Chapter 1: Introduction: oxidative stress, cellular antioxidant systems, and the importance of the thioredoxin system in cells

A. The functions of thioredoxin and thioredoxin reductase: the thioredoxin system

The thioredoxin system is composed of thioredoxin (Trx) and thioredoxin reductase (TrxR; EC 1.6.4.5). TrxR catalyzes the following reaction in which Trx is reduced.

$$\text{Trx-S}_2 + \text{NADPH} + \text{H}^+ \xrightleftharpoons{\text{Thioredoxin reductase}} \text{Trx-(SH)}_2 + \text{NADP}^+ \quad (1.1)$$

In 1964, Trx was first shown to donate reducing equivalents to ribonucleotide reductase (RNR) to enable its catalysis in *Escherichia coli* (*1*). Trx was also shown to serve as a donor of reducing equivalents in the reduction of sulfate, and methionine sulfoxide in yeast (*2, 3*). Human Trx was described by different names such as adult-T cell leukemia-derived factor (ADF), interleukin-2 receptor factor, and early pregnancy factor (*4, 5*). These proteins were attributed to be Trx, on the basis of their sequences of amino acid residues being homologous to that of Trx. The Trx system is widely distributed in eukaryotic and prokaryotic species and has been shown to mediate a variety of physiological functions (*6, 7*): it is involved in cell growth, the inflammation reaction, and apoptosis. In addition to serving as an electron donor to other enzymes, the Trx system is one of the antioxidant systems in cells. Trx is able to regulate the DNA binding activities of several transcription factors (*8-10*). Trx can inhibit the onset of apoptosis (*7, 11, 12*). Several isoenzymes of TrxRs are responsible for mediating various functions in

mammals: a cytosolic form of TrxR (TrxR-1) is required for embryogenesis (*13*), a mitochondrial TrxR (TrxR-2) is essential for hematopoiesis and heart function (*14*), and TrxR-3 is needed for sperm maturation (*15*).

1. The function of Trx in antioxidant systems

In an aerobic environment, the formation of reactive oxygen species (ROS) in cells is inevitable. Low concentrations of ROS are compatible with normal physiological functions, whereas high concentrations of ROS are considered to be harmful to cells, leading to oxidative stress. A variety of enzymatic and nonenzymatic antioxidant systems has been developed to neutralize ROS. The glutathione (GSH) and Trx systems constitute two of the four most important antioxidant systems in most cells. Trx has a redox-active cysteine pair through which it interacts with other proteins to regenerate proteins damaged by ROS, e.g., reduced Trx can restore activity to H_2O_2-inactivated glyceraldehyde-3-phosphate dehydrogenase (*16*). Trx also is a cofactor for methionine sulfoxide reductase, which can reduce methionine sulfoxide residues in oxidized protein caused by ROS (*6, 7*). Trx acts as an electron donor to peroxiredoxin (Prx; thioredoxin peroxidase) and glutathione peroxidase (Gpx) to reduce hydrogen peroxide (*17, 18*). Reduced Trx is oxidized upon passing reducing equivalents to oxidized proteins; oxidized Trx is reduced by TrxR using NADPH (Reaction 1.1). Mammalian TrxRs appear to be directly involved in removing ROS. They are able to directly reduce several oxidants, such as quinones, hydrogen peroxide, and alkylhydroperoxides, due to their highly reactive selenocysteine (*18-20*) (discussion below); however, the turnover numbers for these compounds are low compared to that of the reaction toward Trx (*20,*

21). Moreover, mammalian TrxR can also regenerate other antioxidants e.g., ascorbyl free radicals, α-tocopherol, and lipoic acid. Ascorbic acid is a nonenzymatic antioxidant in cells. After reacting with ROS, the ascorbic acid will be oxidized to an ascorbyl free radical. Mammalian TrxR is capable of reducing this free radical to ascorbic acid (*18*). α-Tocopherol (Vitamin E) can be cycled by ascorbate, which is reduced by mammalian TrxR, to regulate the amount of reduced α-tocopherol in cells. Lipoic acid, another antioxidant in cells, can be regenerated directly by mammalian TrxR (*22*).

2. Trx as an enzyme cofactor

As mentioned previously, Trx is able to donate reducing equivalents to RNR in *E. coli* and methionine sulfoxide reductase in yeast as a cofactor in their catalysis (*1, 2, 23*). RNR is an essential enzyme because it catalyzes the reduction of ribonucleotide to deoxyribonucleotides for DNA synthesis (*1, 24*). However, Trx is not the only electron donor for DNA synthesis (*4*). Glutaredoxin (Grx), a protein related to Trx, also has been shown to be able to donate reducing equivalents to RNR to facilitate DNA synthesis (*6*). In *E. coli*, glutaredoxin-1 (Grx-1) is the main donor of reducing equivalents to RNR, whereas in yeast, both Grx and Trx are able to provide reducing equivalents to RNR (*12*). The reaction whereby Trx also is able to donate reducing equivalents to methionine sulfoxide reductase is Reaction 1.2 (*4*).

$$R\text{-}SO + Trx(SH)_2 \longrightarrow R\text{-}S + Trx\text{-}S_2 + H_2O \quad (1.2)$$

Trx is also involved in sulfur assimilation: it can donate reducing equivalents to PAPS (adenosine 3'-phosphate-5'-phosphosulfate) reductase to reduce PAPS to obtain sulfate (SO_3^-) (*3*, *25*).

3. The function of Trx in the immune system

It has been shown that Trx can stimulate the growth of some transformed lymphocytes and synergize the activity of cytokines on lymphocytes. For example, Trx enhances the growth of human T-lymphotropic virus type I (HTLV I)- and Epstein-Barr virus (EBV)-transformed lymphocytes (*26*). As T-lymphocyte cell lines are stimulated by tetradecanoyl phorbolacetate, Trx can co-stimulate the expression of several cytokines, such as interleukin-1 (IL-1), interleukin-2 (IL-2), and tumor necrosis factor (TNF); the co-stimulative effect results from the activation of nuclear factor-κB (NF-κB) and activator protein 1 (AP-1) by Trx (*27*).

Truncated Trx (Trx 80) contains residue 1-80 of full-length human Trx. Trx 80 does not exhibit a dithiol reductase activity but is a potent chemoattractant for neutrophils, monocytes, and T-lymphocytes (*28*). Trx 80 is mainly secreted by monocytes and also can be produced by T-lymphocytes, and cytotrophblasts. Trx 80 can enhance cytotoxicity of eosinophils (*29*); in addition, Trx 80 can stimulate proliferation of monocytes and regulate the expression of surface antigens on monocytes (*30*).

4. Function of Trx in redox regulation of signal transduction

Several transcription factors are redox-sensitive, and their activities are regulated by the intracellular redox status. Trx is also capable of regulating the DNA-binding

activities of several redox-sensitive transcriptional factors, such as NF-κB, AP-1, HIF-1α (hypoxia-inducible factor 1 α), estrogen receptor, glucocorticoid receptor, and Ref-1 (redox factor-1) (*31-34*). A well-known example is the regulation of NF-κB by Trx. NF-κB is an inducible heterodimeric protein. The most predominant form of NF-κB in cells is p50/p65 (*35*). Activated NF-κB is able to increase the expression of genes associated with the immune response and antioxidant systems. I-κB (inhibitory protein κB) can bind to NF-κB to inactivate NF-κB activity. Under oxidative stress or some other stimuli, I-κB will be phosphorylated by I-κB kinase complex, signaling it to be degraded, and leading to dissociation of the NF-κB-I-κB complex. The resulting NF-κB will translocate into the nucleus to activate certain genes (*36*). Trx in the cytosol is able to prevent the dissociation of the complex of NF-κB and I-κB; e.g., in TNF-α or IL-1 stimulated cells, Trx interfaces the signal pathway required for phosphorylation of I-κB, thereby inhibiting I-κB phosphorylation and degradation (*6, 36*). In contrast, in the nucleus, Trx can facilitate the DNA-binding activity of NF-κB: Cys-62 of the p50 subunit can be reduced by Trx to increase the binding activity of NF-κB to DNA (*8, 35, 37*). Trx can also regulate AP-1 to up-regulate the genes for cell growth, differentiation, and stress (*8*). AP-1 is regulated by Trx through Ref-1: Trx is able to donate reducing equivalents to Cys-63 and Cys-95 of Ref-1, and the resultant Ref-1 can reduce two cysteine residues of AP-1 to increase the DNA-binding activity of AP-1 (*9, 38, 39*). The DNA binding activity of estrogen receptor (ER) is susceptible to oxidative stress and Trx can enhance the transcriptional activity of ER (*31*). Glucocorticoid receptor, which binds to the glucocorticoid response element, can trigger gene expression for hormone production. Both the ligand-binding domain and the DNA-binding domain of glucocorticoid receptor

are regulated by Trx independently (*40, 41*). Trx can regulate the DNA binding activity of p53: under oxidative stress, Trx is able to translocate into the nucleus where Trx increases the activity of p53 directly or through Ref-1 to activate the genes for DNA repair (*10*). In summary, Trx can regulate the DNA binding activities of redox-sensitive transcription factors.

5. The function of Trx in apoptosis

ASK-1 (apoptotic signal kinase-1) is a MAP kinase kinase kinase (MAPKKK). ASK-1 activates C-Jun N-terminal kinase (JNK) and p38 MAP kinase, both of which are required to initiate TNF-α-induced apoptosis (*12, 42*). Reduced Trx is a negative regulator of ASK-1 by binding to the N-terminal region of ASK-1 to inhibit the kinase activity (*43*). The binding of Trx to ASK-1 leads to ubiquitination of ASK-1 (*7*). Oxidation of Trx stimulated by oxidative stress results in the dissociation of the complex of Trx and ASK-1. Consequently, ASK-1 will be activated to initiate apoptosis (*32*). In addition, the relationship between mitochondrial-dependent apoptosis and the Trx system resident in mitochondria has been explored. In mitochondria, induction of the permeability transition pores (PTP) can increase the permeability of the inner membrane to water and solutes < 1.5 kDa; this event is called the membrane permeability transition (MPT). The MPT results in dissipation of mitochondrial membrane potential ($\Delta\psi_m$) and rupture of mitochondria. The disruption of the mitochondrial membrane releases the caspase-9 activator, cytochrome c, and other apoptosis-inducing factors. Adenine nucleotide translocator (ANT), a constituent member of the mitochondria permeability transition pore complex, is a target of ROS. Apoptosis will be initiated upon oxidation of

Cys-56 and the formation of a disulfide bond between Cys-56 and Cys-159 on ANT (*44*). The Trx-2 system resident in mitochondria has been shown to be involved in mitochondria-dependent apoptosis; however, the explicit function of the Trx system in mitochondria is still not clear. Previous studies showed that deletion of Trx-2 resulted in apoptotic cell death (*45*). In addition, overexpression of Trx-2 is able to increase $\Delta\psi_m$ (*46*), but overexpression of TrxR-2 does not have any direct effect on $\Delta\psi_m$ (*44*). Trx-2 can prevent apoptosis in several ways. One way is for Trx-2 to bind to ASK-1 to inhibit its kinase activity. Trx-2 also acts as an endogenous ROS scavenger by donating reducing equivalents to peroxiredoxin-3 to neutralize oxidants such as *tert*-butylhydroperoxide (*t*-BH) (*47*). TrxR-2 has a peroxidase activity to neutralize oxidants (*47*). In addition, Trx-2 can prevent pore formation in the mitochondrial membrane (*45, 48*).

B. Diseases in which Trx is thought to play a role

As mentioned previously, a variety of physiological functions are affected by the Trx system. Thus, once dysfunction of the Trx system occurs, certain diseases will develop (*18*). The functions of the Trx system in several diseases are currently under investigation, and it is hoped that it will be possible to develop new therapeutic drugs on the basis of the Trx system. A few Trx-related diseases will be described briefly below.

1. Cancer

The most striking result caused by ROS is DNA damage, which potentially leads to mutagenesis and/or carcinogenesis. The Trx system is one of the antioxidant systems in cells, and the Trx system is able to regulate the activities of redox-sensitive transcription factors to deal with oxidative stress. Therefore, the Trx system appears to be important in tumor prevention (*18*).

However, once tumor cells are established, the effects of the Trx system on tumor cells will no longer be an advantage for cancer patients. Human Trx, which was first identified in leukemia patients and was referred to as adult T-cell leukemia derived factor (ADF), shows that the Trx system can promote tumor growth. Indeed, secreted Trx is an autocrine growth factor in various tumor cells (*18*). In addition, overexpression of Trx is found in aggressive tumor cells (*49*), and the expression of TrxR is also upregulated in tumor cells (*33, 50*). Overexpression of the Trx system appears to be a consequence of high metabolic rates and high proliferation rates of tumor cells (*12, 33, 50*). Tumor cells inevitably produce excess ROS because of an unusually high metabolic rate. Thus, as oxidative stress is sensed, tumor cells will elevate their antioxidant capacity and the genes

associated with oxidative stress will be activated (*33*). The elevated Trx system has multiple effects on tumor growth and survival. Cancer cells require fast DNA synthesis due to rapid growth, and Trx serves as a donor of reducing equivalents to RNR for DNA synthesis. In addition, Trx acts as an anti-apoptotic factor in cancer cells. As discussed above, Trx can inhibit the activity of ASK-1. Also, Trx inhibits the tumor suppressor gene, PTEN, a tyrosine phosphatase, which is capable of triggering apoptosis (*51*). Moreover, Trx can regulate the activities of the redox-sensitive transcription factors, NF-κB and AP-1. Both of them are responsible for activating the genes for anti-oxidative stress (*33*). Thus, tumor cells will have a higher antioxidant capacity to neutralize ROS and/or anti-tumor drugs. It has also been shown that Trx induces hypoxia-inducible factor-α, which increases the expression of VEGF (vascular endothelial growth factor) resulting in promoting tumor angiogenesis (*50*). Furthermore, the Trx system can act as a ROS scavenger (*50*). Thus, TrxR and Trx are considered to be attractive targets for the development of anti-cancer drugs. Indeed, several TrxR inhibitors, such as gold- and platinum–containing drugs and nitrosoureas are being studied to assess their possible applications in cancer therapy (*33, 51, 52*). Recently, TrxR and Trx inhibitors have been applied to enhance the cytotoxic effects caused by other antitumor drugs (*53, 54*).

Thioredoxin-binding protein-2 (TBP-2), also called vitamin D3 upregulated protein 1, acts as a Trx suppressor by binding to Trx (*50*). The downregulation of TBP-2 has been observed in numerous tumor cells (*50*). Thus, elevation of TBP-2 in tumor cells may be a potential therapy to treat cancers. In addition, it is possible that TBP-2 has a Trx-independent antitumor activity, because TBP-2 seems to have a suppressive effect on tumor growth by enhancing the immune system (*50*). Furthermore, a study also shows

that TBP-2 is involved in the antitumor mechanism of histone deacetylase inhibitors (HDACi) (*49*).

2. Rheumatoid arthritis and Sjögren syndrome

Rheumatoid arthritis (RA) is a chronic autoimmune disease characterized by the proliferation of synovial cells and massive infiltration of immune cells in the joints (*55, 56*). Although the underlying pathophysiological basis of this disease is not known, ROS produced by immune cells (e.g., macrophages and polymorphonuclear cells) have been shown to contribute to the development of RA (*55, 57*). Many oxidizing agents have been observed to affect enzymes and cells. Hydrogen peroxide can inhibit cartilage proteoglycan synthesis. Hypochlorous acid can activate collagenase and gelatinase in neutrophils. Hydrogen peroxide and superoxide anion are able to accelerate bone absorption by osteoclasts. Increased levels of Trx and TrxR are observed in the synovial fluid and tissues in RA patients (*18, 55, 58*). Oxidative stress and TNF-α lead to overexpression of Trx. Overexpression of Trx has a potent capacity to induce proinflammatory cytokines, and Trx is a chemoattractant for neutrophils, monocytes, and T-cells (*57, 58*). Therefore, the up-regulation of Trx will lead to more severe immune reactions in the joints of RA patients. The reason that TrxR is overexpressed in RA is not clear. Organic gold compounds such as auranofin and aurithioglucose applied in treatment of RA are shown to be TrxR-inhibitors, showing that TrxR should be involved in the pathophysiological mechanism of RA (*59*).

Sjögren syndrome is also a chronic autoimmune disease caused by Epstein-Barr virus infection and is characterized by infiltration of lymphocytes in mucosal and other

tissues (*6*). Sjögren syndrome and RA share the same features: a massive inflammatory reaction in the joints. Trx can enhance inflammatory reactions in the joints of the patients with Sjögren syndrome (*18*).

3. Cardiovascular diseases

ROS have been shown to be associated with several cardiovascular diseases such as atherosclerosis and hypertension (*60, 61*). The expression of Trx and TrxR is increased in the endothelial cells and infiltrating macrophages in artherosclerotic plaques, suggesting that Trx and TrxR are involved in antioxidant defense in atherosclerosis (*60, 62*). S-nitrosylation of Cys-69 on Trx-1 is associated with an anti-apoptotic activity in the cardiovascular tissue. An HMG-CoA reductase inhibitor may function in the prevention of atherosclerosis by enhancing S-nitrosylation of Trx-1 (*63*). However, some reports showed that the Trx system is involved in the formation of artherosclerotic plaques (*6, 62*). Thus, more research is required to address the roles of Trx in atherosclerosis. A decrease in Trx expression is found in the animal models of hypertension. This suggests hypertension results from a decrease in Trx expression, although the explicit role of Trx in hypertension is questionable (*61*). In addition, Trx was shown to have a protective role against myocarditis, and adriamycin-induced cardiotoxicity (*62*).

4. Human immunodeficient virus infection

Human immunodeficient virus (HIV) infection leads to dysregulation of Trx expression (*6, 12*). In T cells the expression of Trx in HIV-infected individuals is decreased, allowing viral replication in T-cells (*64*). However, an elevated Trx level is

found in the plasma of HIV-infected patients, and this elevated level is negatively correlated to the life spans of AIDS patients. The proposed mechanism is that elevated levels of plasma Trx can suppress the recruitment of neutrophils to the infection site. Thus, innate immunity is blocked, allowing other infections in these immunodeficient individuals (*65*). The administration of exogenous Trx has been shown to inhibit expression of HIV in marcrophages by 70%, whereas the truncated form, Trx 80, will enhance the expression of HIV by 67% (*12, 66*). This apparent dichotomy of results will require further elucidation to understand the relationship of Trx to HIV infection.

5. Reperfusion injury

Ischemia reperfusion injury occurs as blood flow is restored to an ischemic organ, leading to excess ROS and dysfunction of the organ. Excess ROS is a main cause for reperfusion injury. The accumulated data indicated that increased concentrations of antioxidants are able to ameliorate the injury. Indeed, Trx has been shown to protect the lung, heart, and brain against oxidative stress caused by reperfusion (*67-69*). In reperfusion injury, Trx serves as a ROS scavenger and is involved in signal transduction for cell survival (*6, 69*). A Trx-mediated anti-apoptotic pathway is proposed to be involved in the protection of cerebral ischemia against reperfusion injury (*6*).

C. The redox environment in cells

Redox reactions in cells are required to build and maintain cellular structures and to generate energy (*70*). Therefore, the redox status of cells is very crucial for physiological functions. Under an aerobic environment, the intracellular redox status is tightly regulated within a narrow range (*71*). A variety of signal transduction pathways are redox-dependent. Once the redox status is disrupted, various physiological functions no longer function well, leading to development of several diseases.

1. Reactive oxygen species and oxidative stress

Cells acquire energy derived from oxidative phosphorylation linked to oxygen utilization. Approximately 1-3% of electrons passing through the respiratory chain in the mitochondria will react with oxygen to generate superoxide anion instead of water (*72*). Superoxide anion can be converted by other enzymes to other reactive species. All of these species are called reactive oxygen species (ROS), and include superoxide anion ($^{\bullet}O_2^-$), hydrogen peroxide (H_2O_2), singlet oxygen ($^1O_2^-$), and hydroxyl radical ($^{\bullet}OH$) and anion (OH^-).

Actually, low concentrations of ROS can participate in regulatory mechanisms, acting as messengers to regulate cell growth, differentiation, and the immune system (*22, 73*). For example, ROS can stimulate extracellular signal-regulated kinase (ERK) for cell growth (*74*). It has been shown that hydrogen peroxide and nitric oxide act as signaling molecules, and these active species can be used to kill the invading microbes. ROS can affect the signal transduction pathways in cells leading to cell proliferation or cell death

including apoptosis and necrosis. These effects mediated by ROS are dependent on the dosage and the duration of ROS and are cell-specific (*74*).

ROS can also be generated by exogenous sources such as environmental toxicants, ionizing radiation, and ultraviolet radiation (*72*). Among the species of ROS, hydroxyl radical is the most highly reactive, whereas H_2O_2 is less active (*22*).

2. Superoxide anion

Superoxide anion can be formed from oxygen during enzymatic catalysis, e.g., xanthine oxidase, lipoxygenase, and cyclooxygenase (*22, 73*). Furthermore, superoxide anion can also be generated by NADPH-oxidase in phagocytic immune cells to act as a messenger of signal transduction pathways (*22*). Because of its negative charge, superoxide anion is not able to freely cross membranes. Therefore, the superoxide anion cannot escape the organelle where it is produced (*22, 73*). Superoxide anion is considered to be a primary ROS and it can interact with other molecules to produce secondary ROS (*72*). For example, in the presence of metals, the reaction of superoxide ion and hydrogen peroxide will produce hydroxyl radicals. Superoxide anion can also spontaneously dismutate to hydrogen peroxide and oxygen in aqueous solution, especially at lower pH or in the presence of superoxide dismutase (SOD) (*73*).

3. Hydrogen peroxide

Hydrogen peroxide is one of the less reactive ROS. Unlike superoxide anion, hydrogen peroxide can penetrate biological membranes and is used to act as a signaling molecule. Most of the intracellualar hydrogen peroxide is contributed by dismutation of

superoxide anion, but hydrogen peroxide can be formed by the 2-electron reduction of oxygen mediated by other enzymes (*75*). Although hydrogen peroxide is less reactive than other ROS, it can interact with other molecules to generate more highly reactive ROS. In the presence of transition metals, hydroxyl radicals can be generated from hydrogen peroxide via the Fenton reaction (Reaction 1.3), and these radicals are highly reactive (*22, 73*). Superoxide anion can react with metal ions to recycle the transition metal ions (Reaction 1.4). The sum of Reactions 1.3 and 1.4 is called the Haber-Weiss reaction. Hydrogen peroxide can also react with chloride to form hypochlorous acid (Reaction 1.6). Hydrogen peroxide can be removed by catalases, glutathione peroxidases, and peroxiredoxins.

$$H_2O_2 + Fe^{2+} \longrightarrow {\cdot}OH + OH^- + Fe^{3+} \quad (1.3)\ \text{(Fenton reaction)}$$

$$Fe^{3+} + {\cdot}O_2^- \longrightarrow Fe^{2+} + O_2 \quad (1.4)$$

$$H_2O_2 + {\cdot}O_2^- \longrightarrow {\cdot}OH + OH^- + O_2 \quad (1.5)\ \text{(Haber-Weiss reaction)}$$

$$H^+ + Cl^- + H_2O_2 \longrightarrow HOCl + H_2O \quad (1.6)$$

4. Hydroxyl radical

The highly reactive hydroxyl radical has a half life of approximately 10^{-9} s in aqueous solutions. It is the most dangerous ROS because it can react with almost all chemicals including cellular macromolecules such as DNA, lipid, and proteins. Hydroxyl

radicals can be generated via the Fenton reaction *in vitro*. However, the Fenton reaction is not favorable *in vivo* because of the limited availability of free transition metal ions (*76*). Hydroxyl radicals can be generated through various mechanisms. In addition to the Fenton reaction (Reaction 1.3), hydroxyl radicals can be generated from decomposition of water by ionizing radiation, and hydroxyl radicals are also generated from reactions involving alkylhydroperoxides (*76*).

5. Nitric oxide

Nitric oxide (NO) is formed from the reaction of L-arginine and oxygen catalyzed by NO synthetase using NADPH (Reaction 1.7).

$$\text{L-arginine} + O_2 + \text{NADPH} \xrightarrow{\text{NO synthase}} \text{L-citrulline} + {}^{\cdot}\text{NO} + \text{NADP}^+ \quad (1.7)$$

NO has a short half-life of a few seconds in aqueous solution (*76*). Because NO is readily able to cross biological membranes, it acts as a messenger mediating neutrotransmission, dilation of blood vessels, inhibition of platelet aggregation, angiogenesis, neurotransmission, and functions of the immune system (*77*).

Nitrosative stress is caused by excess NO that is able to interact with superoxide anion to form peroxynitrite anion ($ONOO^-$), which is highly reactive causing DNA fragmentation and lipid peroxidation. Nitrosative stress affects immune defense; peroxynitrite anion readily crosses the membrane to effect cytotoxic actions on invading microbes (*78*). Moreover, peroxynitrite is able to interact with carbon dioxide to form the reactive intermediate ($ONOOCO_2^-$), which will further oxidize proteins (*79*).

D. Roles of the thioredoxin-thioredoxin reductase system in toxicology

Oxidative stress will be generated as ROS exceed the intrinsic capacity of intracellular antioxidants. Excess ROS attack cellular macromolecules leading to mutagenesis, carcinogenesis, dysfunction of proteins, and cell death (apoptosis and necrosis). Several antioxidant systems have evolved to deal with oxidative stress. The cellular targets of ROS and the antioxidant systems are described in the appendix 1. The GSH and the Trx systems constitute major cellular antioxidants in cells (*80*). The intracellular concentration of Trx is in the micromolar range, whereas that of GSH is at the millimolar level. However, the lower concentration of intracellular Trx is offset by its lower redox potential, i.e., its greater reductive capacity (*81*). In this section, the roles of the Trx system in toxicology will be addressed.

The expression of Trx can be induced by a variety of stresses such as viral infection, UV light and X-ray exposure, and hydrogen peroxide. The promoters of human Trx include an SP-1 site, the cyclic AMP responsive element, the antioxidative responsive element, and the xenobiotic responsive element. This shows that Trx is strongly associated with oxidative stress caused by endogenous and exogenous ROS, as well as xenobiotics (*32, 62*). It appears that the functions mediated by the Trx system are associated with signaling pathways rather than acting as oxidant scavengers, because the concentrations of Trx in cells are less than those of intracellular GSH (*7*).

Trx-1 can affect the DNA-binding activities of NF-κB, AP-1 and p53. NF-κB is able to exhibit anti-apoptotic activity including the inhibition of the activation of caspases and the upregulation of the Bcl-2 family against DNA-damaging chemotherapeutic drugs (*82*). The expression of AP-1 can be induced by various stress factors (e.g., hydrogen

peroxide, UV light, asbestos and dioxin) (*83*). AP-1 is able to regulate a variety of genes including collagenase, cyclin D, and TGF-1 (transforming growth factor-1) (*83*); the activation of AP-1 has been shown to promote cell proliferation and differentiation (*7, 83*). Moreover, a tumor suppressor gene, p53, is also regulated by the Trx system. The activation of p53 can result in cell-cycle arrest, the initiation of DNA repair, and if the repair of damaged DNA is not successful, to the onset of apoptosis (*7, 84*). As discussed previously, Trx-1 promotes cell growth and prevents initiation of the apoptotic pathways. Overexpression of Trx-2 leads to human osteosarcoma cells becoming more resistant to oxidant-induced apoptosis (*7*).

Trx is able to donate reducing equivalents to Prx to reduce hydrogen peroxide and various alkyl hydroperoxides as has mentioned above (*17, 85*). Zhang et al. showed that Prx inhibits the production of hydrogen peroxide as cells are treated with a ceramide analogue and prevents the release of cytochrome c from mitochondria, a critical step for apoptosis. Also, they showed that Prx can inhibit lipid peroxidation (*86*). Moreover, Trx acts as a donor of reducing equivalents to methionone sulfoxide reductase for protein repair.

It was believed that the GSH and the Trx systems function independently. Some studies showed that even though the ratio of GSH/GSSG is decreased by some oxidants, most Trx remains in the reduced state (*87*). However, some evidence has shown the existence of the interaction between GSSG and Trx in some species such as *Plasmodium falciparum* and *Drosophila melanogaster* (*88, 89*). GSSG can be reduced by Trx nonenzymatically. The maintenance of the ratio of GSH/GSSG by Trx in these organisms may be due to the difference of redox potentials between Trx and GSH: the redox

potentials of DmTrx-2, PfTrx, and GSSG are -275.4 mV, -271.9 mV, and -241mV, respectively. Thus, electrons can be passed from Trx to GSSG. Also, the structures of these Trxs may also help the binding of GSSG to Trx (*81*).

S-glutathionylation was found to be a regulator of mammalian Trx-1. In addition to a redox-active cysteine pair, human Trx-1 has three additional cysteine residues, Cys-62, Cys-69, and Cys-73. S-glutathionylation on Cys-73 results in the loss of Trx activity (*90*).

The balance between formation of ROS and antioxidants is essential in cells; therefore, imbalance of the redox status leads to the occurrence of various diseases. Indeed, a variety of diseases associated with ROS has been identified, such as cancer, aging, several neurodegenerative diseases, atherosclerosis, and rheumatoid arthritis (*22, 74, 86*). Thus, disruption of the redox status of cells can be a strategy applied in the development of new drugs. Development of antimalarial drugs is such an example.

1. Malaria

Malaria causes a serious global public health issue; 500 million cases are reported and 2.5 million people die of this disease annually (*91*). Four species of the *Plasmodium* family are able to cause human malaria: *P. falciparum, P. vivax, P. ovale, and P. malariae*. The malaria in western Africa is mainly caused by *P. falciparum*, the malaria in eastern and southern Africa is caused by *P. falciparum* and *P. vivax*, while most malarial cases are caused by *P. vivax* outside of Africa, such as southern Asia, the Western Pacific, South America and Central America *(92).* Among these 4 species, *P. falciparum* is the most lethal species (*91*). Malaria parasites have been developing

resistance to anti-malarial drugs, causing the failure of clinical drug applications and the need to develop new antimalarials (*93, 94*).

As shown in Fig 1.1, the life cycle of a malarial parasite can be divided into three stages: mosquito, liver, and blood stages (*91*). Sporozoites can infect humans via a mosquito vector. After entering the human body, sporozoites reach the liver via the circulation system. In the liver, sporozoites form schizonts which release merozoites into bloodstream as liver cells become ruptured. Merozoites can then invade the red blood cells (RBCs) where they mature to trophozoites. Trophozoites undergo asexual division to form schizonts; each schizont contains 24-32 meroziotes. After disruption of RBCs, the released merozoites will infect other RBCs immediately. The symptoms develop upon release of schizonts into blood: malarial parasites will induce cytokine dysfunction in the host, causing fever, chills, headaches, muscle pains, nausea and vomiting (*95*) and also cause malarial anemia (*96*).

During the blood stage, because of the high oxygen tension of the RBCs, the parasite requires antioxidants to deal with oxidative stress. As haemoglobin is taken into the parasite's vacuole, superoxide anions are produced via the Fenton Reaction (Reaction 1.3) (*94, 97*). The parasites have a variety of cellular antioxidants to cope with oxidative stress; and these include the GSH and the Trx systems, and superoxide dismutase (SOD). However, catalase and Gpx are absent in malarial parasites, showing that they have a lower capacity for reducing hydrogen peroxide than other organisms (*97, 98*). In addition, it has been shown that glutathione reductase (GR) inhibition does not affect the parasites because the Trx system is able to substitute for GR and recycle GSSG to GSH (*88*). Thus, the Trx system is thought to constitute a primary antioxidant system in malarial parasites

(*99*). The TrxR from *P. falciparum* (PfTrxR), unlike mammalian TrxR, does not contain a selenocysteine residue, thereby suggesting a new direction for the development of anti-malarial drugs (*99*) (discussion below).

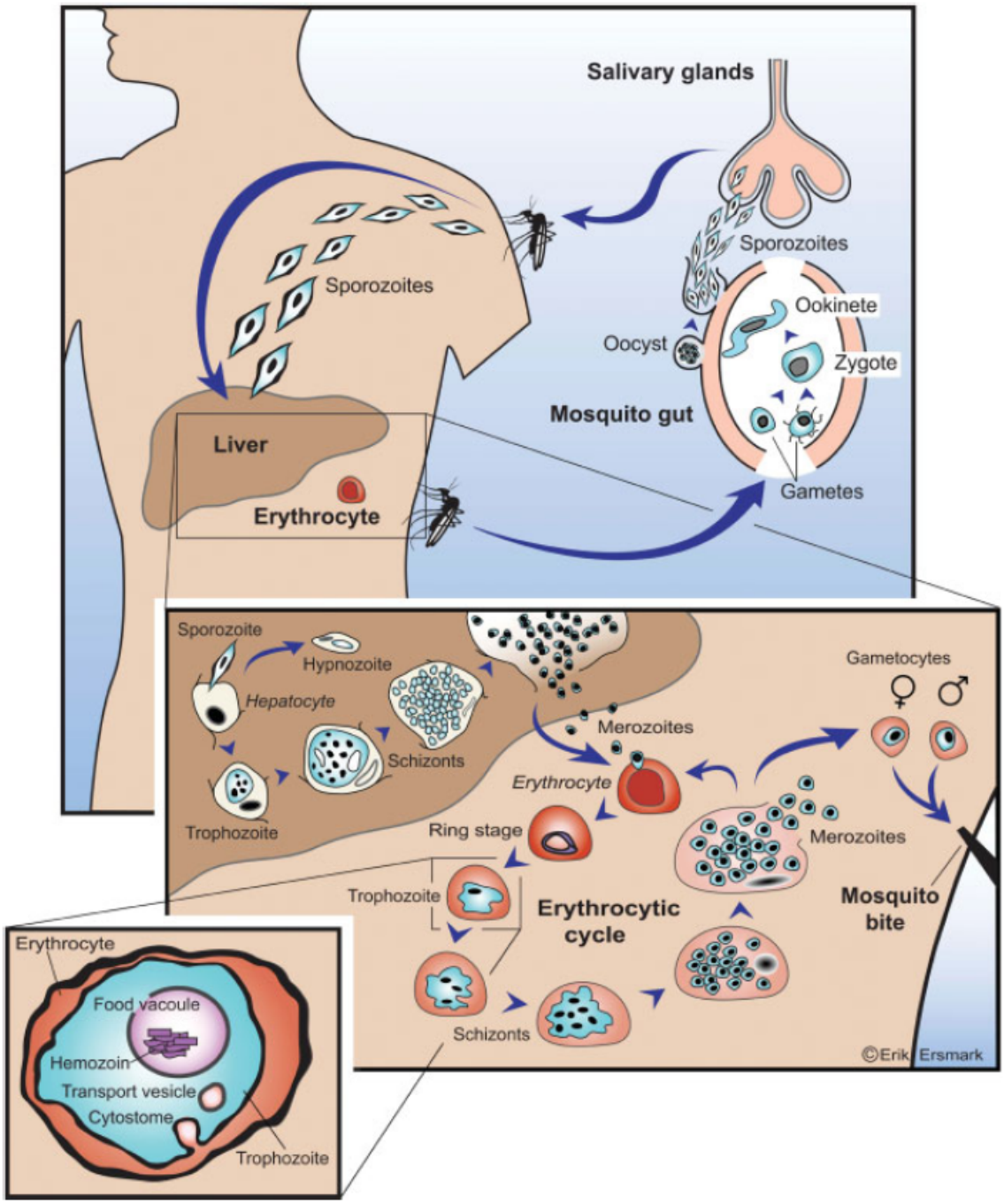

Fig. 1.1 The life cycle of malarial parasites (*100*)

Anopheles gambiae is an insect vector of the malaria parasite. This type of mosquito has a special antioxidant system of which the Trx system comprises the main component (discussion below). Malaria parasites and the insect vector have high demand for the Trx system and differences among TrxRs from human, *A. gambiae*, and *P. falciparum* are observed. Therefore, it is hoped to develop inhibitors specific for TrxR from the host, parasites and the vector.

2. Thioredoxin reductase from dipteran insects

Dipteran insects such as *D. melanogaster* and *A. gambiae* have to deal with high levels of ROS because of their trachea (the insects have an extensive tracheal tubular respiratory system to distributes oxygen to nearly all tissues; during respiration, all tissues in these insects will be exposed to high concentrations of oxygen, leading to oxidative stress (*101*).) and exposure to ionizing radiation (*102*). The antioxidant systems in this type of insect are different from those of mammals; dipteran insects have no GPx or GR (*103*). In order to maintain a high GSH/GSSG ratio, they depend on the ability of $Trx(SH)_2$ to reduce GSSG nonenzymatically (rate constant ~ 170 M^{-1} s^{-1}) (*89*); therefore, the TrxR/Trx system has been shown to be even more important in dipteran insects.

The active sites of TrxRs from *D. melanogaster* and *A. gambiae* have been shown to be virtually identical and Trx-2 from *D. melanogaster* (DmTrx-2) is a good substrate for TrxR from *A. gambiae* (*104*).

D. melanogaster has several different forms of Trx: DmTrx-1 (DHD protein) and TrxT were found in the nucleus of the ovary and the testis, respectively (*105, 106*). A cytosolic form, DmTrx-2, is a better substrate for Prx and its function is similar to that of

human Trx-1 (*105, 106*). The TrxrR-1 gene codes for two isoforms, TrxR-1^{cyto} and TrxR-1^{mito} with different splicing. Both of them have almost identical biochemical properties but their physiological roles are not interchangeable. The null mutation of TrxR-1^{cyto} is lethal (*107*).

E. Biochemical properties of Trx and peroxiredoxin

1. Mechanism of thioredoxin reactions

Trx is a small protein with a M_r ~12 kD_a having a redox-active disulfide (Cys-32 Cys-35 *E. coli* numbers) in a WCGPCK motif. Trx can undergo reversible reduction-oxidation in interactions with targeted proteins. Cys-32 is solvent-accessible and Cys-35 is buried. The microscopic pK_a value of Cys-32 is close to physiological pH, allowing the deprotonation of Cys-32 at physiological pH. A thiolate anion on Cys-32 can initiate a nucleophilic attack on certain exposed protein disulfdes to generate intermolecular mixed disulfides (MDS). Cys-35 acts as a resolving cysteine to attack the MDS and release the targeted protein and oxidized Trx. The pK_a value of Cys-35 is a matter of dispute, but it is higher than that of Cys-32, and nearby Asp-26 has been shown to act as a base to facilitate the formation of thiolate anion on Cys-35 (*108*).

2. Structure of thioredoxin

The overall three-dimensional structures of Trxs from different species are similar; the amino acid residues responsible for catalysis and for the tertiary structure are highly conserved (*106, 109*). This typical Trx-fold is characterized by a central core of four (or five) strands of β-sheet surrounded by three or four α-helixes as shown in Fig. 1.2. This fold is conserved in several redox proteins (e.g., protein disulfide isomerase, glutaredoxin (Grx), glutathione-S-transferase (GST), and GPx) (*110*). The redox–active cysteine pair is located on a protrusion allowing Trx to interact with targeted proteins (*111*). Unlike other Trxs, human Trx-1 has three additional cysteine residues (Cys-62, Cys-69 and Cys-73). Cys-62 and Cys-69 can form an intramolecular disulfide bond under

condition of oxidative stress. The formation of the second disulfide can transiently impair Trx activity. In addition, a homodimeric human Trx-1 can be formed under conditions of oxidative stress via Cys-73; the dimer is not a substrate for TrxR (*112*). Nitrosylation on Cys-69 of human Trx-1 by NO decreases Trx activity; the amount of intracellular NO can be regulated by this nitrosylation reaction (*113*).

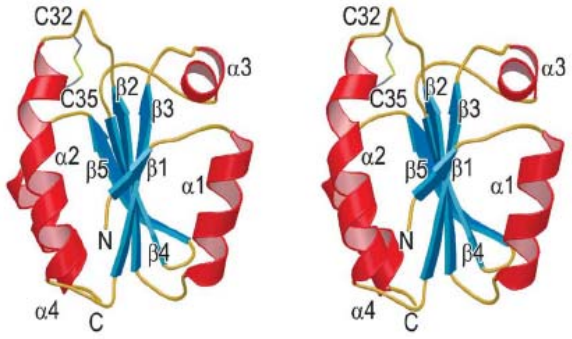

Fig. 1.2 Stereo view of the structure of a thioredoxin fold. The figure used here to demonstrate the structure of a thioredoxin fold is from DmTrx *(106)*.

3. Peroxiredoxin

Peroxiredoxin; Prx (or thioredoxin peroxidase; TPx) is widely present in living organisms (*114*). Mammalian cells have at least six isoforms. Based on the catalytic mechanism, Prx can be divided into 3 subgroups: classic 2-Cys Prx, atypical 2-Cys Prx, and 1-Cys Prx (*115*). All of them contain an N-terminal cysteine residue that deprotonates at neutral pH because a nearby arginine residue lowers the pK_a (*115*). Typical 2-Cys Prxs (Prx I-IV) contain an additional C-terminal cysteine residue. During catalysis, the N-terminal cysteine residue will be oxidized to a sulfenic acid that reacts with the C-terminal cysteine residue from another Prx to form an intermolecular disulfide bond. This disulfide bond can be reduced by Trx but not by GSH or Grx. In one atypical

2-Cys Prx (Prx V), the resulting sulfenic acid on the N-terminal cysteine residue will react with another cysteine residue in the same Prx to form an intramolecular disulfide bond that can be reduced by Trx but not by GSH and Grx. 1-Cys Prx (Prx VI) has one catalytic cysteine residue that forms a sulfenic acid that can be reduced by other thiol compounds. The physiological thiolate donor for 1-Cys Prx has not been determined (*114*). It should be noted that Trx is not the only electron donor for Prx. AphC, a Prx from *Salmonella typhimurium*, can be reduced by AphF from *S. typhimurium* or NADH oxidase from *Amphibacillus xylanus*, both of which are pyridine nucleotide disulfide oxidoreductases, utilizing NADH (*116-118*). A plant Prx can accept electrons from Trx and Grx (*115*). Each Prx is tissue-specific and substrate-specific in different organisms (*119*). Prx II, one of the typical 2-Cys Prxs, has a remarkable rate constant (~1.3×10^7 M^{-1} s^{-1}) in its reaction with hydrogen peroxide (*120*). It was believed that the primary function of Prx is to neutralize hydrogen peroxide. However, some isoforms of Prx are able to react with other reactive species. For example, AphC, the yeast Prx and mammalian Prx V and VI have been shown to exhibit peroxynitrite reductase activity (*115*). In addition, recently, Prx has been shown to be involved in signal transduction. Hydrogen peroxide is often used to act as a second messenger in signal cascades. Prx is able to neutralize hydrogen peroxide allowing Prx to regulate the signal pathways associated with hydrogen peroxide (*114*).

F. Thioredoxin reductase (TrxR) and thioredoxin-glutathione reductase (TGR)

Thioredoxin reductase (E.C. 1.6.4.5) is a member of the family of pyridine nucleotide-disulfide oxidoreductases including GR, lipoamide dehydrogenase, and mercuric ion reductase (*121*). Two classes of TrxRs have been identified: low molecular weight TrxR (low M_r TrxR) and high molecular weight TrxR (high M_r TrxR). Low M_r TrxR, which consists of a dimer of monomers with a M_r 35,000, exists in prokaryotes, plants, and other lower eukaryotes, whereas high M_r TrxR, is a dimer with a monomer M_r of 55,000; it is found in higher eukaryotes. The green alga, *Clamydomonas reinhardtii*, has been found to possess both types of TrxRs (*6*).

1. Low molecular weight thioredoxin reductase

Low M_r TrxR is a dimeric flavoprotein (*24, 122*). The active site contains an NADPH binding site, an FAD binding site, a redox-active cysteine pair, and a Trx binding site. The reducing equivalents from the physiological substrate, NADPH, are passed successively to FAD, to a redox-active disulfide, and then to oxidized Trx. The structure of *E. coli* TrxR showed (*123*) that $FADH^-$, reduced by NADPH, is able to pass reducing equivalents to a redox-active disulfide. However, in that conformation, which is referred to as the FO conformation, the distance between the nicotinamide ring of NADPH and FAD is more than 17 Å, which clearly does not allow the transfer of a hydride ion from NADPH to the isoalloxazine ring of FAD. Moreover, the buried redox-active cysteine pair is far removed from the putative Trx binding site. Thus, it was proposed that a 66 degree domain rotation is required to achieve a conformation referred to as the FR conformation, in which NADPH approaches FAD and the nascent dithiol of

the redox-active cysteine pair is able to interact with the disulfide bond of Trx (*123-125*). The proposed FR conformation was later demonstrated by X-ray crystallogrphy (*125*).

The redox-active disulfide (Cys-135 and Cys-138) in *E. coli* TrxR is responsible for interacting with oxidized Trx; Cys-135 is proposed to initiate a nucleophilic attack on the disulfide bond of oxidized Trx. The formation of the required thiolate anion is catalyzed by Asp-139 (*126*).

2. High molecular weight thioredoxin reductase

High M_r TrxR, a dimeric flavoprotein, has an NADPH binding site, an FAD binding site, and a redox-active disulfide (cysteine pair toward the N-terminus) all from one monomer; it also has either an additional redox-active disulfide or a selenenylsulfide formed from a conserved cysteine-cysteine or a cysteine-selenocysteine dyad, respectively; the cysteine pair or selenocysteine-cysteine pairs are penultimate to the C-terminus from the other monomer. Any conformational change in high M_r TrxR during catalysis is assumed to be comparatively small (*127-130*). The movement of a C-terminal tail has recently been modeled into the structure of human TrxR (*131*). The C-terminal tail not only brings the reducing equivalents from the apolar active site to oxidized Trx bound at the protein surface, but also blocks the approach of GSSG to the N-terminal dithiol so that GSSG is not a substrate of high M_r TrxRs (*130, 132*).

Three major types of high M_r TrxRs have been identified: mammalian, *P. falciparum*, and insect TrxRs. The structures and mechanisms of these three types of enzymes are generally very similar (*93, 128, 130, 131, 133*). The major structural difference is located in the C-terminal redox-active group, where mammalian TrxR has a

cysteine adjacent to a selenocysteine (Gly-Cys-SecC-Gly), *P. falciparum* TrxR contains two cysteine residues separated by 4 amino acid residues (Cys-xxxx-Cys), and insect TrxR has two adjacent Cys residues flanked by serine residues (Ser-Cys-Cys-Ser) (*134*). The sequence similarity between low and high M_r TrxR is only approximately 35%, whereas there is much more similarity between high M_r TrxR and other members of the same family (e.g., GR and lipoamide dehydrogenase). Therefore, the catalytic mechanism of high M_r TrxR is similar to those of GR and lipoamide dehydrogenase rather than to low M_r TrxR, but the mechanism of high M_r TrxR is more complicated due to the additional redox active group (*127*).

The following is a review of three types of high M_r TrxRs; mammalian TrxR and PfTrxR are discussed first for historical reasons. The catalytic mechanism and structure of thioredoxin reductase from *D. melanogaster* (DmTrxR), which is the subject of this dissertation, will then be addressed in more detail.

Three types of mammalian TrxRs have been identified: cytosolic TrxR-1, mitochondrial TrxR-2, and TrxR-3 (TGR; thioredoxin/glutathione reductase), highly expressed in the microsomal fraction of spermatozoa (*5*). All of them are selenocysteine (Sec)-containing proteins (*132, 135, 136*). The codon for Sec is UGA, which is also a stop codon for translation. A SECIS element (cis-acting Sec insertion sequence) is required for incorporation of selenocysteine into the enzymes (*137*). Selenocysteine is essential for the activity of mammalian TrxRs (*138*). The selenosulfide is thought to confer broad substrate tolerance to mammalian TrxRs, allowing it to function not only with Trx but also with several low molecular weight compounds (e.g., hydrogen peroxide, lipid dehydrogenase, ubiquinone, and lipoic acid) (*22, 129, 139*). Also, the

formation of a selenosulfide bond can relieve the ring strain of a disulfide bond formed between two adjacent cysteine residues, because the length of a selenosulfide bond is 15% longer than that of a disulfide bond (*6*). The mechanisms of TrxR-1 and TrxR-2 are similar. A hydride ion from NADPH is passed to FAD and the resulting $FADH^-$ reduces the N-terminal redox-active disulfide; the nascent dithiol interchanges with the C-terminal selenylsulfide that finally interchanges with Trx (*127, 128, 130, 140*).

The biochemical properties of PfTrxR have been characterized (*93, 141, 142*). The passage of reducing equivalents is like that in TrxR-1 and TrxR-2, (*141, 142*).

TGR (TrxR-3), in contrast to TrxR-1 and TrxR-2, displays the activities of TrxR, GR, and Grx (*132, 143*). The molecular weight of the monomer of TGR is 65 kDa. TGR has an additional N-terminal glutaredoxin domain that is responsible for the GR and Grx activities. A selenocysteine has been shown to be required for these activities. A mechanism for TGR has been proposed in which a hydride ion from NADPH is passed to FAD that in turn reduces the N-terminal redox-active disulfide; the nascent dithiol interchanges with the C-terminal redox-active selenylsulfide. Then, reducing equivalents from the C-terminal redox center can be passed either to the Grx domain for Grx activity or to Trx for Trx activity (*132, 143*).

3. The catalytic mechanism and structural properties of DmTrxR

The spectral, structural, and kinetic properties of DmTrxR have been explored (*129, 144*). The catalytic mechanism of DmTrxR is similar to those of TrxRs from both mammals and *P. falciparum* (*93, 127, 129, 141, 142, 144*). Interestingly, the adjacent cysteine residues (SCCS) in the C-terminal redox center in DmTrxR are very efficient for

catalysis. In contrast, the variant of mammalian TrxR in which selenocysteine is replaced by cysteine (GCUG by GCCG) retains only 1.1% of wild-type activity (*138*). It has been proposed that the flanking serine residues facilitate the formation of a thiolate ion on C-terminal cysteine residue in DmTrxR, whereas mammalian TrxR does not need serine residues because of the low pK_a of selenocysteine (*129*). However, *Caenorhabditis elegans* TrxR-2 with two adjacent cysteine residues (Gly-Cys-Cys-Gly) still retains high activity (*145*). In addition, the mammalian TrxR variant with a SCCS sequence inserted in the C-terminal redox center only has <0.5 % of wild-type activity (*146*). These data indicate that serine residues are not the only factors leading to high activity of DmTrxR.

The X-ray structures of high M_r TrxRs from rat, mouse, and human have been determined (*128, 130, 131, 133*). The structure of a truncated DmTrxR, excluding the C-terminal redox-active disulfide (Cys-489' and Cys-490') has also been determined (*133*). As shown in Fig. 1.2, two conserved histidine residues are identified in the active site: His-464' and His-106. Both of them were proposed to be involved in the catalytic mechanism (*129*). The functions of His-464' will be addressed in this study. His-106 was initially proposed to act as a proton donor to the thiol group of the departing Trx (*21*). However, recently, His-106 was shown to play a structural role rather than acting as an acid-base catalyst (*147*).

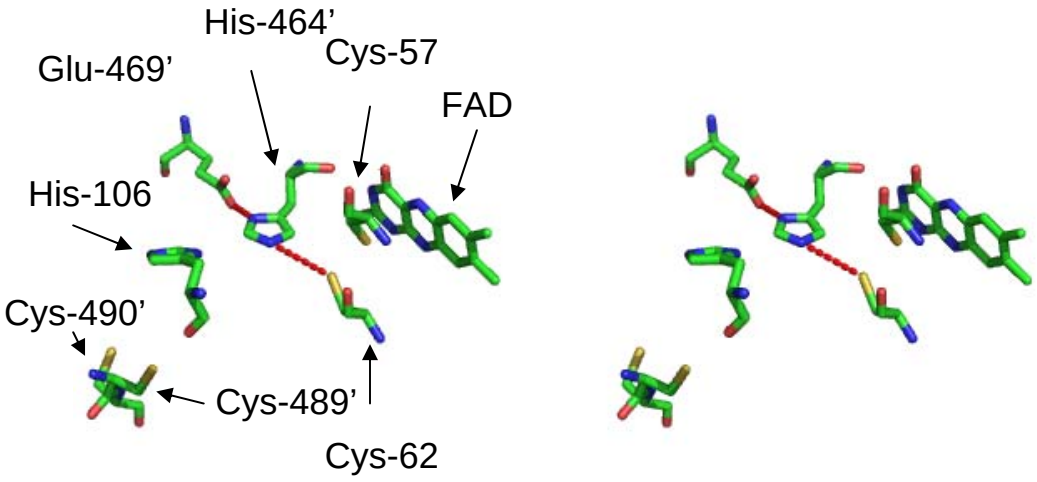

Fig. 1.3 Stereo view showing the relative positions of amino acid residues in the active site of DmTrxR. The active site contains an FAD, an N-terminal redox-active disulfide (Cys-57 and Cys-62), and a C-terminal terminal redox-active disulfide (Cys-489' and Cys-490'). His-464' is adjacent to the N-terminal redox-active disulfide and the distance between NE2 of His-464' and the sulfur atom of Cys-57 is 3.69 Å. The distance between ND1 of His-464' and OE2 of Glu-469' is 2.8 Å (*133*). His-106 was shown to play a structural role rather than acting as an acid-base catalyst. PyMol was applied to generate the figure, and the structure used here is based on the structure of rat TrxR (pdb accession code: 1H6V) (*128*).

The catalytic mechanism of DmTrxR has been proposed (*144*). At the time it was proposed, it was the most detailed mechanism available for high M_r TrxR. The flow of reducing equivalents is like that presented above for human- and PfTrxR. The overall reaction can be separated by two half reactions as shown in Scheme 1.1. In the reductive half-reaction, oxidized enzyme, denoted by E_{ox}, is reduced by the first equiv of NADPH to form 2-electron reduced enzyme (EH_2); NADPH is bound to the *re* side of the isoalloxazine ring of FAD and a charge-transfer complex (CTC) of $FADH^-$-$NADP^+$ is produced (EH_2^A in Scheme 1.1). $FADH^-$ passes reducing equivalents to an N-terminal

redox-active disulfide (Cys-57 and Cys-62) that is on the *si* side of the isoalloxazine ring of FAD, and the thiolate-FAD CTC involving Cys-62 is produced (EH_2^B in Scheme 1.1). The reducing equivalents interchange between the nascent N-terminal dithiol and the C-terminal disulfide (Cys-489' and Cys-490') (EH_2^B and EH_2^D). Subsequently, a second NADPH molecule reduces EH_2 to produce 4-electron reduced enzyme (EH_4). EH_4^A is converted to EH_4^B and $NADP^+$ dissociates (EH_4^C) to complete the reductive half-reaction. In the oxidative half-reaction the nascent C-terminal dithiol interchanges with the disulfide of Trx to return the enzyme to the EH_2 state. Thus, the enzyme cycles between EH_2 and EH_4 in the catalysis (*93, 144*).

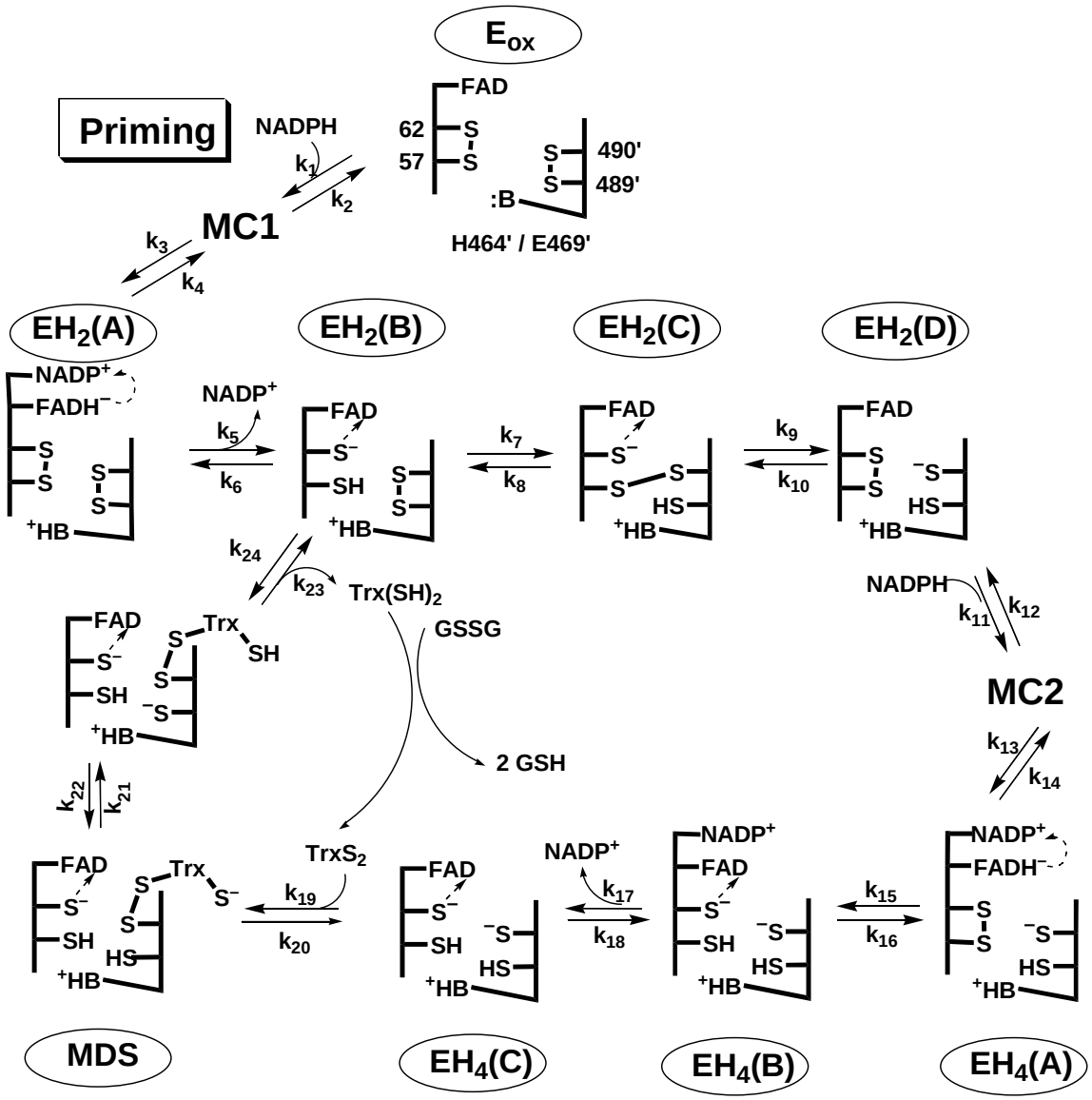

Scheme 1.1 The proposed catalytic mechanism of wild-type DmTrxR. The reductive half- reaction involves the steps denoted by rate constants, k_1-k_{18} and the oxidative half-reaction involves the steps k_{19}-k_{24}. MC, Michaelis complex; MDS, mixed disulfide. Residues numbered without a prime come from one monomer and those with a prime come from the other monomer.

As the catalytic mechanism for DmTrxR as shown in Scheme 1.1 implies, two dithiol-disulfide interchange reactions are involved in the catalysis of DmTrxR. Thiol groups are chemically inactive species (*148*). Thus, formation of a reactive thiolate anion is required to initiate the interchange reaction. However, the pK_a value of a thiol group in aqueous solution is approximately 8.3, which is considerably above physiological pH (*148*). The protein milieu is needed to lower the pK_a value of the thiol to facilitate the reaction. A glutamate-histidine dyad is the acid-base catalyst in other members of the same family such as GR and lipoamide dehydrogenase (*149-151*). The alignment of amino acid sequences of high M_r TrxRs shows that histidine and glutamate residues are conserved among the TrxRs from different species (*93*). Therefore, the dyad is proposed to act as an acid-base catalyst of TrxRs.

The analogous dyad (His-509' and Glu-514') in PfTrxR has been shown to be essential in catalysis, and theoretical calculations showed that the function of the dyad is important in human TrxR (*93, 152, 153*). In studies described in this dissertation, the functions of the dyad of His-464'and Glu-469' in the catalytic mechanism of DmTrxR were investigated.

a. The function of the histidine residue in the catalytic mechanism

In GR, a histidine residue in the active site is able to facilitate the formation of a thiolate anion by acting as a base catalyst, and by stabilizing the thiolate anion as an ion pair between thiolate and the imidazolium ion. In addition, it also is capable of serving as a donor to protonate the thiolate of glutathione to prevent the back reaction (*154, 155*). In lipoamide dehydrogenase, a histidine residue also acts as an acid-base catalyst (*156*).

However, an aspartate residue rather than a histidine residue is involved in the catalytic mechanism of low M_r, *E. coli* TrxR (*126*). It has been shown in PfTrxR that the analogous histidine residue (His-509') is involved in the reductive and oxidative half reactions (*93*). Thus, His-464' is proposed to act as an acid-base catalyst in the catalytic mechanism of DmTrxR. Details of the functions of the histidine residue in human TrxR have been a matter of dispute: Brandt *et al.* suggested that the catalytic triad of asparate-histidine-selenocysteine is essential to stabilize a selenolate in human TrxR (*152*), whereas Eckenroth *et al*. showed that it was unlikely that selenocysteine could interact with the histidine residue because of structural restrictions in human TrxR (*133*).

b. The function of glutamate residue in the catalytic mechanism

The triad of serine, histidine and aspartate has been observed in the putative active site of the serine proteases (*157-159*). The catalytic triad of Ser-195, His-57 and Asp-102 has been extensively studied in chymotrypsin. Initially, Asp-102 was thought to be involved in a charge-relay system with His-57 to convert a weakly nucleophilic $-CH_2OH$ group on Ser195 to a more reactive alkoxide ion, $-CH_2O^-$. The charge-relay was later found to be unlikely because the pK_a value of the histidine residue is higher than that of the glutamate residue (*157*). The emerging NMR data suggested that a low barrier hydrogen bond (LBHB) is involved in the catalytic mechanism (*158*).

In serine proteases, a weak hydrogen bond is formed between Asp-102 and His-57 in the ground state where the distance between these two amino acid residues is 3.3 Å (*160*). In the transition state, the formation of a LBHB between these two amino acid residues can lower the activation barrier of the reaction. During the catalysis by serine

proteases, the LBHB is formed when the pK_a values of the hydrogen donor and acceptor are closely matched and the distance between Asp-102 and His-57 is less than the sum of van der Waals radii, i.e., the distance must be less than 2.65 Å (*158, 161*). It was thought that the formation of a LBHB is unlikely in water: a nearby water molecule can form a hydrogen bond with the hydrogen acceptor and/or the hydrogen donor, leading to the failure of the formation of a LBHB (*158*). However, recently, it has been suggested on the basis of theroretical calculations that LBHBs can exist in water (*161*). The formation of a LBHB can also be favorable in a hydrophobic environment. The strength of a LBHB is dependent on how closely the pK_a values of a hydrogen acceptor and donor are matched (*161*). The pK_a values of two amino acid residues of a dyad might be nearly identical during catalysis in a hydrophobic environment (*162*). The free energy of a normal hydrogen bond is approximately 2.4 to 12 kJ/mol, whereas the free energy of a LBHB is 12-24 kJ/mol (*158*). Thus, it is clear that the formation of an LBHB is able to stabilize an intermediate species during the catalysis of chymotrypsin. Nevertheless, the LBHB mechanism is still contentious (*163*).

A histidine residue is capable of facilitating catalysis in enzymes in the absence of an adjacent acidic amino acid. His-176 in glyceraldehyde-3-phosphate dehydrogenase has been shown to act as a base catalyst for Cys-149 and to stabilize the thiolate anion on Cys-149 by the formation of an ion pair (*164, 165*). A hydrogen bond forming between the essential histidine residue with the hydroxyl group from a threonine (or a serine) residue is able to fix the orientation of the histidine residue, allowing the histidine to be correctly juxtaposed to the sulphur atom of Cys-149 (*166*). However, there is no acidic amino acid (e.g., glutamate or asparate) adjacent to the histidine residue in this enzyme,

showing that a histidine residue is able to facilitate the catalysis in absence of an acidic amino acid residue.

The functions of a glutamate residue in the family of pyridine nucleotide-disulfide oxidoreductases have barely been studied. The structure of GR shows a distance of only 2.8 Å between the glutamate and histidine residues (*149*). The kinetic, spectroscopic and catalytic properties of the glutamate variants of lipoamide dahydrogenase from *Azotobacter vinelandii* have been explored briefly (*150, 151*). The activities of E455'D and E455'Q lipoamide dehydrogenases from *Azotobacter vinelandii*, in which Glu-455' is replaced by Asp and Gln, respectively, are 1.6% and 1.3% that of wild-type enzyme, respectively, when the NAD^+ analog, 3-acetylpyridine-adenine-dinucleotide, was used as the acceptor (*151*). This NAD analog has a considerably higher redox potential than NAD, and therefore is a better electron acceptor. The glutamate residue in that lipoamide dehydrogenase has also been shown to affect the acid-base properties of the histidine residue and to help the orientation of the histidine residue (*150, 151*). The glutamate variant of PfTrxR showed slower rates in the reductive and oxidative half-reactions relative to wild-type enzyme, indicating the glutamate residue makes the histidine residue a better catalyst (*93*).

In DmTrxR, as shown in Fig. 1.2, the distance between the oxygen atom of Glu-469' and the nitrogen atom of His-464' is 2.8 Å (*133*). The active site of DmTrxR is in a hydrophobic environment. This made it important to study the role of Glu-469' in the catalysis of DmTrxR in detail.

In the studies described in this thesis, the roles of His-464' and Glu-469' in the catalysis of DmTrxR were explored. In Chapter 2, we compared the kinetic,

spectroscopic, and catalytic properties of wild-type and H464'Q DmTrxR, in which His-464' is replaced by Gln, to investigate the function of His-464' in the acid-base catalysis of DmTrxR. Because thiolate formation is pH dependent, the pH effect on these biochemical properties of wild-type and H464'Q DmTrxR were also compared. In Chapter 3, E469'Q and E469'A DmTrxR, in which Glu-469' is replaced by Gln and Ala, respectively, were studied kinetically, spectroscopically, and in terms of their catalytic properties to develop a better understanding of the function of Glu-469' in the acid-base catalyst of DmTrxR.

References

1. Laurent, T. C., Moore, E. C., and Reichard, P. (1964) Enzymatic Synthesis of Deoxyribonucleotides. Iv. Isolation and Characterization of Thioredoxin, the Hydrogen Donor from Escherichia Coli B, *J Biol Chem 239*, 3436-3444.
2. Asahi, T., Bandurski, R. S., and Wilson, L. G. (1961) Yeast sulfate-reducing system. II. Enzymatic reduction of protein disulfide, *J Biol Chem 236*, 1830-1835.
3. Gonzalez Porque, P., Baldesten, A., and Reichard, P. (1970) Purification of a thioredoxin system from yeast, *J Biol Chem 245*, 2363-2370.
4. Holmgren, A. (1985) Thioredoxin, *Annu Rev Biochem 54*, 237-271.
5. Powis, G., Mustacich, D., and Coon, A. (2000) The role of the redox protein thioredoxin in cell growth and cancer, *Free Radic Biol Med 29*, 312-322.
6. Gromer, S., Urig, S., and Becker, K. (2004) The thioredoxin system--from science to clinic, *Med Res Rev 24*, 40-89.
7. Watson, W. H., Yang, X., Choi, Y. E., Jones, D. P., and Kehrer, J. P. (2004) Thioredoxin and its role in toxicology, *Toxicol Sci 78*, 3-14.
8. Schenk, H., Klein, M., Erdbrugger, W., Droge, W., and Schulze-Osthoff, K. (1994) Distinct effects of thioredoxin and antioxidants on the activation of transcription factors NF-kappa B and AP-1, *Proc Natl Acad Sci U S A 91*, 1672-1676.
9. Hirota, K., Matsui, M., Iwata, S., Nishiyama, A., Mori, K., and Yodoi, J. (1997) AP-1 transcriptional activity is regulated by a direct association between thioredoxin and Ref-1, *Proc Natl Acad Sci U S A 94*, 3633-3638.
10. Ueno, M., Masutani, H., Arai, R. J., Yamauchi, A., Hirota, K., Sakai, T., Inamoto, T., Yamaoka, Y., Yodoi, J., and Nikaido, T. (1999) Thioredoxin-dependent redox regulation of p53-mediated p21 activation, *J Biol Chem 274*, 35809-35815.
11. Saitoh, M., Nishitoh, H., Fujii, M., Takeda, K., Tobiume, K., Sawada, Y., Kawabata, M., Miyazono, K., and Ichijo, H. (1998) Mammalian thioredoxin is a direct inhibitor of apoptosis signal-regulating kinase (ASK) 1, *Embo J 17*, 2596-2606.
12. Lillig, C. H., and Holmgren, A. (2007) Thioredoxin and related molecules--from biology to health and disease, *Antioxid Redox Signal 9*, 25-47.
13. Bondareva, A. A., Capecchi, M. R., Iverson, S. V., Li, Y., Lopez, N. I., Lucas, O., Merrill, G. F., Prigge, J. R., Siders, A. M., Wakamiya, M., Wallin, S. L., and Schmidt, E. E. (2007) Effects of thioredoxin reductase-1 deletion on embryogenesis and transcriptome, *Free Radic Biol Med 43*, 911-923.
14. Conrad, M., Jakupoglu, C., Moreno, S. G., Lippl, S., Banjac, A., Schneider, M., Beck, H., Hatzopoulos, A. K., Just, U., Sinowatz, F., Schmahl, W., Chien, K. R., Wurst, W., Bornkamm, G. W., and Brielmeier, M. (2004) Essential role for mitochondrial thioredoxin reductase in hematopoiesis, heart development, and heart function, *Mol Cell Biol 24*, 9414-9423.
15. Su, D., Novoselov, S. V., Sun, Q. A., Moustafa, M. E., Zhou, Y., Oko, R., Hatfield, D. L., and Gladyshev, V. N. (2005) Mammalian selenoprotein thioredoxin-glutathione reductase. Roles in disulfide bond formation and sperm maturation, *J Biol Chem 280*, 26491-26498.

16. Fernando, M. R., Nanri, H., Yoshitake, S., Nagata-Kuno, K., and Minakami, S. (1992) Thioredoxin regenerates proteins inactivated by oxidative stress in endothelial cells, *Eur J Biochem 209*, 917-922.
17. Chae, H. Z., Chung, S. J., and Rhee, S. G. (1994) Thioredoxin-dependent peroxide reductase from yeast, *J Biol Chem 269*, 27670-27678.
18. Becker, K., Gromer, S., Schirmer, R. H., and Muller, S. (2000) Thioredoxin reductase as a pathophysiological factor and drug target, *Eur J Biochem 267*, 6118-6125.
19. Mustacich, D., and Powis, G. (2000) Thioredoxin reductase, *Biochem J 346 Pt 1*, 1-8.
20. Cenas, N., Nivinskas, H., Anusevicius, Z., Sarlauskas, J., Lederer, F., and Arner, E. S. (2004) Interactions of quinones with thioredoxin reductase: a challenge to the antioxidant role of the mammalian selenoprotein, *J Biol Chem 279*, 2583-2592.
21. Gromer, S., and Gross, J. H. (2002) Methylseleninate is a substrate rather than an inhibitor of mammalian thioredoxin reductase. Implications for the antitumor effects of selenium, *J Biol Chem 277*, 9701-9706.
22. Nordberg, J., and Arner, E. S. (2001) Reactive oxygen species, antioxidants, and the mammalian thioredoxin system, *Free Radic Biol Med 31*, 1287-1312.
23. Williams, C. H., Jr. (2000) Thioredoxin-thioredoxin reductase--a system that has come of age, *Eur J Biochem 267*, 6101.
24. Moore, E. C., and Reichard, P. (1964) Enzymatic Synthesis of Deoxyribonucleotides. Vi. the Cytidine Diphosphate Reductase System from Novikoff Hepatoma, *J Biol Chem 239*, 3453-3456.
25. Gonzalez Porque, P., Baldesten, A., and Reichard, P. (1970) The involvement of the thioredoxin system in the reduction of methionine sulfoxide and sulfate, *J Biol Chem 245*, 2371-2374.
26. Wakasugi, N., Tagaya, Y., Wakasugi, H., Mitsui, A., Maeda, M., Yodoi, J., and Tursz, T. (1990) Adult T-cell leukemia-derived factor/thioredoxin, produced by both human T-lymphotropic virus type I- and Epstein-Barr virus-transformed lymphocytes, acts as an autocrine growth factor and synergizes with interleukin 1 and interleukin 2, *Proc Natl Acad Sci U S A 87*, 8282-8286.
27. Schenk, H., Vogt, M., Droge, W., and Schulze-Osthoff, K. (1996) Thioredoxin as a potent costimulus of cytokine expression, *J Immunol 156*, 765-771.
28. Bertini, R., Howard, O. M., Dong, H. F., Oppenheim, J. J., Bizzarri, C., Sergi, R., Caselli, G., Pagliei, S., Romines, B., Wilshire, J. A., Mengozzi, M., Nakamura, H., Yodoi, J., Pekkari, K., Gurunath, R., Holmgren, A., Herzenberg, L. A., Herzenberg, L. A., and Ghezzi, P. (1999) Thioredoxin, a redox enzyme released in infection and inflammation, is a unique chemoattractant for neutrophils, monocytes, and T cells, *J Exp Med 189*, 1783-1789.
29. Silberstein, D. S., McDonough, S., Minkoff, M. S., and Balcewicz-Sablinska, M. K. (1993) Human eosinophil cytotoxicity-enhancing factor. Eosinophil-stimulating and dithiol reductase activities of biosynthetic (recombinant) species with COOH-terminal deletions, *J Biol Chem 268*, 9138-9142.
30. Pekkari, K., and Holmgren, A. (2004) Truncated thioredoxin: physiological functions and mechanism, *Antioxid Redox Signal 6*, 53-61.

31. Hayashi, S., Hajiro-Nakanishi, K., Makino, Y., Eguchi, H., Yodoi, J., and Tanaka, H. (1997) Functional modulation of estrogen receptor by redox state with reference to thioredoxin as a mediator, *Nucleic Acids Res 25*, 4035-4040.
32. Yodoi, J., Masutani, H., and Nakamura, H. (2001) Redox regulation by the human thioredoxin system, *Biofactors 15*, 107-111.
33. Nguyen, P., Awwad, R. T., Smart, D. D., Spitz, D. R., and Gius, D. (2006) Thioredoxin reductase as a novel molecular target for cancer therapy, *Cancer Lett 236*, 164-174.
34. Berndt, C., Lillig, C. H., and Holmgren, A. (2007) Thiol-based mechanisms of the thioredoxin and glutaredoxin systems: implications for diseases in the cardiovascular system, *Am J Physiol Heart Circ Physiol 292*, H1227-1236.
35. Hayashi, T., Ueno, Y., and Okamoto, T. (1993) Oxidoreductive regulation of nuclear factor kappa B. Involvement of a cellular reducing catalyst thioredoxin, *J Biol Chem 268*, 11380-11388.
36. Hirota, K., Murata, M., Sachi, Y., Nakamura, H., Takeuchi, J., Mori, K., and Yodoi, J. (1999) Distinct roles of thioredoxin in the cytoplasm and in the nucleus. A two-step mechanism of redox regulation of transcription factor NF-kappaB, *J Biol Chem 274*, 27891-27897.
37. Kabe, Y., Ando, K., Hirao, S., Yoshida, M., and Handa, H. (2005) Redox regulation of NF-kappaB activation: distinct redox regulation between the cytoplasm and the nucleus, *Antioxid Redox Signal 7*, 395-403.
38. Nakamura, H., Nakamura, K., and Yodoi, J. (1997) Redox regulation of cellular activation, *Annu Rev Immunol 15*, 351-369.
39. Diamond, D. A., Parsian, A., Hunt, C. R., Lofgren, S., Spitz, D. R., Goswami, P. C., and Gius, D. (1999) Redox factor-1 (Ref-1) mediates the activation of AP-1 in HeLa and NIH 3T3 cells in response to heat shock, *J Biol Chem 274*, 16959-16964.
40. Grippo, J. F., Holmgren, A., and Pratt, W. B. (1985) Proof that the endogenous, heat-stable glucocorticoid receptor-activating factor is thioredoxin, *J Biol Chem 260*, 93-97.
41. Makino, Y., Okamoto, K., Yoshikawa, N., Aoshima, M., Hirota, K., Yodoi, J., Umesono, K., Makino, I., and Tanaka, H. (1996) Thioredoxin: a redox-regulating cellular cofactor for glucocorticoid hormone action. Cross talk between endocrine control of stress response and cellular antioxidant defense system, *J Clin Invest 98*, 2469-2477.
42. Ichijo, H., Nishida, E., Irie, K., ten Dijke, P., Saitoh, M., Moriguchi, T., Takagi, M., Matsumoto, K., Miyazono, K., and Gotoh, Y. (1997) Induction of apoptosis by ASK1, a mammalian MAPKKK that activates SAPK/JNK and p38 signaling pathways, *Science 275*, 90-94.
43. Fujino, G., Noguchi, T., Takeda, K., and Ichijo, H. (2006) Thioredoxin and protein kinases in redox signaling, *Semin Cancer Biol 16*, 427-435.
44. Patenaude, A., Ven Murthy, M. R., and Mirault, M. E. (2004) Mitochondrial thioredoxin system: effects of TrxR2 overexpression on redox balance, cell growth, and apoptosis, *J Biol Chem 279*, 27302-27314.
45. Tanaka, T., Hosoi, F., Yamaguchi-Iwai, Y., Nakamura, H., Masutani, H., Ueda, S., Nishiyama, A., Takeda, S., Wada, H., Spyrou, G., and Yodoi, J. (2002)

Thioredoxin-2 (TRX-2) is an essential gene regulating mitochondria-dependent apoptosis, *Embo J 21*, 1695-1703.
46. Damdimopoulos, A. E., Miranda-Vizuete, A., Pelto-Huikko, M., Gustafsson, J. A., and Spyrou, G. (2002) Human mitochondrial thioredoxin. Involvement in mitochondrial membrane potential and cell death, *J Biol Chem 277*, 33249-33257.
47. Zhang, H., Go, Y. M., and Jones, D. P. (2007) Mitochondrial thioredoxin-2/peroxiredoxin-3 system functions in parallel with mitochondrial GSH system in protection against oxidative stress, *Arch Biochem Biophys 465*, 119-126.
48. Rigobello, M. P., Callegaro, M. T., Barzon, E., Benetti, M., and Bindoli, A. (1998) Purification of mitochondrial thioredoxin reductase and its involvement in the redox regulation of membrane permeability, *Free Radic Biol Med 24*, 370-376.
49. Marks, P. A. (2006) Thioredoxin in cancer--role of histone deacetylase inhibitors, *Semin Cancer Biol 16*, 436-443.
50. Kaimul, A. M., Nakamura, H., Masutani, H., and Yodoi, J. (2007) Thioredoxin and thioredoxin-binding protein-2 in cancer and metabolic syndrome, *Free Radic Biol Med 43*, 861-868.
51. Engman, L., McNaughton, M., Gajewska, M., Kumar, S., Birmingham, A., and Powis, G. (2006) Thioredoxin reductase and cancer cell growth inhibition by organogold(III) compounds, *Anticancer Drugs 17*, 539-544.
52. Urig, S., and Becker, K. (2006) On the potential of thioredoxin reductase inhibitors for cancer therapy, *Semin Cancer Biol 16*, 452-465.
53. Lu, J., Chew, E. H., and Holmgren, A. (2007) Targeting thioredoxin reductase is a basis for cancer therapy by arsenic trioxide, *Proc Natl Acad Sci U S A 104*, 12288-12293.
54. Marzano, C., Gandin, V., Folda, A., Scutari, G., Bindoli, A., and Rigobello, M. P. (2007) Inhibition of thioredoxin reductase by auranofin induces apoptosis in cisplatin-resistant human ovarian cancer cells, *Free Radic Biol Med 42*, 872-881.
55. Lemarechal, H., Anract, P., Beaudeux, J. L., Bonnefont-Rousselot, D., Ekindjian, O. G., and Borderie, D. (2007) Impairment of thioredoxin reductase activity by oxidative stress in human rheumatoid synoviocytes, *Free Radic Res 41*, 688-698.
56. Lemarechal, H., Anract, P., Beaudeux, J. L., Bonnefont-Rousselot, D., Ekindjian, O. G., and Borderie, D. (2007) Expression and extracellular release of Trx80, the truncated form of thioredoxin, by TNF-alpha- and IL-1beta-stimulated human synoviocytes from patients with rheumatoid arthritis, *Clin Sci (Lond) 113*, 149-155.
57. Jikimoto, T., Nishikubo, Y., Koshiba, M., Kanagawa, S., Morinobu, S., Morinobu, A., Saura, R., Mizuno, K., Kondo, S., Toyokuni, S., Nakamura, H., Yodoi, J., and Kumagai, S. (2002) Thioredoxin as a biomarker for oxidative stress in patients with rheumatoid arthritis, *Mol Immunol 38*, 765-772.
58. Maurice, M. M., Nakamura, H., Gringhuis, S., Okamoto, T., Yoshida, S., Kullmann, F., Lechner, S., van der Voort, E. A., Leow, A., Versendaal, J., Muller-Ladner, U., Yodoi, J., Tak, P. P., Breedveld, F. C., and Verweij, C. L. (1999) Expression of the thioredoxin-thioredoxin reductase system in the inflamed joints of patients with rheumatoid arthritis, *Arthritis Rheum 42*, 2430-2439.

59. Kerimova, A. A., Atalay, M., Yusifov, E. Y., Kuprin, S. P., and Kerimov, T. M. (2000) Antioxidant enzymes; possible mechanism of gold compound treatment in rheumatoid arthritis, *Pathophysiology 7*, 209-213.
60. Okuda, M., Inoue, N., Azumi, H., Seno, T., Sumi, Y., Hirata, K., Kawashima, S., Hayashi, Y., Itoh, H., Yodoi, J., and Yokoyama, M. (2001) Expression of glutaredoxin in human coronary arteries: its potential role in antioxidant protection against atherosclerosis, *Arterioscler Thromb Vasc Biol 21*, 1483-1487.
61. World, C. J., Yamawaki, H., and Berk, B. C. (2006) Thioredoxin in the cardiovascular system, *J Mol Med 84*, 997-1003.
62. Shioji, K., Nakamura, H., Masutani, H., and Yodoi, J. (2003) Redox regulation by thioredoxin in cardiovascular diseases, *Antioxid Redox Signal 5*, 795-802.
63. Nakamura, H. (2005) Thioredoxin and its related molecules: update 2005, *Antioxid Redox Signal 7*, 823-828.
64. Masutani, H., Ueda, S., and Yodoi, J. (2005) The thioredoxin system in retroviral infection and apoptosis, *Cell Death Differ 12 Suppl 1*, 991-998.
65. Nakamura, H., De Rosa, S. C., Yodoi, J., Holmgren, A., Ghezzi, P., Herzenberg, L. A., and Herzenberg, L. A. (2001) Chronic elevation of plasma thioredoxin: inhibition of chemotaxis and curtailment of life expectancy in AIDS, *Proc Natl Acad Sci U S A 98*, 2688-2693.
66. Powis, G., and Montfort, W. R. (2001) Properties and biological activities of thioredoxins, *Annu Rev Pharmacol Toxicol 41*, 261-295.
67. Aota, M., Matsuda, K., Isowa, N., Wada, H., Yodoi, J., and Ban, T. (1996) Protection against reperfusion-induced arrhythmias by human thioredoxin, *J Cardiovasc Pharmacol 27*, 727-732.
68. Okubo, K., Kosaka, S., Isowa, N., Hirata, T., Hitomi, S., Yodoi, J., Nakano, M., and Wada, H. (1997) Amelioration of ischemia-reperfusion injury by human thioredoxin in rabbit lung, *J Thorac Cardiovasc Surg 113*, 1-9.
69. Hattori, I., Takagi, Y., Nakamura, H., Nozaki, K., Bai, J., Kondo, N., Sugino, T., Nishimura, M., Hashimoto, N., and Yodoi, J. (2004) Intravenous administration of thioredoxin decreases brain damage following transient focal cerebral ischemia in mice, *Antioxid Redox Signal 6*, 81-87.
70. Schafer, F. Q., and Buettner, G. R. (2001) Redox environment of the cell as viewed through the redox state of the glutathione disulfide/glutathione couple, *Free Radic Biol Med 30*, 1191-1212.
71. Arrigo, A. P. (1999) Gene expression and the thiol redox state, *Free Radic Biol Med 27*, 936-944.
72. Valko, M., Leibfritz, D., Moncol, J., Cronin, M. T., Mazur, M., and Telser, J. (2007) Free radicals and antioxidants in normal physiological functions and human disease, *Int J Biochem Cell Biol 39*, 44-84.
73. Thannickal, V. J., and Fanburg, B. L. (2000) Reactive oxygen species in cell signaling, *Am J Physiol Lung Cell Mol Physiol 279*, L1005-1028.
74. Seifried, H. E., Anderson, D. E., Fisher, E. I., and Milner, J. A. (2007) A review of the interaction among dietary antioxidants and reactive oxygen species, *J Nutr Biochem 18*, 567-579.
75. Massey, V. (1994) Activation of molecular oxygen by flavins and flavoproteins, *J Biol Chem 269*, 22459-22462.

76. Valko, M., Rhodes, C. J., Moncol, J., Izakovic, M., and Mazur, M. (2006) Free radicals, metals and antioxidants in oxidative stress-induced cancer, *Chem Biol Interact 160*, 1-40.
77. Govers, R., and Oess, S. (2004) To NO or not to NO: 'where?' is the question, *Histol Histopathol 19*, 585-605.
78. Marnett, L. J. (2000) Oxyradicals and DNA damage, *Carcinogenesis 21*, 361-370.
79. Carr, A. C., McCall, M. R., and Frei, B. (2000) Oxidation of LDL by myeloperoxidase and reactive nitrogen species: reaction pathways and antioxidant protection, *Arterioscler Thromb Vasc Biol 20*, 1716-1723.
80. Holmgren, A. (1989) Thioredoxin and glutaredoxin systems, *J Biol Chem 264*, 13963-13966.
81. Cheng, Z., Arscott, L. D., Ballou, D. P., and Williams, C. H., Jr. (2007) The relationship of the redox potentials of thioredoxin and thioredoxin reductase from Drosophila melanogaster to the enzymatic mechanism: reduced thioredoxin is the reductant of glutathione in Drosophila, *Biochemistry 46*, 7875-7885.
82. Lin, A., and Karin, M. (2003) NF-kappaB in cancer: a marked target, *Semin Cancer Biol 13*, 107-114.
83. Dalton, T. P., Shertzer, H. G., and Puga, A. (1999) Regulation of gene expression by reactive oxygen, *Annu Rev Pharmacol Toxicol 39*, 67-101.
84. Lane, D. P. (1992) Cancer. p53, guardian of the genome, *Nature 358*, 15-16.
85. Gon, Y., Sasada, T., Matsui, M., Hashimoto, S., Takagi, Y., Iwata, S., Wada, H., Horie, T., and Yodoi, J. (2001) Expression of thioredoxin in bleomycin-injured airway epithelium: possible role of protection against bleomycin induced epithelial injury, *Life Sci 68*, 1877-1888.
86. Zhang, P., Liu, B., Kang, S. W., Seo, M. S., Rhee, S. G., and Obeid, L. M. (1997) Thioredoxin peroxidase is a novel inhibitor of apoptosis with a mechanism distinct from that of Bcl-2, *J Biol Chem 272*, 30615-30618.
87. Watson, W. H., and Jones, D. P. (2003) Oxidation of nuclear thioredoxin during oxidative stress, *FEBS Lett 543*, 144-147.
88. Kanzok, S. M., Schirmer, R. H., Turbachova, I., Iozef, R., and Becker, K. (2000) The thioredoxin system of the malaria parasite Plasmodium falciparum. Glutathione reduction revisited, *J Biol Chem 275*, 40180-40186.
89. Kanzok, S. M., Fechner, A., Bauer, H., Ulschmid, J. K., Muller, H. M., Botella-Munoz, J., Schneuwly, S., Schirmer, R., and Becker, K. (2001) Substitution of the thioredoxin system for glutathione reductase in Drosophila melanogaster, *Science 291*, 643-646.
90. Casagrande, S., Bonetto, V., Fratelli, M., Gianazza, E., Eberini, I., Massignan, T., Salmona, M., Chang, G., Holmgren, A., and Ghezzi, P. (2002) Glutathionylation of human thioredoxin: a possible crosstalk between the glutathione and thioredoxin systems, *Proc Natl Acad Sci U S A 99*, 9745-9749.
91. Linares, G. E., and Rodriguez, J. B. (2007) Current status and progresses made in malaria chemotherapy, *Curr Med Chem 14*, 289-314.
92. Mendis, K., Sina, B. J., Marchesini, P., and Carter, R. (2001) The neglected burden of Plasmodium vivax malaria, *Am J Trop Med Hyg 64*, 97-106.
93. McMillan, P. J., Arscott, L. D., Ballou, D. P., Becker, K., Williams, C. H., Jr., and Muller, S. (2006) Identification of acid-base catalytic residues of high-Mr

thioredoxin reductase from Plasmodium falciparum, *J Biol Chem 281*, 32967-32977.
94. Kawazu, S. I., Komaki-Yasuda, K., Oku, H., and Kano, S. (2008) Peroxiredoxins in malaria parasites: Parasitologic aspects, *Parasitol Int 57*, 1-7.
95. Clark, I. A., Budd, A. C., Alleva, L. M., and Cowden, W. B. (2006) Human malarial disease: a consequence of inflammatory cytokine release, *Malar J 5*, 85.
96. Ghosh, K., and Ghosh, K. (2007) Pathogenesis of anemia in malaria: a concise review, *Parasitol Res 101*, 1463-1469.
97. Muller, S. (2004) Redox and antioxidant systems of the malaria parasite Plasmodium falciparum, *Mol Microbiol 53*, 1291-1305.
98. Nickel, C., Rahlfs, S., Deponte, M., Koncarevic, S., and Becker, K. (2006) Thioredoxin networks in the malarial parasite Plasmodium falciparum, *Antioxid Redox Signal 8*, 1227-1239.
99. Krnajski, Z., Gilberger, T. W., Walter, R. D., and Muller, S. (2001) The malaria parasite Plasmodium falciparum possesses a functional thioredoxin system, *Mol Biochem Parasitol 112*, 219-228.
100. Ersmark, K., Samuelsson, B., and Hallberg, A. (2006) Plasmepsins as potential targets for new antimalarial therapy, *Med Res Rev 26*, 626-666.
101. Hetz, S. K., and Bradley, T. J. (2005) Insects breathe discontinuously to avoid oxygen toxicity, *Nature 433*, 516-519.
102. Kanzok, S. M., and Zheng, L. (2003) The mosquito genome--a turning point?, *Trends Parasitol 19*, 329-331.
103. Morozova, N., Forry, E. P., Shahid, E., Zavacki, A. M., Harney, J. W., Kraytsberg, Y., and Berry, M. J. (2003) Antioxidant function of a novel selenoprotein in Drosophila melanogaster, *Genes Cells 8*, 963-971.
104. Bauer, H., Gromer, S., Urbani, A., Schnolzer, M., Schirmer, R. H., and Muller, H. M. (2003) Thioredoxin reductase from the malaria mosquito Anopheles gambiae, *Eur J Biochem 270*, 4272-4281.
105. Bauer, H., Kanzok, S. M., and Schirmer, R. H. (2002) Thioredoxin-2 but not thioredoxin-1 is a substrate of thioredoxin peroxidase-1 from Drosophila melanogaster: isolation and characterization of a second thioredoxin in D. Melanogaster and evidence for distinct biological functions of Trx-1 and Trx-2, *J Biol Chem 277*, 17457-17463.
106. Wahl, M. C., Irmler, A., Hecker, B., Schirmer, R. H., and Becker, K. (2005) Comparative structural analysis of oxidized and reduced thioredoxin from Drosophila melanogaster, *J Mol Biol 345*, 1119-1130.
107. Missirlis, F., Ulschmid, J. K., Hirosawa-Takamori, M., Gronke, S., Schafer, U., Becker, K., Phillips, J. P., and Jackle, H. (2002) Mitochondrial and cytoplasmic thioredoxin reductase variants encoded by a single Drosophila gene are both essential for viability, *J Biol Chem 277*, 11521-11526.
108. Chivers, P. T., and Raines, R. T. (1997) General acid/base catalysis in the active site of Escherichia coli thioredoxin, *Biochemistry 36*, 15810-15816.
109. Eklund, H., Gleason, F. K., and Holmgren, A. (1991) Structural and functional relations among thioredoxins of different species, *Proteins 11*, 13-28.

110. Fernandes, A. P., and Holmgren, A. (2004) Glutaredoxins: glutathione-dependent redox enzymes with functions far beyond a simple thioredoxin backup system, *Antioxid Redox Signal 6*, 63-74.
111. Holmgren, A., Soderberg, B. O., Eklund, H., and Branden, C. I. (1975) Three-dimensional structure of Escherichia coli thioredoxin-S2 to 2.8 A resolution, *Proc Natl Acad Sci U S A 72*, 2305-2309.
112. Watson, W. H., Pohl, J., Montfort, W. R., Stuchlik, O., Reed, M. S., Powis, G., and Jones, D. P. (2003) Redox potential of human thioredoxin 1 and identification of a second dithiol/disulfide motif, *J Biol Chem 278*, 33408-33415.
113. Haendeler, J., Hoffmann, J., Tischler, V., Berk, B. C., Zeiher, A. M., and Dimmeler, S. (2002) Redox regulatory and anti-apoptotic functions of thioredoxin depend on S-nitrosylation at cysteine 69, *Nat Cell Biol 4*, 743-749.
114. Rhee, S. G., Kang, S. W., Chang, T. S., Jeong, W., and Kim, K. (2001) Peroxiredoxin, a novel family of peroxidases, *IUBMB Life 52*, 35-41.
115. Rhee, S. G., Chae, H. Z., and Kim, K. (2005) Peroxiredoxins: a historical overview and speculative preview of novel mechanisms and emerging concepts in cell signaling, *Free Radic Biol Med 38*, 1543-1552.
116. Niimura, Y., Poole, L. B., and Massey, V. (1995) Amphibacillus xylanus NADH oxidase and Salmonella typhimurium alkyl-hydroperoxide reductase flavoprotein components show extremely high scavenging activity for both alkyl hydroperoxide and hydrogen peroxide in the presence of S. typhimurium alkyl-hydroperoxide reductase 22-kDa protein component, *J Biol Chem 270*, 25645-25650.
117. Poole, L. B., Reynolds, C. M., Wood, Z. A., Karplus, P. A., Ellis, H. R., and Li Calzi, M. (2000) AhpF and other NADH:peroxiredoxin oxidoreductases, homologues of low Mr thioredoxin reductase, *Eur J Biochem 267*, 6126-6133.
118. Reynolds, C. M., and Poole, L. B. (2001) Activity of one of two engineered heterodimers of AhpF, the NADH:peroxiredoxin oxidoreductase from Salmonella typhimurium, reveals intrasubunit electron transfer between domains, *Biochemistry 40*, 3912-3919.
119. Park, S. G., Cha, M. K., Jeong, W., and Kim, I. H. (2000) Distinct physiological functions of thiol peroxidase isoenzymes in Saccharomyces cerevisiae, *J Biol Chem 275*, 5723-5732.
120. Peskin, A. V., Low, F. M., Paton, L. N., Maghzal, G. J., Hampton, M. B., and Winterbourn, C. C. (2007) The high reactivity of peroxiredoxin 2 with H(2)O(2) is not reflected in its reaction with other oxidants and thiol reagents, *J Biol Chem 282*, 11885-11892.
121. Williams, C. H. (1992) *Lipoamide Dehydrogenase, Glutathione Reductase, Thioredoxin reductase, and Mercuric ion reductase-A family of Flavoenzyme Transhydrogenase*, Vol. 3, CRC press, Inc, Boca Raton. FL.
122. Thelander, L. (1967) Thioredoxin reductase. Characterization of a homogenous preparation from Escherichia coli B, *J Biol Chem 242*, 852-859.
123. Waksman, G., Krishna, T. S., Williams, C. H., Jr., and Kuriyan, J. (1994) Crystal structure of Escherichia coli thioredoxin reductase refined at 2 A resolution. Implications for a large conformational change during catalysis, *J Mol Biol 236*, 800-816.

124. Lennon, B. W., and Williams, C. H., Jr. (1996) Enzyme-monitored turnover of Escherichia coli thioredoxin reductase: insights for catalysis, *Biochemistry 35*, 4704-4712.
125. Lennon, B. W., Williams, C. H., Jr., and Ludwig, M. L. (2000) Twists in catalysis: alternating conformations of Escherichia coli thioredoxin reductase, *Science 289*, 1190-1194.
126. Mulrooney, S. B., and Williams, C. H., Jr. (1994) Potential active-site base of thioredoxin reductase from Escherichia coli: examination of histidine245 and aspartate139 by site-directed mutagenesis, *Biochemistry 33*, 3148-3154.
127. Arscott, L. D., Gromer, S., Schirmer, R. H., Becker, K., and Williams, C. H., Jr. (1997) The mechanism of thioredoxin reductase from human placenta is similar to the mechanisms of lipoamide dehydrogenase and glutathione reductase and is distinct from the mechanism of thioredoxin reductase from Escherichia coli, *Proc Natl Acad Sci U S A 94*, 3621-3626.
128. Sandalova, T., Zhong, L., Lindqvist, Y., Holmgren, A., and Schneider, G. (2001) Three-dimensional structure of a mammalian thioredoxin reductase: implications for mechanism and evolution of a selenocysteine-dependent enzyme, *Proc Natl Acad Sci U S A 98*, 9533-9538.
129. Gromer, S., Johansson, L., Bauer, H., Arscott, L. D., Rauch, S., Ballou, D. P., Williams, C. H., Jr., Schirmer, R. H., and Arner, E. S. (2003) Active sites of thioredoxin reductases: why selenoproteins?, *Proc Natl Acad Sci U S A 100*, 12618-12623.
130. Biterova, E. I., Turanov, A. A., Gladyshev, V. N., and Barycki, J. J. (2005) Crystal structures of oxidized and reduced mitochondrial thioredoxin reductase provide molecular details of the reaction mechanism, *Proc Natl Acad Sci U S A 102*, 15018-15023.
131. Fritz-Wolf, K., Urig, S., and Becker, K. (2007) The structure of human thioredoxin reductase 1 provides insights into C-terminal rearrangements during catalysis, *J Mol Biol 370*, 116-127.
132. Sun, Q. A., Kirnarsky, L., Sherman, S., and Gladyshev, V. N. (2001) Selenoprotein oxidoreductase with specificity for thioredoxin and glutathione systems, *Proc Natl Acad Sci U S A 98*, 3673-3678.
133. Eckenroth, B. E., Rould, M. A., Hondal, R. J., and Everse, S. J. (2007) Structural and biochemical studies reveal differences in the catalytic mechanisms of mammalian and Drosophila melanogaster thioredoxin reductases, *Biochemistry 46*, 4694-4705.
134. Williams, C. H., Arscott, L. D., Muller, S., Lennon, B. W., Ludwig, M. L., Wang, P. F., Veine, D. M., Becker, K., and Schirmer, R. H. (2000) Thioredoxin reductase two modes of catalysis have evolved, *Eur J Biochem 267*, 6110-6117.
135. Gladyshev, V. N., Jeang, K. T., and Stadtman, T. C. (1996) Selenocysteine, identified as the penultimate C-terminal residue in human T-cell thioredoxin reductase, corresponds to TGA in the human placental gene, *Proc Natl Acad Sci U S A 93*, 6146-6151.
136. Gasdaska, P. Y., Berggren, M. M., Berry, M. J., and Powis, G. (1999) Cloning, sequencing and functional expression of a novel human thioredoxin reductase, *FEBS Lett 442*, 105-111.

137. Berry, M. J., Banu, L., Chen, Y. Y., Mandel, S. J., Kieffer, J. D., Harney, J. W., and Larsen, P. R. (1991) Recognition of UGA as a selenocysteine codon in type I deiodinase requires sequences in the 3' untranslated region, *Nature 353*, 273-276.
138. Zhong, L., and Holmgren, A. (2000) Essential role of selenium in the catalytic activities of mammalian thioredoxin reductase revealed by characterization of recombinant enzymes with selenocysteine mutations, *J Biol Chem 275*, 18121-18128.
139. Xia, L., Nordman, T., Olsson, J. M., Damdimopoulos, A., Bjorkhem-Bergman, L., Nalvarte, I., Eriksson, L. C., Arner, E. S., Spyrou, G., and Bjornstedt, M. (2003) The mammalian cytosolic selenoenzyme thioredoxin reductase reduces ubiquinone. A novel mechanism for defense against oxidative stress, *J Biol Chem 278*, 2141-2146.
140. Zhong, L., Arner, E. S., and Holmgren, A. (2000) Structure and mechanism of mammalian thioredoxin reductase: the active site is a redox-active selenolthiol/selenenylsulfide formed from the conserved cysteine-selenocysteine sequence, *Proc Natl Acad Sci U S A 97*, 5854-5859.
141. Gilberger, T. W., Walter, R. D., and Muller, S. (1997) Identification and characterization of the functional amino acids at the active site of the large thioredoxin reductase from Plasmodium falciparum, *J Biol Chem 272*, 29584-29589.
142. Gilberger, T. W., Bergmann, B., Walter, R. D., and Muller, S. (1998) The role of the C-terminus for catalysis of the large thioredoxin reductase from Plasmodium falciparum, *FEBS Lett 425*, 407-410.
143. Sun, Q. A., Su, D., Novoselov, S. V., Carlson, B. A., Hatfield, D. L., and Gladyshev, V. N. (2005) Reaction mechanism and regulation of mammalian thioredoxin/glutathione reductase, *Biochemistry 44*, 14528-14537.
144. Bauer, H., Massey, V., Arscott, L. D., Schirmer, R. H., Ballou, D. P., and Williams, C. H., Jr. (2003) The mechanism of high Mr thioredoxin reductase from Drosophila melanogaster, *J Biol Chem 278*, 33020-33028.
145. Lacey, B. M., and Hondal, R. J. (2006) Characterization of mitochondrial thioredoxin reductase from C. elegans, *Biochem Biophys Res Commun 346*, 629-636.
146. Johansson, L., Arscott, L. D., Ballou, D. P., Williams, C. H., Jr., and Arner, E. S. (2006) Studies of an active site mutant of the selenoprotein thioredoxin reductase: the Ser-Cys-Cys-Ser motif of the insect orthologue is not sufficient to replace the Cys-Sec dyad in the mammalian enzyme, *Free Radic Biol Med 41*, 649-656.
147. Jacob, J., Schirmer, R. H., and Gromer, S. (2005) The conserved histidine 106 of large thioredoxin reductases is likely to have a structural role but not a base catalyst function, *FEBS Lett 579*, 745-748.
148. Huber, R. E., and Criddle, R. S. (1967) Comparison of the chemical properties of selenocysteine and selenocystine with their sulfur analogs, *Arch Biochem Biophys 122*, 164-173.
149. Karplus, P. A., and Schulz, G. E. (1989) Substrate binding and catalysis by glutathione reductase as derived from refined enzyme: substrate crystal structures at 2 A resolution, *J Mol Biol 210*, 163-180.

150. Benen, J., van Berkel, W., Zak, Z., Visser, T., Veeger, C., and de Kok, A. (1991) Lipoamide dehydrogenase from Azotobacter vinelandii: site-directed mutagenesis of the His450-Glu455 diad. Spectral properties of wild type and mutated enzymes, *Eur J Biochem 202*, 863-872.
151. Benen, J., van Berkel, W., Dieteren, N., Arscott, D., Williams, C., Jr., Veeger, C., and de Kok, A. (1992) Lipoamide dehydrogenase from Azotobacter vinelandii: site-directed mutagenesis of the His450-Glu455 diad. Kinetics of wild-type and mutated enzymes, *Eur J Biochem 207*, 487-497.
152. Brandt, W., and Wessjohann, L. A. (2005) The functional role of selenocysteine (Sec) in the catalysis mechanism of large thioredoxin reductases: proposition of a swapping catalytic triad including a Sec-His-Glu state, *Chembiochem 6*, 386-394.
153. Gromer, S., Wessjohann, L. A., Eubel, J., and Brandt, W. (2006) Mutational studies confirm the catalytic triad in the human selenoenzyme thioredoxin reductase predicted by molecular modeling, *Chembiochem 7*, 1649-1652.
154. Boggaram, V., and Mannervik, B. (1978) An essential histidine residue in the catalytic mechanism of mammalian glutathione reductase, *Biochem Biophys Res Commun 83*, 558-564.
155. Rietveld, P., Arscott, L. D., Berry, A., Scrutton, N. S., Deonarain, M. P., Perham, R. N., and Williams, C. H., Jr. (1994) Reductive and oxidative half-reactions of glutathione reductase from Escherichia coli, *Biochemistry 33*, 13888-13895.
156. Sahlman, L., and Williams, C. H., Jr. (1989) Titration studies on the active sites of pig heart lipoamide dehydrogenase and yeast glutathione reductase as monitored by the charge transfer absorbance, *J Biol Chem 264*, 8033-8038.
157. Craik, C. S., Roczniak, S., Largman, C., and Rutter, W. J. (1987) The catalytic role of the active site aspartic acid in serine proteases, *Science 237*, 909-913.
158. Frey, P. A., Whitt, S. A., and Tobin, J. B. (1994) A low-barrier hydrogen bond in the catalytic triad of serine proteases, *Science 264*, 1927-1930.
159. Tobin, J. B., Whitt, S. A., Cassidy, C. S., and Frey, P. A. (1995) Low-barrier hydrogen bonding in molecular complexes analogous to histidine and aspartate in the catalytic triad of serine proteases, *Biochemistry 34*, 6919-6924.
160. Tsukada, H., and Blow, D. M. (1985) Structure of alpha-chymotrypsin refined at 1.68 A resolution, *J Mol Biol 184*, 703-711.
161. Cleland, W. W. (2000) Low-barrier hydrogen bonds and enzymatic catalysis, *Arch Biochem Biophys 382*, 1-5.
162. Cleland, W. W., Frey, P. A., and Gerlt, J. A. (1998) The low barrier hydrogen bond in enzymatic catalysis, *J Biol Chem 273*, 25529-25532.
163. Warshel, A., Papazyan, A., and Kollman, P. A. (1995) On low-barrier hydrogen bonds and enzyme catalysis, *Science 269*, 102-106.
164. Polgar, L. (1975) Ion-pair formation as a source of enhanced reactivity of the essential thiol group of D-glyceraldehyde-3-phosphate dehydrogenase, *Eur J Biochem 51*, 63-71.
165. Soukri, A., Mougin, A., Corbier, C., Wonacott, A., Branlant, C., and Branlant, G. (1989) Role of the histidine 176 residue in glyceraldehyde-3-phosphate dehydrogenase as probed by site-directed mutagenesis, *Biochemistry 28*, 2586-2592.

166. Skarzynski, T., Moody, P. C., and Wonacott, A. J. (1987) Structure of holo-glyceraldehyde-3-phosphate dehydrogenase from Bacillus stearothermophilus at 1.8 A resolution, *J Mol Biol 193*, 171-187.

Chapter 2: The function of His-464' in acid-base catalysis of thioredoxin reductase from *Drosophila melanogaster*

A. Abstract

Thioredoxin reductase (TrxR) catalyses the reduction of thioredoxin (Trx) by NADPH. Like other members of the pyridine nucleotide-disulfide oxidoreductase enzyme family, the enzyme from *Drosophila melanogaster* is a homodimer, and each catalytically active unit consists of three redox centers: FAD and an N-terminal Cys-57/Cys-62 redox-active disulfide from one monomer, and a Cys-489'/Cys-490' C-terminal redox-active disulfide from the second monomer. Because dipteran insects such as *D. melanogaster* lack glutathione reductase, thioredoxin reductase (DmTrxR) is particularly important; in addition to its normal functions, it also reduces GSSG for antioxidant protection. DmTrxR, used as a model for the enzyme from the malaria vector, *Anopheles gambiae*, has been shown to cycle in catalysis between the two-electron and four-electron reduced states, EH_2 and EH_4 [Bauer et al. (2003) *J. Biol. Chem. 278*, 33020-33028]. His-464' acts as an acid-base catalyst of the dithiol-disulfide interchange reactions required in catalysis. The H464'Q enzyme has only 2% of the wild-type activity, emphasizing the importance of this residue. The pH dependence of V_{max} for wild-type DmTrxR has pK_a values of 6.4 and 9.3 on the DmTrxR-DmTrx-2 complex, whereas H464'Q DmTrxR only has an observable pK_a at 6.4, indicating that the pK_a at pH 9.3 is contributed mainly by His-464'. The pK_a at pH 6.4 has been assigned to Cys-57 and Cys-490'; the thiolate on Cys-490' is the nucleophile in the reduction of Trx. In

contrast to wild-type DmTrxR, H464'Q DmTrxR does not stabilize a thiolate-FAD charge-transfer complex in the presence of excess NADPH. The rates of steps in both the reductive and oxidative half reactions are markedly diminished in H464'Q DmTrxR compared with those of wild-type enzyme, indicating that His-464' is involved in both half reactions.

B. Introduction

Thioredoxin reductase (EC 1.6.4.5) (TrxR) belongs to the family of pyridine nucleotide-disulfide oxidoreductases that includes glutathione reductase (GR), lipoamide dehydrogenase, trypanothione reductase, and mercuric ion reductase (*1, 2*). The enzyme catalyzes the reaction: NADPH + H^+ + $Trx(S)_2$ <=> $NADP^+$ + $Trx(SH)_2$ (*3*). The TrxR/Trx system has been shown to be involved in important physiological functions, such as cell growth, inflammation reactions, and apoptosis. Trx has also been shown to be an anti-apoptotic factor by binding to ASK-1 (*4*). TrxR functions as one of the major antioxidant systems in biology (*5-8*). Reduced thioredoxin ($Trx(SH)_2$) is able to donate reducing equivalents to both ribonucleotide reductase and methionine sulfoxide reductase to enable their catalyses (*9, 10*). Trx is also capable of regulating the DNA-binding activities of several redox-sensitive transcriptional factors, such as NF-κB, AP-1, HIF-1α, the estrogen receptor, the glucocorticoid receptor, and Ref-1 (*11-13*). Moreover, $Trx(SH)_2$, the product of the Trx/TrxR system, is an important antioxidant for reducing reactive oxygen species and providing reducing equivalents to thioredoxin peroxidase to reduce hydrogen peroxide (*14*).

The TrxR/Trx system has been shown to be particularly important in dipteran insects, such as *Drosophila melanogaster* and *Anopheles gambiae*, the vector of tropical malaria, because GR is absent in these organisms (*15, 16*). Thus, to maintain a high ratio of glutathione (GSH) to glutathione disulfide (GSSG) in the cell, $Trx(SH)_2$ is necessary to reduce GSSG nonenzymatically. TrxRs from *D. melanogaster* and *A. gambiae* share 69% similarity and the residues that contribute to the active sites of the two enzymes are virtually identical. Another indication of similarity is the fact that the substrate for the fly

enzyme, DmTrx-2, is a good substrate of TrxR from *A. gambiae* and is used in the present work (*16*). Compared to DmTrx-1, DmTrx-2 is now thought to be the major form of Trx (>50 μM) in *D. melanogaster* (*17*). For these reasons, TrxR from *D. melanogaster* is an excellent model of the catalytic mechanism of the enzyme from *Diptera*.

Two forms of TrxR have been identified: low M_r TrxR with a monomer M_r of ~ 35,000 and high M_r TrxR with a monomer M_r of ~ 55,000 (*2*). Low M_r TrxR exists in prokaryotes, plants, and lower eukaryotes, whereas high M_r TrxR is found in higher eukaryotes. Both forms of TrxR are homodimeric flavoenzymes (*3, 18, 19*). The active site of low M_r TrxR contains an NADPH binding site, a FAD binding site, and one redox-active disulfide (*18, 20, 21*). High M_r TrxR has either an additional redox-active disulfide or a selenenylsulfide formed from conserved cysteine-cysteine or cysteine-selenocysteine dyads in the neighboring subunit (*22-24*). It has been shown that low M_r TrxR and high M_r TrxR have different catalytic mechanisms: in low M_r TrxR, a large conformational change is required to move reducing equivalents from the apolar flavin site to the surface of the protein where Trx binds (*25*); in high M_r TrxR, this transfer is mediated by a second disulfide or selenylsulfide, and any conformational changes required are comparatively small (*22, 26-28*). Comparisons to other members in the family of pyridine nucleotide-disulfide oxidoreductases reveal that the sequence of high M_r TrxR is more homologous to GR and lipoamide dehydrogenase than to low M_r TrxR (*2, 26*). Thus, it is likely that the catalytic mechanism of high M_r TrxR is similar to those of GR and lipoamide dehydrogenase, although somewhat more complicated because of the presence of the required additional redox active group (*22-24, 27*).

The active site of TrxR from *D. melanogaster* (DmTrxR), a high M_r TrxR, contains three redox centers: FAD, an N-terminal disulfide (Cys57-Cys62) adjacent to the flavin, both from one subunit, and a second disulfide (Cys489'-Cys490') penultimate to the C-terminal serine residue from the other subunit (*29*) as shown in Fig. 2.1. The C-terminal polypeptide chain containing Cys-489'and Cys-490' is flexible; it is proposed that it assumes alternate positions, first near His-464', the acid-base catalyst, to form a mixed disulfide between Cys-57 and Cys-490', and then at the protein surface, as shown in Fig. 2.1, in order to react with Trx. A catalytic mechanism for DmTrxR has been proposed (*30*), as shown in Scheme 1. NADPH reduces FAD via hydride transfer. The resulting $FADH^-$ passes reducing equivalents to the adjacent redox-active-disulfide (Cys57-Cys62), which is on the *si* side of the flavin ring, to produce a thiolate-FAD CTC involving Cys-62 (EH_2^B in Scheme 2.1). This nascent dithiol reduces the C-terminal cysteine pair (Cys489'-Cys490') via a dithiol-disulfide interchange reaction. Finally, the resultant reduced C-terminal cysteine pair reduces the disulfide of the substrate, Trx. Most of these intermediate species in catalysis have identifiable spectral properties that were reported in McMillan et al., Table 1 (*31*).

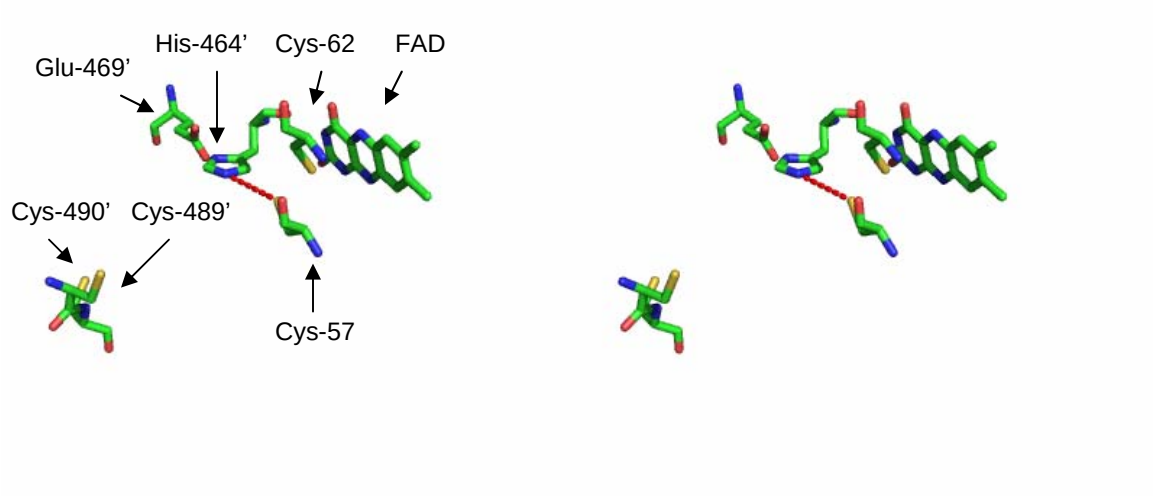

Fig. 2.1 Stereo view showing the relative positions of amino acid residues in the active site of DmTrxR. The active site contains an FAD, an N-terminal redox-active disulfide (Cys-57 and Cys-62), and a C-terminal terminal redox-active disulfide (Cys-489' and Cys-490'). His-464' is adjacent to the N-terminal redox-active disulfide and the distance between NE2 of His-464' and the sulfur atom of Cys-57 is 3.69 Å. PyMol was applied to generate the figure, and the structure used here is based on the structure of rat TrxR (pdb accession code: 1H6V) (*26*).

It has been shown that high M_r TrxR cycles between EH_2 and EH_4 in catalysis (*30, 31*). As implied in Scheme 2.1, to initiate the interchange reaction, deprotonation of Cys-57 to form its thiolate is required for nucleophilic attack on the C-terminal disulfide, similarly to that reported for lipoamide dehydrogenase (*32*). In all members of the pyridine nucleotide-disulfide oxidoreductase family, with the exception of low M_r TrxR, a histidine residue in the active site, and derived from the adjacent subunit, acts as an acid-base catalyst in the dithiol-disulfide interchange (*33-36*). Furthermore, in the high M_r TrxRs from human, *D. melanogaster,* and *Plasmodium falciparum*, analogous histidine residues act as acid-base catalysts to facilitate the interchange reactions between disulfides and dithiols (*29, 31, 37*). Based on the structures of GR and the related TrxRs from rat, mouse, human, and *D. melanogaster*, it is suggested that NE2 of the imidazole

ring of His-464' is close to the interchange thiol (Cys-57) in DmTrxR (*26, 28, 29, 31, 34-36, 38*). Thus, in DmTrxR, it appears that the function of His-464' is to act as the acid-base catalyst for the dithiol-disulfide interchange reactions. In this work, the role of His-464' was examined by measuring the pH dependence of various enzyme properties using steady-state kinetics methods, static NADPH titrations, and stopped-flow spectrophotometric methods to determine the kinetics of the reductive and oxidative half reactions of the enzyme.

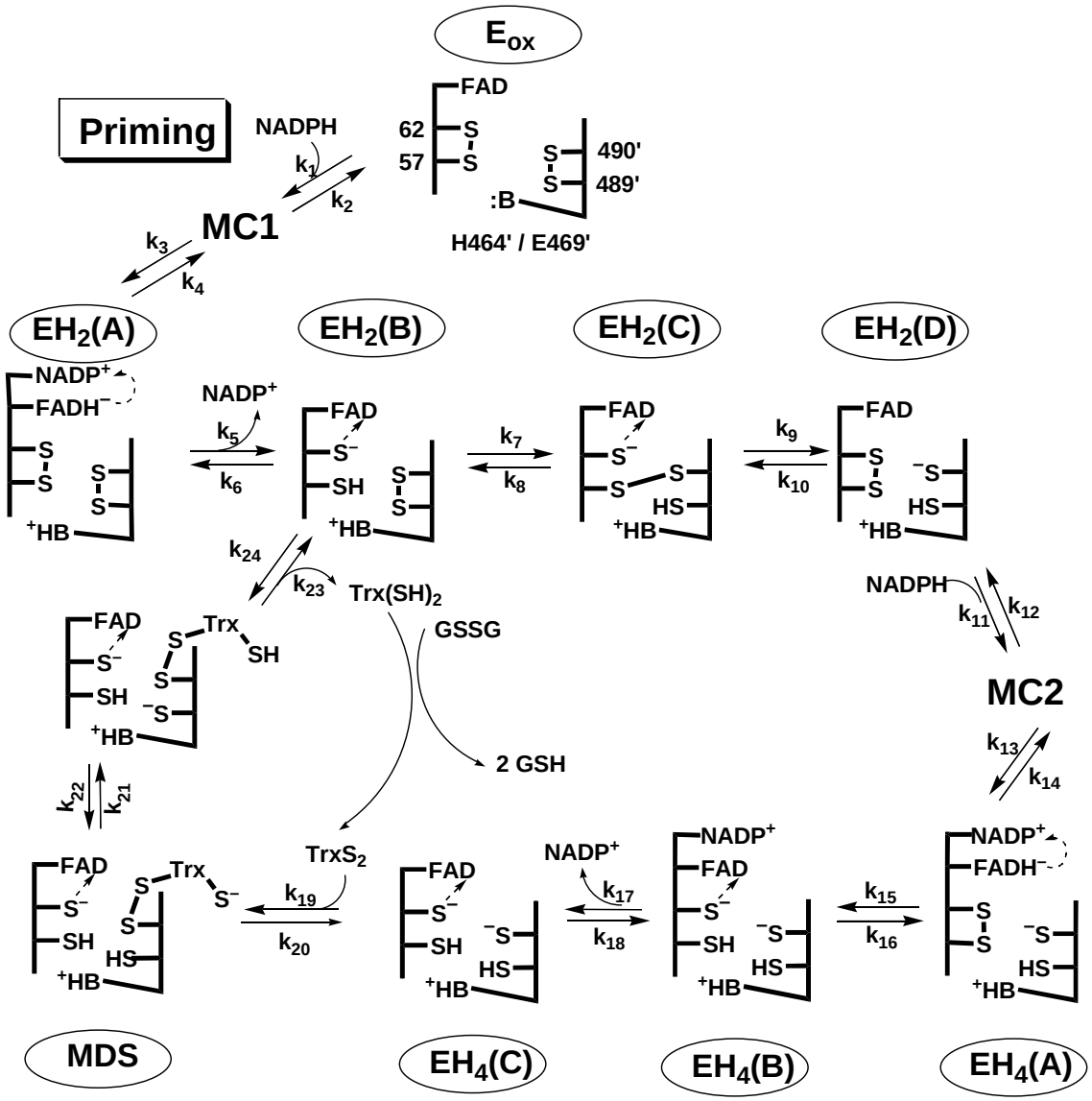

Scheme 2.1 The proposed catalytic mechanism of wild-type DmTrxR. The reductive half- reaction involves the steps denoted by rate constants, k_1-k_{18} and the oxidative half-reaction involves the steps k_{19}-k_{24}. MC, Michaelis complex; MDS, mixed disulfide. Charge transfer is indicated by a dashed arrow. Residues numbered without a prime come from one monomer and those with a prime come from the other monomer. While there is no direct evidence to show that Cys-490' is the nucleophile that attacks the disulfide bond of DmTrx, Cys-490' in DmTrxR occupies the same position as Sec-489' in mammalian TrxR. Because the Sec-489' is believed to initiate nucleophilic attack on Trx, Cys-490' in DmTrxR is thought to be the nucelphile to attack the disulfide bond of DmTrx. Data in Bauer et al. indicate that the S of Cys-490' is attacked by Cys-57 in the step k_7 and that the thiol of Cys-490' initiates the dithiol-disulfide interchange with Trx (*30*).

C. Materials and Methods

1. Chemicals

NADPH, lysozyme, FAD, phenylmethylsulfonyl fluoride, leupeptin, pepstatin, tricine, boric acid, citric acid, and GSSG were purchased from Sigma-Aldrich. Nickel-nitrilotriacetic acid agarose for purification of His-tagged proteins was from QIAGEN. Isopropyl-beta-D-thiogalactopyranoside was supplied by Invitrogen. 4-20% SDS-PAGE gels were purchased from NuSep. All other chemicals and reagents were from Fisher Scientific unless stated.

2. DNA sequencing of wild-type DmTrxR-1 and the histidine mutant

The plasmids containing cDNA for wild-type DmTrxR, H464'Q DmTrxR, and DmTrx-2 were kindly provided by S. Gromer. The cDNA fragments encoding the genes of interest were inserted into the pQE-30 plasmid that allows for expression of N-terminal His-tagged proteins. pQE-30 was obtained from QIAGEN. The sequence of each plasmid was verified by the sequencing core facility at the University of Michigan.

3. Preparation of wild-type DmTrxR-1, the histidine mutant, and DmTrx-2

The preparation methods were similar to those described previously (*15, 17*). Briefly, the bacterial strain, NovaBlue from Novagen, was used for protein expression with induction by isopropyl-beta-D-thiogalactopyranoside. The harvested cells were suspended in 50 mM potassium phosphate, containing 300 mM NaCl and 10 mM imidazole. In the preparation of enzymes, FAD (100 μM) was added to the lysate solution. The bacteria then were treated with lysozyme to weaken the cell walls. The

protease inhibitors, phenylmethylsulfonyl fluoride, leupeptin and pepstatin, were added to the cell lysate, which was then sonicated. The His_6-tagged proteins were applied to a nickel-nitrilotriacetic acid column and eluted by a step-gradient of imidazole. All elution buffers for the preparation of enzymes contained 100 μM FAD. The procedures for isolation of proteins were performed at 4 ºC.. The purity of each fraction of enzyme and of DmTrx-2 was estimated by 4-20% SDS-PAGE. The imidazole in each fraction was removed using a 10-DG desalting column from Bio-Rad to avoid the known instability of these proteins during dialysis. The concentrations of DmTrxR and of the histidine mutants, as well as of DmTrx-2 were determined spectrally using values of ε_{462nm} = 11,900 M^{-1} cm^{-1} for DmTrxRs and ε_{277nm} = 7,320 M^{-1} cm^{-1} for DmTrx-2 (*30, 39*).

4. Determination of the activities of DmTrxR and of the histidine variant

The activities of both wild-type DmTrxR and the histidine variant were measured by rates of consumption of NADPH, monitored at 340 nm in the presence of 100 μM NADPH, 50 μM DmTrx-2, and 0.3 mM GSSG in a universal buffer, pH 7.6 containing 25 mM monobasic phosphate, 25 mM borate, 25 mM tricine and 25 mM citrate (*40*); this buffer mixture does not maintain constant ionic strength. Results were corrected for acid-catalyzed hydrolysis of NADPH; the corrections were significant only in assays of the altered enzyme having low activity.

5. Steady-state kinetics of wild-type DmTrxR and the histidine variant over a range of pH.

The reaction rates of wild-type and H464'Q DmTrxR were determined at different pH values in the universal buffer by following the consumption of NADPH with various concentrations of DmTrx-2 and a fixed concentration of NADPH (100 μM) in the presence of GSSG (0.3 mM). Results were corrected for the acid-catalyzed hydrolysis of NADPH. K_m and V_{max} values were derived from a Michaelis-Menten graph of turnover numbers versus concentration of DmTrx-2 fit to the equation for a rectangular hyperbola. The profiles of pH were fit to equations 1 and 2 to obtain the two pK_a value(s).

$$v = \frac{V_{max}}{\frac{10^{-pH}}{10^{-pK_{a1}}} + 1} \qquad \text{Equation 2.1}$$

$$v = \frac{V_{max}}{\frac{10^{-pH}}{10^{-pK_{a1}}} + \frac{10^{-pK_{a2}}}{10^{-pH}} + 1} \qquad \text{Equation 2.2}$$

6. Titrations of wild-type DmTrxR and the histidine variant with NADPH.

The enzymes were made anaerobic in cuvettes by ~10 cycles of evacuation followed by flushing with purified argon. This procedure was performed on ice to minimize evaporation of the sample. A Hamilton titrating syringe containing an anaerobic solution of NADPH was attached to the cuvette and small aliquots of NADPH were added during the titration. Spectra of enzymes were recorded with a Cary 3 spectrophotometer from Varian after each addition of NADPH.

7. The kinetics of the reductive half-reactions of wild-type DmTrxR and the histidine variant using stopped-flow spectrophotometry.

The reductive half-reactions of wild-type and H464'Q DmTrxR were studied by placing NADPH in anaerobic buffer in one syringe, and oxidized enzyme in anaerobic buffer in the other syringe of the SF-61 DX2 stopped-flow system from Hi-Tech at 25 °C. The evolving changes in the spectra during the reaction with NADPH were observed using the photodiode array detector, and absorbance changes at single wavelengths were collected using the monochromator and a photomultiplier detector. The dead-time of the stopped-flow instrument is 1.5 ms and the first spectrum is recorded starting 1.5 ms after the dead-time of instrument. The apparent rate constants were derived from single-wavelength data with KinetAsyst (version 3.16) from Hi-Tech.

8. **The kinetics of the oxidative half-reactions of wild-type DmTrxR and the histidine variant using stopped-flow spectrophotometry.**

The oxidative half-reactions of wild-type or H464'Q enzyme were studied using the SF-61 DX 2 double-mixing stopped-flow spectrophotometer from Hi-Tech, at 25 °C. Wild-type or H464'Q DmTrxR were pre-reduced with 2 equiv of NADPH anaerobically for 10 seconds in the first mix to produce EH_4, and the pre-reduced enzymes were mixed with various concentrations of Trx. The data were collected as described above for the reductive half-reaction. The turbidity introduced by DmTrx-2 increases the absorbance especially between 300 and 400 nm. To correct the spectra after mixing enzymes and Trx-2, we have subtracted the spectrum that was generated after mixing buffer and Trx-2

from the original spectra. The apparent rate constants of the reactions were derived from single-wavelength datawith KinetAsyst (version 3.16 from Hi-Tech).

D. Results and Discussion

1. Effect of pH on the activity of wild-type and variant TrxR

We have investigated the pattern of macroscopic pK_a values in the H464'Q variant of DmTrxR to further understand the roles of His-464' as an acid-base catalyst in the catalytic mechanism, in particular in the steps involving dithiol-disulfide interchange reactions (Scheme 2.1, steps k_7, k_9, k_{19}, k_{23}). H464'Q DmTrxR was cloned and expressed, and its properties were compared with those of wild-type DmTrxR. The activity of H464'Q DmTrxR was only 2 % that of wild-type DmTrxR under standard assay conditions (k_{cat} = 0.33±0.02 s^{-1} *vs* 15.3±0.1 s^{-1}), which highlights the importance of His464 in catalysis. The effect of the mutation on the activity of DmTrxR is comparable to those changes observed upon analogous mutations of GR and lipoamide dehydrogenase (*41, 42*). Because the K_m for NADPH is less than 2 μM, its value could not be determined accurately (data not shown). Therefore, V_{max} and K_m values for the substrate, DmTrx-2, for wild-type or H464'Q DmTrxR at different pH values were determined using a fixed concentration of NADPH (100 μM). As shown in Fig. 2.2, two apparent pK_a values are present in the pH profile of V_{max} of wild-type DmTrxR; one is at pH 6.4, and the other is at pH 9.3; however, only one pK_a value (6.4) can be discerned in the pH profile of V_{max} for H464'Q DmTrxR. The group with a pK_a of ~9.3 is missing in the complex of H464'Q DmTrxR and DmTrx-2, implying that the higher pK_a value is contributed by His-464'; this residue must be protonated in order to stabilize Cys-57 or Cys-490', the likely the thiolates initiating dithiol-disulfide interchange reactions (Scheme 2.1 and discussion below). The high pK_a value attributed to His-464' is

reminiscent of the active site of papain; in papain, the pK_a value of His-157 is increased by formation of an ion pair with Cys-25 (*43, 44*).

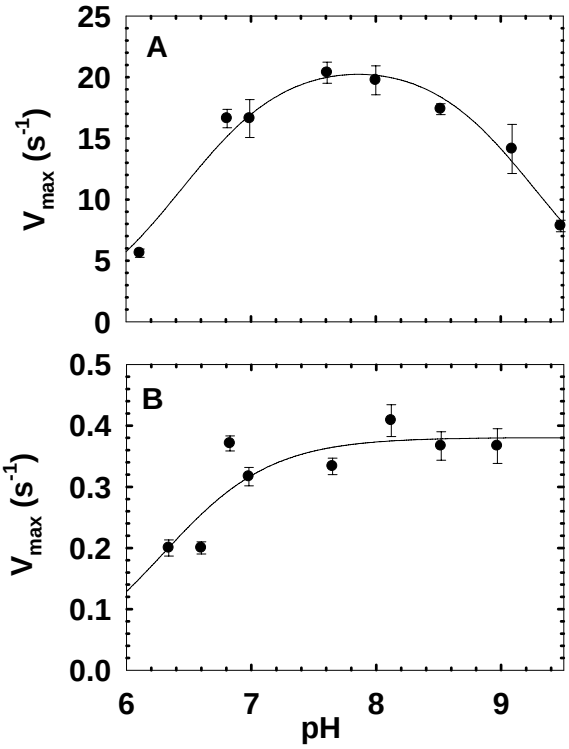

Fig. 2.2 The pH profiles of V_{max} for wild-type DmTrxR (A) and H464'Q DmTrxR (B). The turnover numbers were determined from the rate of NADPH consumption with various concentrations of DmTrx2 and a fixed concentration of NADPH (100 μM), in the presence of GSSG (0.3 mM) at different pH values. The K_m and V_{max} were derived from a graph of turnover number versus concentration of DmTrx-2 fit to an equation for a rectangular hyperbola. The data were fit to Equations 2.1 and 2.2 to calculate the pK_a values.

Plots of V_{max}/K_m for wild-type DmTrxR allow for the estimation of macroscopic pK_a values of 7.0 and 8.7 on the free wild-type DmTrxR; similar values are observed in the plot of V_{max} vs. pH. V_{max}/K_m values for H464'Q DmTrxR do not yield clear pK_a values, as shown in Fig. 2.3. Our preliminary interpretation is that the pattern at low pH suggests a pK_a similar to that derived for wild-type DmTrxR, but the data at high pH for the variant are ambiguous.

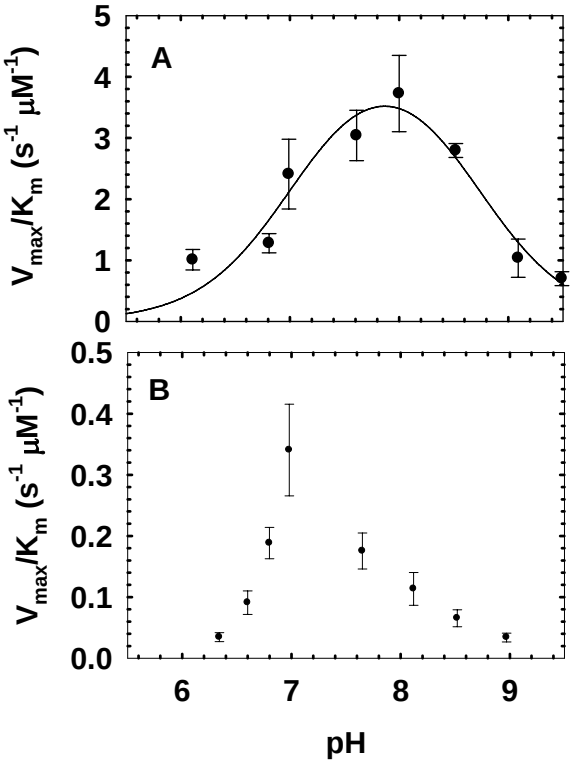

Fig. 2.3 The pH profiles of V_{max}/K_m for wild-type DmTrxR (A) and H464'Q DmTrxR (B). The turnover numbers were determined from the rate of NADPH consumption with various concentrations of DmTrx2 and a fixed concentration of NADPH (100 μM), in the presence of GSSG (0.3 mM), at different pH values. The K_m and V_{max} values were derived from graphs of turnover number versus concentration of DmTrx-2 fit to an equation for a rectangular hyperbola (Michaelis-Menten equation). The data were fit to Equations 2.2 to calculate the pK_a values.

The most obvious assignments of the macroscopic pK_a value of 6.4 are to the two interchange thiols, Cys-57 and Cys-490', which must be deprotonated in order to initiate dithiol-disulfide interchange (steps k_7, k_9 and k_{19}, k_{23}, respectively, Scheme 2.1). The fact that the pK_a value is observed in plots of V_{max} as well as of V_{max}/K_m (see above) reflects the complexity of the substrate, DmTrx-2, that, after binding, reacts with the enzyme to form a covalent intermediate (MDS in Scheme 2.1). However, it seems highly probable that Cys-57 and Cys-490' contribute significantly to the macroscopic pK_a at pH 6.4 on

the enzyme-substrate complex. There may be an analogy between the situation at this point in catalysis and that existing in GR just prior to interchange with GSSG (*32*). The pK_a of the interchange thiol of GR is much higher than that of the charge-transfer thiol, and base catalysis is therefore essential to initiate interchange. The base in GR is slightly closer to the interchange thiol than to the flavin-interacting thiol (*34-36*). His-464' in DmTrxR would be positioned in such a way that it can interact with Cys-57 in one conformation, and with Cys-490' in a slightly different conformation (*38*). Surprisingly, this pK_a value is not changed by mutation of His-464', suggesting that in H464'Q DmTrxR, deprotonation of cysteine residues may be feasible at physiological pH. However, in this variant, the cysteine thiolate anions are less stable because of the loss of the stabilizing protonated His-464'. The imidazole group of His-464' must be uncharged in order to assist in the formation of thiolate, and the resulting imidazolium can stabilize the thiolate by ion-pair interaction. Plots of V_{max} vs pH show that His-464' must be protonated for maximal activity; therefore, stabilization by ion-pair formation must be more important than base catalysis.

It has been shown that imidazole will partially restore the activity in variants of thioredoxin for which the putative catalyst of thiol-disulfide interchange has been altered (*45*). Thus, it was of interest to investigate the effect of imidazole and imidazolium on the activity of the histidine variant at different pH values. The imidazole/imidazolium ratio is pH dependent; therefore, the concentration of active species, imidazole, was calculated and is indicated in Fig. 2.4. Relatively high concentrations of imidazole partially restored the activity of H464'Q DmTrxR, but had much smaller effects on wild-type enzyme. Moreover, the effect of imidazole on the activity of H464'Q DmTrxR at pH 8.5 was less

than that at pH 7.5 (Fig. 2.4). This is expected because the deprotonation of thiol groups is more favorable at higher pH, thereby decreasing the effect of imidazole on the activity of H464'Q DmTrxR. The effects due to the addition of imidazole to the variant are consistent with the histidine residue in wild-type enzyme acting as an acid-base catalyst to facilitate the formation of thiolate anion as well as to stabilize the thiolate by ionic interaction.

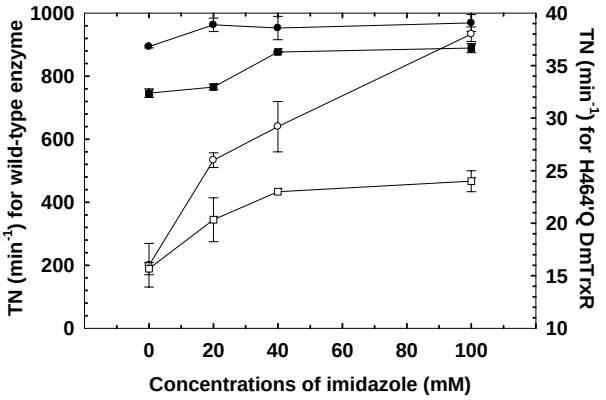

Fig. 2.4 The turnover numbers of wild-type DmTrxR and H464'Q DmTrxR in the presence of imidazole-imidazolium at pH **7.**5 at pH 8.5. (●) wild-type enzyme, pH 7.5, left y-axis; (■) wild-type enzyme, pH 8.5, left-axis. (○) H464'Q DmTrxR, pH 7.5, right y-axis; (□) H464'Q DmTrxR, pH 8.5, right y-axis. The concentration of imidazole, the active species, was calculated using the Henderson-Hasselbalch equation.

A similar example of stabilization by ionic interaction and acid-base catalysis has been studied in papain, where an ion-pair is formed between Cys-25 and His-159. Proton NMR measurements on the resting enzyme have shown that the ion-pair is favored by nearly 100 % over the thiol-imidazole form (*43, 44*). Chymotrypsin is the most commonly referred to example of an enzyme having a catalytic triad, Ser-His-Asp, and this is analogous to Cys-His-Glu in TrxR (*46, 47*).

2. Titrations of wild-type and variant TrxR

Static titrations of wild-type and variant TrxR with NADPH were carried out to ascertain the effects of the mutation of His-464' on the electron distribution among the three redox centers. The titration of wild-type DmTrxR led to a blue-shift of the main flavin band (from 462 nm to 450 nm), and the formation of the thiolate-FAD CTC identified by increased absorbance at 540 nm; formation of the $FADH^{-}$-$NADP^{+}$ CTC, which contributes a broad band around 670 nm, can only be observed transiently using rapid reaction techniques (see below) (*30, 42, 48*) (Fig. 2.5). After 1 equiv of NADPH was added, the wild-type enzyme was reduced to the EH_2 state (2-electron-reduced enzyme), and the high absorbance at 540 nm showed that EH_2^B and EH_2^C predominated among the four EH_2 isoforms (Scheme 2.1). Further addition of NADPH produced EH_4^B and a small amount of EH_4^A (Scheme 2.1), as shown by the slight loss of flavin absorbance at 462 nm. However, in the titration of wild-type DmTrxR the thiolate-FAD CTC observed at 540 nm reached a maximum and did not decrease, even in the presence of excess NADPH. These results are consistent with the previous findings of Bauer et al. for DmTrxR (*30*). Titrations of wild-type enzyme with NADPH at various pH values showed that the intensity and spectral characteristics of the thiolate-FAD CTC were largely unchanged between pH 7 and 9 (Fig. 2.6).

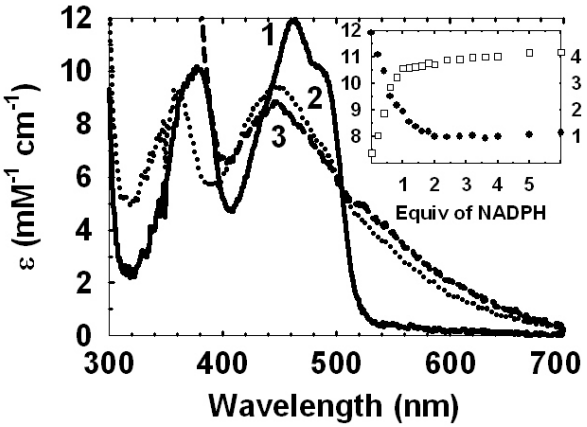

Fig. 2.5 Titration of wild-type with NADPH at pH 8. Spectra are as follows. 1, E_{ox}; 2, after addition of 1 equiv of NADPH; 3, after 6 equiv of NADPH. (Inset) absorbance at 462 nm (●), left y-axis; and 540 nm (□), right y-axis as function of equiv of NADPH added. **B**: Spectra and Inset as in **A**.

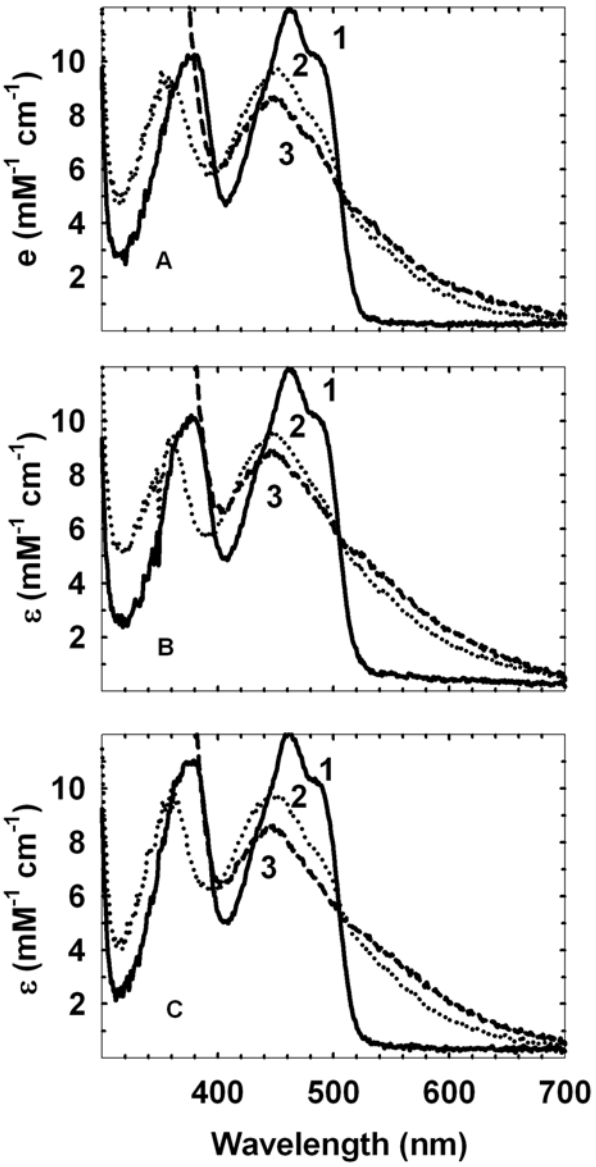

Fig. 2.6 Titration of wild-type DmTrxR with NADPH at pH 7, 8, and 9. A: Titration at pH 7. Spectrum 1, E_{ox}; Spectrum 2, after addition of 1 equiv of NADPH; Spectrum 3, after 6 equiv of NADPH. **B**: Titration at pH 8. Spectra as in **A**. **C**: NADPH titration at pH 9. Spectra as in **A**.

In stark contrast to results with wild-type DmTrxR, the spectra of reduced H464'Q DmTrxR revealed that excess NADPH fully reduced the flavin (Fig. 2.7 cf. Fig. 2.5). This result indicates that the relative redox potentials of FAD, the N-terminal disulfide, and the C-terminal cysteine pair are altered in H464'Q DmTrxR from those of

wide-type enzyme. Fig. 2.7 (inset) shows that the thiolate-FAD CTC reached a maximum and then decreased, indicating that the histidine variant was reduced beyond the EH_4 level in the presence of more than 2 equiv of NADPH, resulting in the loss of the thiolate-FAD CTC. In this family of enzymes, the redox potential of the flavin is normally lower than that of the disulfide(s); the CTC absorbance is diagnostic for the reduction of the disulfides. Even in the mammalian enzyme where the C-terminal redox active group is a selenenylsulfide, titration with dithionite shows uptake of three 2-electron equivalents before unreacted dithionite is detected (*22*). Furthermore, the maximum amount of thiolate-FAD CTC (~2.6 mM^{-1} cm^{-1}) observed was considerably less than that of wild-type enzyme (~4.1 mM^{-1} cm^{-1}), again showing the importance of His-464' for the stabilization of the thiolate-FAD CTC. This titration revealed an interesting difference between H464'Q DmTrxR and the analogous variant in the plasmodium enzyme, H509'Q PfTrxR; no thiolate-FAD CTC was observed in the latter enzyme (*31*). Overall, these results suggest that in the absence of His-464', thiolate formation is still possible in DmTrxR, but is not efficient. The effect of pH on the titration of H464'Q DmTrxR with NADPH was greater than the effect of pH on wild-type enzyme; the fraction of the thiolate-FAD CTC in H464'Q DmTrxR increased as the pH increased (Fig. 2.8 cf. Fig. 2.6). This result is consistent with there being less need for stabilization of the CTC by His-464' at high pH.

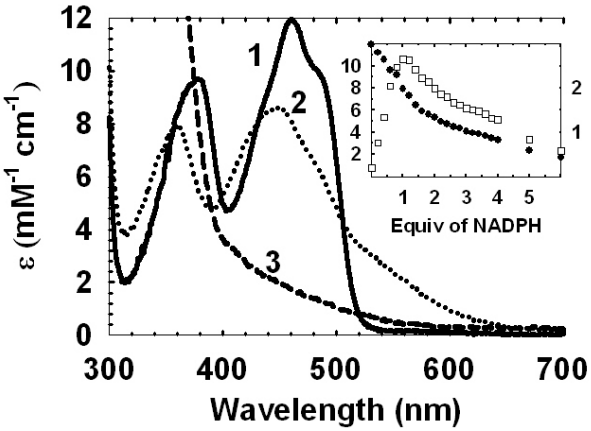

Fig. 2.7 Titration of H464'Q DmTrxR with NADPH at pH 8. Spectra are as follows. 1, E_{ox}; 2, after addition of 1 equiv of NADPH; 3, after 6 equiv of NADPH. (Inset) absorbance at 462 nm (●), left y-axis; and 540 nm (□), right y-axis as function of equiv of NADPH added. **B**: Spectra and Inset as in **A**.

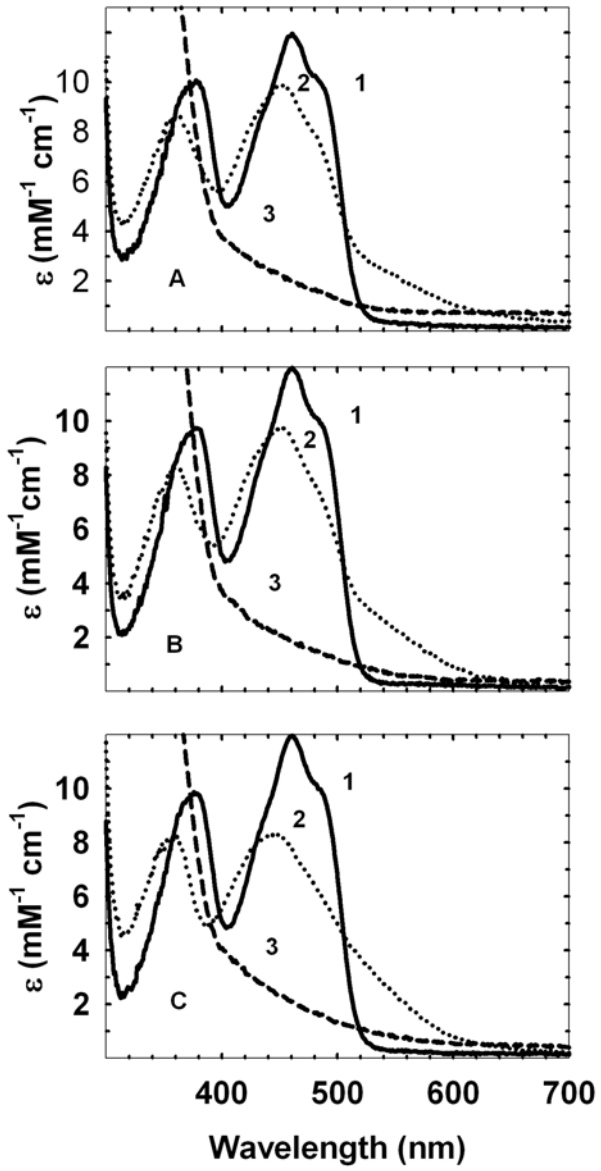

Fig. 2.8 Titration of H464'Q DmTrxR with NADPH at pH 7, 8, and 9 .A: Titration at pH 7**.** Spectrum 1, E_{ox}; Spectrum 2, after addition of 1 equiv of NADPH; Spectrum 3, after 6 equiv of NADPH. **B**: Titration at pH 8. Spectra as in **A**. **C**: Titration at pH 9. Spectra as in **A**.

3. Effect of pH on the reductive half-reaction of wild-type and variant DmTrxR

Because His-464' facilitates the formation of the thiolate of Cys-57, the effects of its mutation on the reductive half-reaction should be apparent, and therefore studies of this reaction were compared to those of wild-type DmTrxR. Fig. 2.9 shows spectra recorded during the reductive half reaction of wild-type DmTrxR; spectra 2-4 are of the enzyme approximately at the end of each of the three phases that were identified from the kinetic traces (Fig. 2.9, Inset). The first phase occurred from the dead time (1.5 ms) to ~ 5 ms, the second phase was from ~ 5 ms to ~ 20 ms, and the final phase was from ~ 20 ms to ~ 300 ms. In the first phase, which was dependent on the concentration of NADPH, the absorbance at 440 nm decreased while that at 670 nm increased, showing reduction of the flavin and formation of the $FADH^{-}$-$NADP^{+}$ CTC, respectively. Thus, this step is associated with the reaction from E_{ox} to EH_2^A (Scheme 2.1). The mechanism proposed in Scheme 2.1 is based on observations made with enzyme family members lacking the C-terminal redox active disulfide and expanded from Bauer et al. *(30)*. Note that even this minimal mechanism for TrxR has at least eight reversible kinetic events associated with the reductive half reaction (Scheme 2.1). The flavin was approximately 60 % reduced in the first phase, but almost half of this change occurred in the dead time of the stopped-flow instrument (~1.5 ms). EH_2^A (Scheme 2.1) was the major enzyme species present at the end of this phase. In the second phase, increased absorbance at 440 and 540 nm indicated that reoxidation of the flavin and formation of the thiolate-FAD CTC occurred in this phase (EH_2^A to EH_2^B in Scheme 2.1). The third and slowest phase may not reflect a single step; rather, it may include dithiol-disulfide interchange (EH_2^B to EH_2^D), as well

as the reaction of the enzyme with the second equivalent of NADPH (EH_2^D to EH_4^A and EH_4^B in Scheme 2.1). Table 2.1 lists the K_d values for NADPH for wild-type DmTrxR derived from the apparent first-order rate constants at each pH value, and these values are similar at pH 7-9. The rates of the second and third phases were independent of the concentration of NADPH.

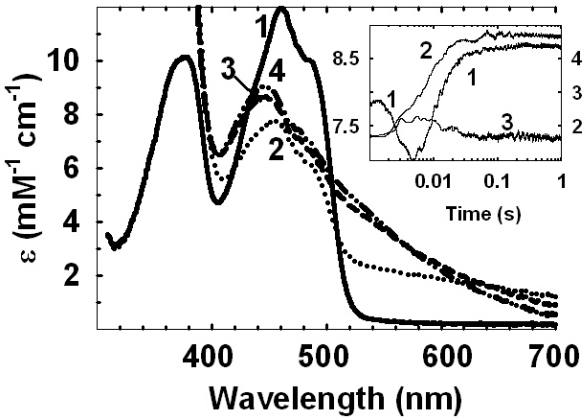

Fig. 2.9 Spectra and kinetics observed in the reductive half-reactions of wild-type DmTrxR. Reduction of DmTrxR (10 μM) with 10 equiv of NADPH at pH 8, 25 °C under anaerobic conditions. Spectrum 1, E_{ox}. Spectra 2-4, 4 ms, 20 ms, and 300 ms. The Inset shows kinetic traces: Curve 1, left y-axis, 440 nm; Curve 2, right y-axis, 540 nm and Curve 3; right y-axis, 670 nm.

Table 2.1. The apparent rate constants measured during the reductive half-reactions of wild-type and H464'Q DmTrxR, at different pH values, at 25 °C.

Enzymes [a]	pH	$K_{d\ app}$ – NADPH (μM)[b]	$k_{1app\ max}$ (s^{-1})	$k_{2\ app}$ (s^{-1})	$k_{3\ app}$ [c] (s^{-1})
WT	7	13 ± 4	629 ± 56	237 ± 37	47.4 ± 9.4
WT	8	8 ± 5	562 ± 83	187 ± 12	38 ± 16
WT	9	9 ± 3	488 ± 36	107 ± 23	16.4 ± 3.5
H464'Q	7	12 ± 2	164 ± 8	0.4 ± 0.1	0.025 ± 0.015
H464'Q	8	22 ± 4	164 ± 8	1 ± 0.1	0.032 ± 0.001
H464'Q[d]	9	38 ± 6	287 ± 20	7.3 ± 0.5	1.3 ± 0.1

[a] The concentration of enzyme was 10 μM.

[b] The $K_{d\ app}$-NADPH values were determined from $k_{1\ app}$ and concentrations of NADPH using an equation for a rectangular hyperbola. The $k_{1\ app}$ reflects the reduction of the flavin.

[c] the $k_{3\ app}$ in the reductive half-reaction of H464'Q DmTrxR at pH 7 and pH 8 cannot be identified in the kinetic traces

[d] A forth phase was observed: $k_{4\ app}$ = 0.011±0.001 s^{-1}.

The effect of pH on all the apparent rate constants is shown in Table 1. An ~ 2-fold decrease in the rate of the flavin reoxidation, $k_{2\ app}$, was observed with wild-type enzyme as the pH was increased and the positive charge on His-464' decreased (Fig. 2.3). It is possible that this charge stabilizes the negative charge on N1 of the flavin indirectly via a solvent molecule, so that loss of the charge would promote dissociation of $NADP^+$ (EH_2^A to EH_2^B, k_5 in Scheme 2.1). The 3-fold decrease in the rate of the third phase as the pH was increased could have been due to diminished need for stabilization of the charge at N1 in the reaction of the second molecule of NADPH (EH_4^A to EH_4^B, k_{15} in Scheme 2.1). Alternatively, in wild-type enzyme, formation of a thiolate on either Cys-57 or Cys-62 is affected by two linked factors, pH, and the formation of an ion pair between the cysteine and histidine residues. As the pH is increased, deprotonation of the thiol group is favored, but formation of the imidazolium group of His-464', which is able to stabilize thiolate, is less favorable. In the reductive half reaction of wild-type enzyme, it was

observed that the second and third rate constants decreased as the pH increased. This observation suggests that for wild-type enzyme, stabilization by ion-pair formation was more significant than the increase of thiolate concentration at higher pH, substantiating our findings in the experiment of steady-state kinetics.

The spectra recorded during the reductive half reaction of H464'Q DmTrxR (Fig. 2.10) demonstrate that the reaction is very different from that of wild-type enzyme. At the end of the first phase, extending from the dead time (1.5 ms) to ~ 30 ms (Fig. 2.10, Inset, curve 1 and 2), the absorbance at 450 nm decreased (Spectra 2 and 3), and absorbance appeared at 670 nm, indicating the presence of the $FADH^{-}$-$NADP^{+}$ CTC species as EH_2^A (Scheme 1). Approximately 81 % of the total flavin was reduced, in contrast to wild-type DmTrxR where only ~ 60 % of the flavin was reduced (Figs. 2.9, spectrum 2 and 2.10, spectrum 3); reduction of the flavin beyond the EH_4 level was also observed in the static titrations (Fig. 2.7). Because the electron transfer from reduced flavin to the N-terminal redox disulfide is decreased in the H464'Q DmTrxR variant (see above; $k_{2\ app}$), increased net flavin reduction would be expected in the reaction of H464'Q DmTrxR with NADPH (E_{ox} to EH_2^A in Scheme 2.1). From ~ 30 ms to ~ 7 s, only one significant phase was identified at pH 7 or at pH 8 ($k_{2\ app}$ in Table 2.1), but 2 phases ($k_{2\ app}$ and $k_{3\ app}$ in Table 2.1) could be discerned at pH 9. In this period, the absorbance at 450 nm increased while the absorbance at 670 nm decreased, indicating reoxidation of the flavin and reduction of the adjacent disulfide without formation of very much of the thiolate-flavin CTC. The phase seen at both pH 7 and 8 ($k_{2\ app}$ in Table 2.1) may be associated with the steps from EH_2^A to EH_4 (Scheme 2.1). At pH 9, the two phases ($k_{2\ app}$ and $k_{3\ app}$ in Table 2.1) were from ~30 ms to ~ 110 ms, and from ~ 110 ms to ~ 7 s. The phase characterized by $k_{2\ app}$

may be associated with the transfer of electron pairs from $FADH^-$ to the N-terminal redox-active disulfide (EH_2^A to EH_2^B in Scheme 2.1). The phase represented by k_{3app} may not reflect a single step; it may be associated with interchange between the nascent N-terminal dithiol and the C-terminal disulfide (EH_2^B to EH_2^D in Scheme 2.1), as well as to the reaction of the enzyme with the second equivalent of NADPH (EH_2^D to EH_4^A and EH_4^B in Scheme 2.1). The phase ($k_{3\ app}$ for pH 7 and pH 8 and $k_{4\ app}$ for pH 9), from ~ 7 s to ~ 60 s may not be relevant to catalysis. It is important to note that during this time period, the absorbance at 540 nm continued to slowly decrease, indicating the loss of stabilization of the thiolate-flavin CTC. After that phase, the flavin in H464'Q DmTrxR became fully bleached, as shown in Fig 2.10 spectrum 5. The FAD-bleached spectra can be observed in the reaction of H464'Q DmTrxR with either 5 equiv or 10 equiv of NADPH.

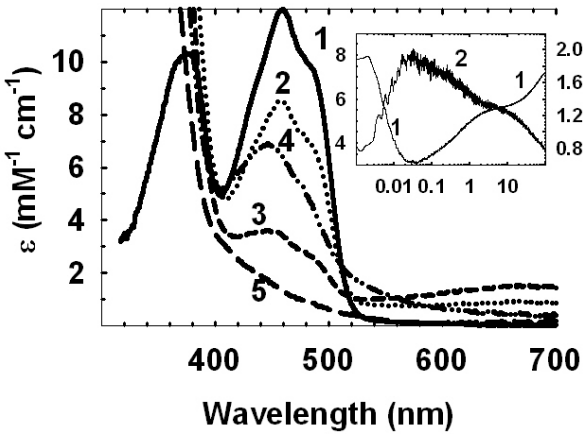

Fig 2.10 Spectra and kinetics observed in the reductive half-reactions of H464'Q DmTrxR. Reduction of H464'Q DmTrxR (10 μM) with 5 equiv of NADPH at pH 9, 25 °C under anaerobic conditions. Spectrum 1, E_{ox}. Spectra 2-5, 1 ms, 29 ms, 70 s, and 10 min. The Inset shows the kinetic traces: Curve 1, left y-axis, 450 nm and Curve 2, right y-axis, 670 nm.

The rates of all three phases decreased in the variant H464'Q DmTrxR compared to wild-type enzyme. As shown in Table 2.1, the effects on $k_{2\ app}$ observed at pH 7 and 8, and on $k_{2\ app}$ and $k_{3\ app}$ at pH 9 were far greater than on $k_{1\ app}$. The results imply that His-464' is important in the step in which reducing equivalents pass from the reduced flavin to the N-terminal disulfide (k_5 in Scheme 2.1) and the step in which reducing equivalents pass from the nascent N-terminal dithiol to the C-terminal disulfide (k_7 and k_9 in Scheme 2.1). The inhibitory effects due to mutation of His-464' on these two steps were lessened at higher pH values where base catalysis is less important (Table 2.1). The rate of flavin reduction in H464'Q DmTrxR compared to wild-type enzyme is affected, but to a much lesser degree, 3.8-fold at pH 7 and 1.7-fold at pH 9. Most importantly, the rates of the second and third phases increased as the pH was increased, because formation of thiolate is favorable at the higher pH values. These results strongly indicate that His-464' acts as the acid-base catalyst to facilitate thiolate formation in DmTrxR.

The K_d values for NADPH derived from the first phase are listed in Table 2.1; the dissociation constants of NADPH for H464'Q DmTrxR increased as the pH was raised. It has been shown that several amino acid residues are responsible for binding NADPH in the rat, mouse, and human TrxR. By analogy, Arg-218 and Arg-223 in DmTrxR would form hydrogen bonds with the 2'-phosphate group of NADPH to facilitate NADPH binding to the enzyme, and Tyr-197 would be able to stack against the nicotinamide ring of NADPH, holding it in an optimal conformation to facilitate hydride ion transfer from NADPH to the flavin. It is unlikely that these amino acid residues would be affected directly by the mutation of His-464', because the structures of rat, mouse, and human TrxRs show that they are far removed from His-464'. However, it is possible that the

mutation of His-464' does affect the positions of these amino acid residues indirectly to alter the binding of NADPH to the enzyme.

4. Effect of pH on the oxidative half reactions of wild-type and variant TrxR

Previous studies suggested that the histidine residue analogous to His-464' in DmTrxR is also involved in the oxidative half reaction of PfTrxR (*31*). Therefore, the oxidative half reactions of wild-type enzyme and H464'Q DmTrxR were studied, and the effects of pH on this half reaction were also explored. The enzymes were pre-reduced to EH_4 by addition of two equivalents of NADPH followed by mixing with various concentrations of DmTrx-2. Fig. 2.11 shows spectra recorded during the oxidative half reaction of wild-type enzyme; spectrum 2 shows the pre-reduced enzyme (EH_4), and spectra 3 and 4 show the enzyme at the end of the two phases, identified in the kinetic traces. The reaction was finished within 10 s. Two phases were assumed in fitting the kinetic traces; the first phase from the dead time (1.5 ms) to ~ 100 ms and the second phase from ~ 100 ms to ~ 10 s are shown in Fig. 2.11, inset. Increases in absorbance at 450 nm and decreases in absorbance at 540 nm were observed in both phases. The first phase has only a small change in absorbance and is frequently referred to as a 'lag phase'. This step may be attributed to dissociation of $NADP^+$ from the enzyme. A similar first phase in the oxidative half reaction of PfTrxR was also observed by McMillan et al. (*31*); the working temperature was 4 °C in their study of PfTrxR, whereas the temperature in this study was 25 °C. The patterns of changes in absorbance at pH 8 and pH 9 were similar to those at pH 7 (data not shown). As pH was increased, the first phase decreased in rate, indicating again that the dissociation of $NADP^+$ from enzyme may be dependent

on pH. In the second phase, most of the loss of the thiolate-FAD CTC and flavin reoxidation were observed. This phase is associated with the conversion of EH_4 to EH_2, as hypothesized for PfTrxR (*31*). Further reoxidation of the enzyme was not observed, even with 15 equiv of DmTrx-2, and this is consistent with the enzyme functioning between EH_2 and EH_4 during catalysis. The second phase showed no pH dependence (Table 2.2).

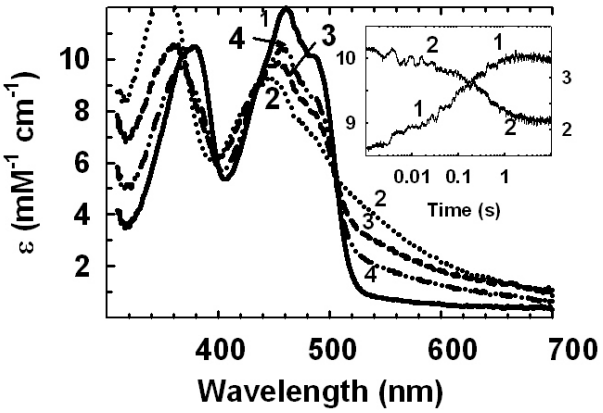

Fig.2.11 The oxidative half-reaction of wild-type DmTrxR at pH 7 under anaerobic conditions carried out in the double mixing stopped-flow instrument. The reaction of DmTrx-2 with wild-type enzyme (10 μM) 10 s after pre-reducing with 2 equiv of NADPH in the first mix. Spectrum 1, E_{ox} as a reference, Spectrum 2, pre-reduced enzyme (EH_4). Spectra were recorded at various times after mixing with 10 equiv DmTrx-2. Spectrum 3, 116 ms and Spectrum 4, 7.1 s. Kinetic traces are shown in the Inset: Curve 1, left y-axis, 450 nm and Curve 2, right y-axis, 540 nm.

Table 2.2. The apparent rate constants of the oxidative half-reactions of wild-type and H464'Q DmTrxR, at different pH values, at 25 °C

Enzymes [a]	pH	$k_{1\ app}$ (s^{-1})	$k_{2\ app}$ (s^{-1})	$k_{3\ app}$ (s^{-1})
WT	7	28 ± 11	2.7 ± 1.4	
WT	8	18-20	2.8 ± 0.5	
WT	9	13.4 ± 4.6	2.4 ± 0.4	
H464'Q [b]	7	29.3 ±6.2	0.5-1.5	0.17±0.03
H464'Q[b]	8	24.2±6.1	1.2±0.4	0.17±0.02
H464'Q[b]	9	ND[c]	ND[c]	0.1 ± 0.03

[a] The concentration of enzyme was 10 μM.
[b] The change of absorbance in the first and the second phases is small. A major absorbance change is observed in the third phase.
[c] ND: not determined; the first and the second phases in the oxidative half-reaction of H464'Q DmTrxR look like a lag phase; therefore, these two phases can not be fit accurately.

The spectra in Fig. 2.12 show that the oxidative half reaction of H464'Q DmTrxR is more complex than that of wild-type enzyme (Fig. 2.11); the reaction in the variant enzyme continued beyond the EH_2 stage, in contrast to wild-type enzyme, and the reaction in the variant was much slower, taking ~ 20 s. Three phases were distinguishable in the kinetic traces (Fig. 2.12, inset), unlike the two phases in wild-type enzyme: the first phase from 1.5 ms to ~ 0.1 s, the second phase from ~ 0.1 s to ~ 1 s and the third phase from ~ 1 s to ~ 20 s. In the first and second phases, changes in absorbance at 450 and 670 nm were small. We believe that these two phases reflect dissociation of $NADP^+$ from the enzyme, as well as the continuous reduction of the enzyme by unreacted NADPH. The third phase, involving the largest change in absorbance at both wavelengths, shows the characteristics of enzyme reoxidation to EH_2 from EH_4, as discussed for the wild-type enzyme, but with extensive further oxidation to E_{ox} (Fig. 2.12). Clearly His-464' is involved in the oxidative half-reaction.

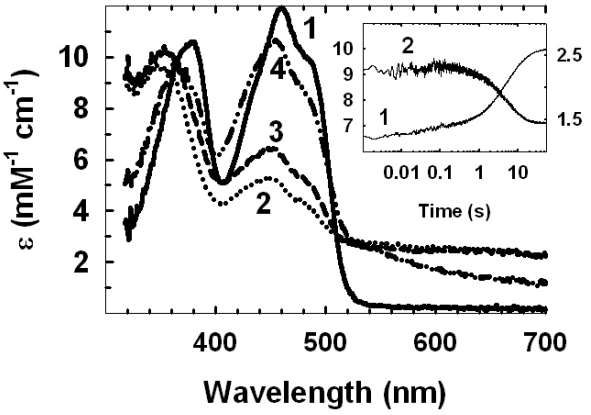

Fig. 2.12 The oxidative half-reaction of H464'Q DmTrxR at pH 7 under anaerobic conditions carried out in the double mixing stopped-flow instrument. The reaction of DmTrx-2 with H464'Q DmTrxR (10 μM) 10 s after pre-reducing with 2 equiv of NADPH in the first mix. Spectrum 1, E_{ox} as a reference, and Spectrum 2, pre-reduced enzyme (EH_4). Spectra were recorded at various times after mixing with 10 equiv DmTrx-2: Spectrum 3, 112 ms, and Spectrum 4, 21 s. Kinetic traces are shown in the Inset: Curve 1, 450 nm, left y-axis and Curve 2, 670 nm, y-right axis.

Based on the structures of rat, mouse, and human TrxRs, the interaction between His-464' and the C-terminal redox dithiol appears to depend on the mobility of the C-terminal tail in DmTrxR that could allow the C-terminal dithiol to approach His-464' (*26, 28, 29, 38*). Thus, it is reasonable that His-464' be involved in the oxidative half reaction as well as the reductive half reaction. The function of His-464' in DmTrxR proposed by Eckenroth et al. (*29*) is based on the mechanism of GR. In the oxidative half reaction of GR, as $_1GSSG_2$ is reduced by GR, GR-S-S-G_1 and $_2GS^-$ are produced and His-467' will protonate the thiolate anion, $_2GS^-$ to suppress the back reaction (*49*). Therefore, it has been proposed that like GR, the function of His-464' in DmTrxR is to protonate the leaving group Cys-490'. Eckenroth et al. used tetrapeptides that represented the last three residues of DmTrxR to react with enzyme in which the last three residues removed; the leaving group of the peptides presumably will be protonated on dissociation from the

enzyme. In contrast, in our enzyme system where the enzyme is in the native state, the thiol of Cys-490' must be a thiolate in order to react with DmTrx-2. Therefore, we propose that the function of His-464' in the oxidative half reaction is to stabilize the thiolate on Cys-490' for nucleophilic attack on the redox-active disulfide of Trx (k_{19}, Scheme 2.1). This is consistent with our interpretation of the data in Fig. 2.3 showing that Cys-490' must be deprotonated and His-464' protonated for maximum activity. In addition, His-464' may serve as the proton donor to Trx to complete the interchange. As a result, the rate of the oxidative half reaction is less in H464'Q DmTrxR than in wild-type DmTrxR. The reasons for the small effects of pH on the reoxidation rate of H464'Q DmTrxR ($k_{3\ app}$) and wild-type enzyme ($k_{2\ app}$) are not obvious (Table 2.2).

E. Concluding remarks

Malaria is a very serious global public health problem; approximately 500 million cases of malaria are reported annually, and more than 2.5 million people, mostly children, die of this disease (*31, 50*). The malarial protozoan parasite, *Plasmodium*, requires the mosquito vector, *A. gambiae*, for transmission of malaria to the human. Dipteran insects such as *A. gambiae* and *D. melanogaster* have an unusual need for an alternative antioxidant system because this genus lacks GR (*15, 17*). The system consisting of Trx and TrxR has been shown to comprise the primary antioxidant system in *Diptera (15)*. As mentioned in the Introduction, similarities in sequence and structure make DmTrxR a good model for the enzyme from *A. gambiae.* The long-term objective of this work is to establish differences between human TrxR, DmTrxR, and PfTrxR, victim, host-vector model, and parasite, respectively. It is hoped that these differences will be helpful to medicinal chemists in the development of inhibitors of the host-vector enzyme relative to the enzyme from the parasite.

The formation of thiolate is required for nucleophilic attack in dithiol-disulfide interchanges that are integral parts of catalysis in this family of enzymes (*1, 45*). Although the pK_a of the thiol group of free cysteine in aqueous solution is about 8.3, considerably above physiological pH (*51*), the protein milieu can lower the pK_a value of sulfhydryl groups in the redox-active dithiol in DmTrxR. A histidine residue is conserved and has been shown to act as the acid-base catalyst in this family (*1, 31, 42, 52, 53*). Therefore, based on the structures of the rat, mouse, human, and *D. melanogaster* TrxRs (*26, 28, 29, 38*), His-464', which is on the subunit adjacent to that containing the FAD and the N-terminal cysteines, is proposed to facilitate the formation of thiolate in

DmTrxR. Indeed, as mentioned above, the histidine variant, H464'Q DmTrxR, showed only 2% of the activity of wild-type enzyme, indicating that this histidine residue is crucial for the enzyme activity of DmTrxR.

How and to what extent acid-base catalysis occurs by His-464' are questions that led to this study of the effects of pH on various enzyme properties. The effect of pH on the activity of wild-type DmTrxR defined a pK_a of 6.4, ascribed to Cys-57 and Cys-490', and a pK_a of 9.3 in the DmTrxR-DmTrx-2 complex and 8.7 in free DmTrxR ascribed to His-464'. The fact that this pK_a was missing in H464'Q DmTrxR substantiates the notion that this residue is important for acid-base catalysis. The rescuing effect of imidazole on the activity of H464'Q DmTrxR corroborated the function of His-464'. In the reductive half reaction of the enzyme, electron-pair transfers from reduced flavin to the N-terminal disulfide, and from the nascent N-terminal dithiol to the C-terminal disulfide ($k_{2\ app}$ and k_{3app}), were profoundly affected in the variant, H464'Q DmTrxR. This suggested that the relative redox potentials of the three redox centers are altered by the mutation of His-464'. The rates of these two steps increased at higher pH values, as expected because base catalysis is less important at high pH. His-464' is also involved in the oxidative half reaction, apparently by stabilizing the charge on Cys-490' and by protonating Trx. Therefore, based on our evidence, it is concluded that His-464' acts as the acid-base catalyst in both half reactions of DmTrxR.

Glu-514' in PfTrxR, analogous to Glu-469' in DmTrxR (Scheme 1), has been shown to enhance the acid-base catalysis by histidine (*31, 37, 53*). In the study by McMillan et al., Glu-514' was replaced by alanine, resulting in a significant decrease in active site polarity that led to enhanced thiolate-flavin charge-transfer. Future studies will

investigate the effect of pH on the enhancement by Glu-469' of acid-base catalysis by His-464' in DmTrxR, utilizing both polar and apolar replacement residues for Glu-469', in particular glutamine.

References

1. Williams, C. H. (1992) *Lipoamide Dehydrogenase, Glutathione Reductase, Thioredoxin reductase, and Mercuric ion reductase-A family of Flavoenzyme Transhydrogenase*, Vol. 3, CRC press, Inc, Boca Raton. FL.
2. Williams, C. H., Arscott, L. D., Muller, S., Lennon, B. W., Ludwig, M. L., Wang, P. F., Veine, D. M., Becker, K., and Schirmer, R. H. (2000) Thioredoxin reductase two modes of catalysis have evolved, *Eur J Biochem 267*, 6110-6117.
3. Moore, E. C., Reichard, P., and Thelander, L. (1964) Enzymatic Synthesis of Deoxyribonucleotides.V. Purification and Properties of Thioredoxin Reductase from Escherichia Coli B, *J Biol Chem 239*, 3445-3452.
4. Watson, W. H., Yang, X., Choi, Y. E., Jones, D. P., and Kehrer, J. P. (2004) Thioredoxin and its role in toxicology, *Toxicol Sci 78*, 3-14.
5. Mau, B. L., and Powis, G. (1992) Inhibition of cellular thioredoxin reductase by diaziquone and doxorubicin. Relationship to the inhibition of cell proliferation and decreased ribonucleotide reductase activity, *Biochem Pharmacol 43*, 1621-1627.
6. Bertini, R., Howard, O. M., Dong, H. F., Oppenheim, J. J., Bizzarri, C., Sergi, R., Caselli, G., Pagliei, S., Romines, B., Wilshire, J. A., Mengozzi, M., Nakamura, H., Yodoi, J., Pekkari, K., Gurunath, R., Holmgren, A., Herzenberg, L. A., and Ghezzi, P. (1999) Thioredoxin, a redox enzyme released in infection and inflammation, is a unique chemoattractant for neutrophils, monocytes, and T cells, *J Exp Med 189*, 1783-1789.
7. Gromer, S., Urig, S., and Becker, K. (2004) The thioredoxin system--from science to clinic, *Med Res Rev 24*, 40-89.
8. Burke-Gaffney, A., Callister, M. E., and Nakamura, H. (2005) Thioredoxin: friend or foe in human disease?, *Trends Pharmacol Sci 26*, 398-404.
9. Boschi-Muller, S., Olry, A., Antoine, M., and Branlant, G. (2005) The enzymology and biochemistry of methionine sulfoxide reductases, *Biochim Biophys Acta 1703*, 231-238.
10. Gon, S., Faulkner, M. J., and Beckwith, J. (2006) In vivo requirement for glutaredoxins and thioredoxins in the reduction of the ribonucleotide reductases of Escherichia coli, *Antioxid Redox Signal 8*, 735-742.
11. Yodoi, J., Masutani, H., and Nakamura, H. (2001) Redox regulation by the human thioredoxin system, *Biofactors 15*, 107-111.
12. Nguyen, P., Awwad, R. T., Smart, D. D., Spitz, D. R., and Gius, D. (2006) Thioredoxin reductase as a novel molecular target for cancer therapy, *Cancer Lett 236*, 164-174.
13. Berndt, C., Lillig, C. H., and Holmgren, A. (2007) Thiol-based mechanisms of the thioredoxin and glutaredoxin systems: implications for diseases in the cardiovascular system, *Am J Physiol Heart Circ Physiol 292*, H1227-1236.
14. Chae, H. Z., Chung, S. J., and Rhee, S. G. (1994) Thioredoxin-dependent peroxide reductase from yeast, *J Biol Chem 269*, 27670-27678.
15. Kanzok, S. M., Fechner, A., Bauer, H., Ulschmid, J. K., Muller, H. M., Botella-Munoz, J., Schneuwly, S., Schirmer, R., and Becker, K. (2001) Substitution of the

thioredoxin system for glutathione reductase in Drosophila melanogaster, *Science 291*, 643-646.
16. Bauer, H., Gromer, S., Urbani, A., Schnolzer, M., Schirmer, R. H., and Muller, H. M. (2003) Thioredoxin reductase from the malaria mosquito Anopheles gambiae, *Eur J Biochem 270*, 4272-4281.
17. Bauer, H., Kanzok, S. M., and Schirmer, R. H. (2002) Thioredoxin-2 but not thioredoxin-1 is a substrate of thioredoxin peroxidase-1 from Drosophila melanogaster: isolation and characterization of a second thioredoxin in D. Melanogaster and evidence for distinct biological functions of Trx-1 and Trx-2, *J Biol Chem 277*, 17457-17463.
18. Thelander, L. (1967) Thioredoxin reductase. Characterization of a homogenous preparation from Escherichia coli B, *J Biol Chem 242*, 852-859.
19. Luthman, M., and Holmgren, A. (1982) Rat liver thioredoxin and thioredoxin reductase: purification and characterization, *Biochemistry 21*, 6628-6633.
20. Zanetti, G., and Williams, C. H., Jr. (1967) Characterization of the active center of thioredoxin reductase, *J Biol Chem 242*, 5232-5236.
21. Thelander, L. (1968) Studies on thioredoxin reductase from Escherichia coli B. The relation of structure and function, *Eur J Biochem 4*, 407-419.
22. Arscott, L. D., Gromer, S., Schirmer, R. H., Becker, K., and Williams, C. H., Jr. (1997) The mechanism of thioredoxin reductase from human placenta is similar to the mechanisms of lipoamide dehydrogenase and glutathione reductase and is distinct from the mechanism of thioredoxin reductase from Escherichia coli, *Proc Natl Acad Sci U S A 94*, 3621-3626.
23. Zhong, L., Arner, E. S., and Holmgren, A. (2000) Structure and mechanism of mammalian thioredoxin reductase: the active site is a redox-active selenolthiol/selenenylsulfide formed from the conserved cysteine-selenocysteine sequence, *Proc Natl Acad Sci U S A 97*, 5854-5859.
24. Zhong, L., and Holmgren, A. (2000) Essential role of selenium in the catalytic activities of mammalian thioredoxin reductase revealed by characterization of recombinant enzymes with selenocysteine mutations, *J Biol Chem 275*, 18121-18128.
25. Lennon, B. W., Williams, C. H., Jr., and Ludwig, M. L. (2000) Twists in catalysis: alternating conformations of Escherichia coli thioredoxin reductase, *Science 289*, 1190-1194.
26. Sandalova, T., Zhong, L., Lindqvist, Y., Holmgren, A., and Schneider, G. (2001) Three-dimensional structure of a mammalian thioredoxin reductase: implications for mechanism and evolution of a selenocysteine-dependent enzyme, *Proc Natl Acad Sci U S A 98*, 9533-9538.
27. Gromer, S., Johansson, L., Bauer, H., Arscott, L. D., Rauch, S., Ballou, D. P., Williams, C. H., Jr., Schirmer, R. H., and Arner, E. S. (2003) Active sites of thioredoxin reductases: why selenoproteins?, *Proc Natl Acad Sci U S A 100*, 12618-12623.
28. Biterova, E. I., Turanov, A. A., Gladyshev, V. N., and Barycki, J. J. (2005) Crystal structures of oxidized and reduced mitochondrial thioredoxin reductase provide molecular details of the reaction mechanism, *Proc Natl Acad Sci U S A 102*, 15018-15023.

29. Eckenroth, B. E., Rould, M. A., Hondal, R. J., and Everse, S. J. (2007) Structural and biochemical studies reveal differences in the catalytic mechanisms of mammalian and Drosophila melanogaster thioredoxin reductases, *Biochemistry 46*, 4694-4705.
30. Bauer, H., Massey, V., Arscott, L. D., Schirmer, R. H., Ballou, D. P., and Williams, C. H., Jr. (2003) The mechanism of high Mr thioredoxin reductase from Drosophila melanogaster, *J Biol Chem 278*, 33020-33028.
31. McMillan, P. J., Arscott, L. D., Ballou, D. P., Becker, K., Williams, C. H., Jr., and Muller, S. (2006) Identification of acid-base catalytic residues of high-Mr thioredoxin reductase from Plasmodium falciparum, *J Biol Chem 281*, 32967-32977.
32. Sahlman, L., and Williams, C. H., Jr. (1989) Titration studies on the active sites of pig heart lipoamide dehydrogenase and yeast glutathione reductase as monitored by the charge transfer absorbance, *J Biol Chem 264*, 8033-8038.
33. Matthews, R. G., Ballou, D. P., Thorpe, C., and Williams, C. H., Jr. (1977) Ion pair formation in pig heart lipoamide dehydrogenase: rationalization of pH profiles for reactivity of oxidized enzyme with dihydrolipoamide and 2-electron-reduced enzyme with lipoamide and iodoacetamide, *J Biol Chem 252*, 3199-3207.
34. Pai, E. F., and Schulz, G. E. (1983) The catalytic mechanism of glutathione reductase as derived from x-ray diffraction analyses of reaction intermediates, *J Biol Chem 258*, 1752-1757.
35. Karplus, P. A., and Schulz, G. E. (1987) Refined structure of glutathione reductase at 1.54 A resolution, *J Mol Biol 195*, 701-729.
36. Karplus, P. A., and Schulz, G. E. (1989) Substrate binding and catalysis by glutathione reductase as derived from refined enzyme: substrate crystal structures at 2 A resolution, *J Mol Biol 210*, 163-180.
37. Gromer, S., Wessjohann, L. A., Eubel, J., and Brandt, W. (2006) Mutational studies confirm the catalytic triad in the human selenoenzyme thioredoxin reductase predicted by molecular modeling, *Chembiochem 7*, 1649-1652.
38. Fritz-Wolf, K., Urig, S., and Becker, K. (2007) The structure of human thioredoxin reductase 1 provides insights into C-terminal rearrangements during catalysis, *J Mol Biol 370*, 116-127.
39. Cheng, Z., Arscott, L. D., Ballou, D. P., and Williams, C. H., Jr. (2007) The relationship of the redox potentials of thioredoxin and thioredoxin reductase from Drosophila melanogaster to the enzymatic mechanism: reduced thioredoxin is the reductant of glutathione in Drosophila, *Biochemistry 46*, 7875-7885.
40. Kooter, I. M., Steiner, R. A., Dijkstra, B. W., van Noort, P. I., Egmond, M. R., and Huber, M. (2002) EPR characterization of the mononuclear Cu-containing Aspergillus japonicus quercetin 2,3-dioxygenase reveals dramatic changes upon anaerobic binding of substrates, *Eur J Biochem 269*, 2971-2979.
41. Benen, J., van Berkel, W., Dieteren, N., Arscott, D., Williams, C., Jr., Veeger, C., and de Kok, A. (1992) Lipoamide dehydrogenase from Azotobacter vinelandii: site-directed mutagenesis of the His450-Glu455 diad. Kinetics of wild-type and mutated enzymes, *Eur J Biochem 207*, 487-497.

42. Rietveld, P., Arscott, L. D., Berry, A., Scrutton, N. S., Deonarain, M. P., Perham, R. N., and Williams, C. H., Jr. (1994) Reductive and oxidative half-reactions of glutathione reductase from Escherichia coli, *Biochemistry 33*, 13888-13895.
43. Johnson, F. A., Lewis, S. D., and Shafer, J. A. (1981) Determination of a low pK for histidine-159 in the S-methylthio derivative of papain by proton nuclear magnetic resonance spectroscopy, *Biochemistry 20*, 44-48.
44. Lewis, S. D., Johnson, F. A., and Shafer, J. A. (1981) Effect of cysteine-25 on the ionization of histidine-159 in papain as determined by proton nuclear magnetic resonance spectroscopy. Evidence for a his-159--Cys-25 ion pair and its possible role in catalysis, *Biochemistry 20*, 48-51.
45. Chivers, P. T., and Raines, R. T. (1997) General acid/base catalysis in the active site of Escherichia coli thioredoxin, *Biochemistry 36*, 15810-15816.
46. Tsukada, H., and Blow, D. M. (1985) Structure of alpha-chymotrypsin refined at 1.68 A resolution, *J Mol Biol 184*, 703-711.
47. Craik, C. S., Roczniak, S., Largman, C., and Rutter, W. J. (1987) The catalytic role of the active site aspartic acid in serine proteases, *Science 237*, 909-913.
48. Krauth-Siegel, R. L., Arscott, L. D., Schonleben-Janas, A., Schirmer, R. H., and Williams, C. H., Jr. (1998) Role of active site tyrosine residues in catalysis by human glutathione reductase, *Biochemistry 37*, 13968-13977.
49. Wong, K. K., Vanoni, M. A., and Blanchard, J. S. (1988) Glutathione reductase: solvent equilibrium and kinetic isotope effects, *Biochemistry 27*, 7091-7096.
50. Linares, G. E., and Rodriguez, J. B. (2007) Current status and progresses made in malaria chemotherapy, *Curr Med Chem 14*, 289-314.
51. Huber, R. E., and Criddle, R. S. (1967) Comparison of the chemical properties of selenocysteine and selenocystine with their sulfur analogs, *Arch Biochem Biophys 122*, 164-173.
52. Boggaram, V., and Mannervik, B. (1978) An essential histidine residue in the catalytic mechanism of mammalian glutathione reductase, *Biochem Biophys Res Commun 83*, 558-564.
53. Brandt, W., and Wessjohann, L. A. (2005) The functional role of selenocysteine (Sec) in the catalysis mechanism of large thioredoxin reductases: proposition of a swapping catalytic triad including a Sec-His-Glu state, *Chembiochem 6*, 386-394.

Chapter 3: The function of Glu-469' as an acid-base catalyst in thioredoxin reductase from *Drosophila melanogaster*

A. Abstract

Thioredoxin reductase (TrxR) catalyses the reduction of thioredoxin (Trx) by NADPH. Like other members of the pyridine nucleotide-disulfide family, TrxR is a homodimer; in the enzyme from *Drosophila melanogaster* (DmTrxR), each catalytically active unit consists of three redox centers: FAD and an N-terminal Cys-57/Cys-62 redox-active disulfide from one monomer, and a Cys-489'/Cys-490' C-terminal redox-active disulfide from the second monomer. Because dipteran insects such as *D. melanogaster* lack glutathione reductase, DmTrxR is particularly important for antioxidant protection; reduced Trx reacts nonenzymatically with glutathione to maintain a high (glutathione disulfide)/(glutathione) ratio. A dyad of His-464' and Glu-469' in TrxR acts as the acid-base catalyst of the dithiol-disulfide interchange reactions required in catalysis [Huang et al., *Biochem.* in press]. In the investigation described in this chapter, the role of Glu-469' in catalysis by DmTrxR was studied. The E469'A and E469'Q DmTrxRs retain 28% and 35% of the wild-type activity, respectively, showing that this glutamate residue is important but not critical to catalysis. The pH dependence of V_{max} for both glutamate variants yields pK_a values of 6.0 and 8.7, compared to those in wild-type enzyme of 6.4 and 9.3, indicating that the basicity of His-464' in TrxR in complex with its substrate, DmTrx-2, is somewhat less in the glutamate variants than in wild type enzyme. The rates of steps in the reductive half reactions in both glutamate variants are less than those of

wild-type enzyme. Based on our observation, it is proposed that the function of Glu-469' is to facilitate the positioning of His-464' toward the interchange thiol, Cys-57, as was suggested for the analogous residue in glutathione reductase.

B. Introduction

The physiological importance and the catalytic mechanism of thioredoxin reductase from *Drosophila melanogaster* (DmTrxR) were described in the second chapter. To summarize, TrxR cycles in catalysis between the EH_2 and EH_4 states; the catalytic mechanism of DmTrxR as shown in Scheme 3.1 implies that Cys-57 attacks the C-terminal disulfide (Cys-489' and Cys-490'). Thus, the thiolate on Cys-57 must be formed to initiate nucleophilic attack. A histidine has been shown to be important in the catalysis of TrxR from *Plasmodium falciparum* and *D. melanogaster* (*1, 2*). This histidine residue is able to act as a base catalyst to facilitate the formation of thiolate anion on Cys-57 and to stabilize the thiolate by forming an ion pair between the cysteine and histidine residues. A glutamate residue nearby the histidine residue has been proposed to be involved in the catalysis of TrxRs from both humans and *P. falciparum* by stabilizing the incipient protonated histidine residue (*2-5*).

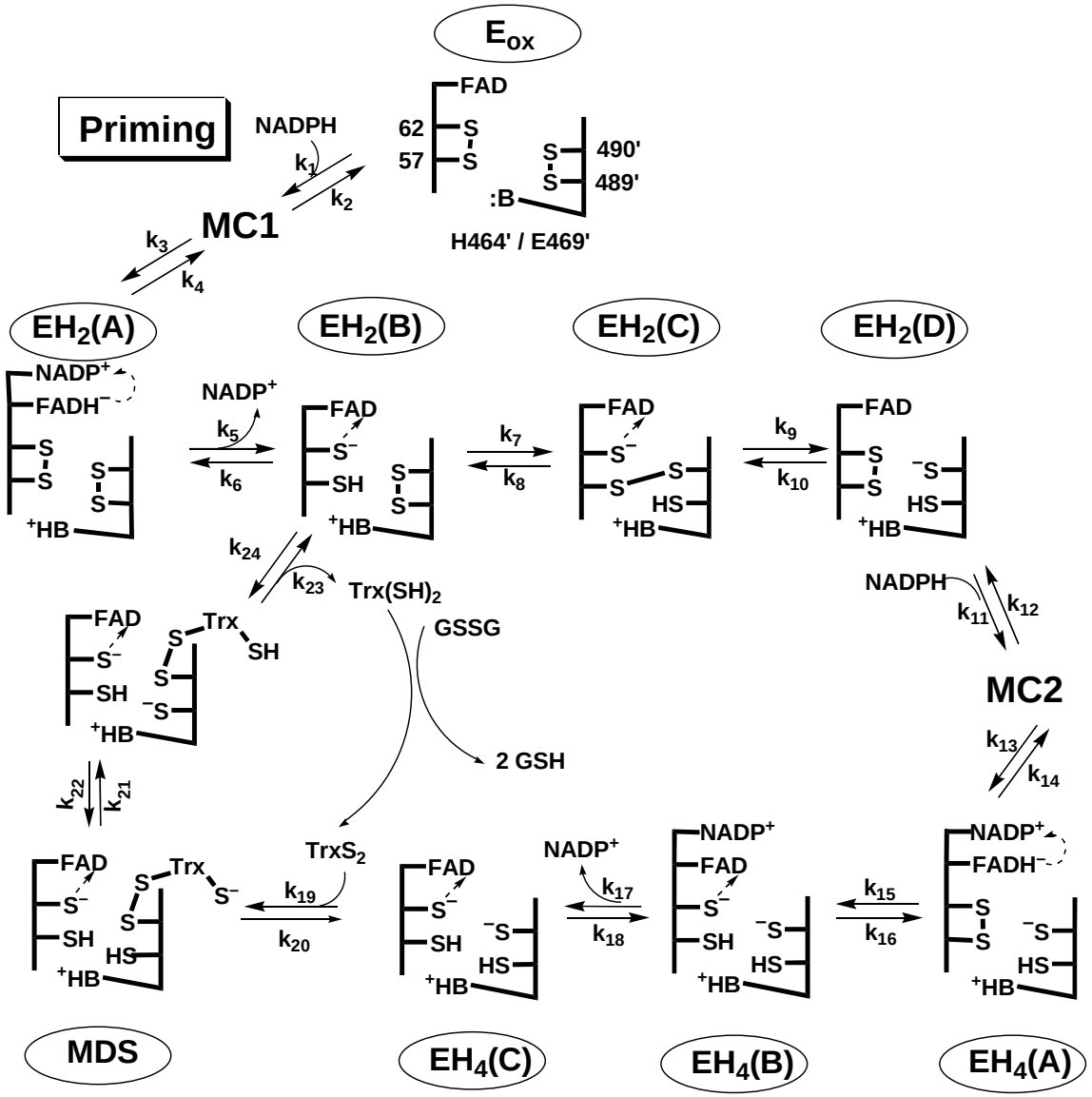

Scheme 3.1 The proposed catalytic mechanism of wild-type DmTrxR. The reductive half-reaction involves the steps denoted by rate constants, k_1-k_{18}, and the oxidative half-reaction involves the steps k_{19}-k_{24}. MC, Michaelis complex; MDS, mixed disulfide. Residues numbered without a prime come from one monomer and those with a prime come from the other monomer. Dashed arrows indicate charge transfer

A similar dyad acting as a general acid-base catalyst has been identified in a variety of enzymes; the dyad, together with the residue that it acts upon, is referred to in this literature as a triad (*6*). The function of such a triad in the serine proteases has been studied extensively (*7-9*); Ser-195, His-57, and Asp-102 form a catalytic triad in chymotrypsin, and initially, Asp-102 was thought to be involved in a so-called charge-relay system with His-57 to convert a weakly nucleophilic $–CH_2OH$ group on Ser-195 to a more reactive alkoxide ion, $–CH_2O^–$. Recently, the charge-relay formalism has been considered to be an unlikely postulate because the pK_a value of His-57 is greater than that of Asp-102, and the pK_a of the Ser hydroxyl is very high (*8*). Thus, Asp-102 would not be expected to be able to sequester a proton from His-57. Subsequent NMR studies suggested that a low barrier hydrogen bond (LBHB, or short, very strong hydrogen bond) is involved in catalysis (*6, 10*). In chymotrypsin, His-57 and Asp-102 form a weak hydrogen bond in the ground state. During catalysis, a LHBH forms when the pK_a values of His-57 and Asp-102 are closely matched, and the distance between the bonding atoms becomes less than the sum of the van der Waals radii (i.e., the distance between oxygen and nitrogen must be less than 2.65 Å) (*10*). Formation of a LBHB is more favorable in a hydrophobic environment, and its formation is thought to lower the activation barrier of a reaction. However, the existence of the LBHB mechanism for chymotrypsin is contentious; the only support for this mechanism comes from results of an NMR study and a low deuterium fractionation factor of the hydrogen in the putative LBHB (*6, 10*).

The structure of GR, a member of the same family of enzymes as TrxR, reveals that the distance between the glutamate oxygen and a histidine nitrogen in the dyad is

only slightly longer than that associated with LBHBs (2.8 Å) (*3, 11*). The role of the analogous glutamate-histidine dyad has been studied in another dithiol-disulfide dehydrogenase, lipoamide dehydrogenase, where it has been found that the glutamate residue is able to modify the acid-base properties of the histidine residue. The glutamate residue also facilitates the orientation of the histidine residue toward the redox-active disulfide to make it more effective. Furthermore, the mutations that substitute glutamine and asparate residues for glutamate change the electron distribution between the FAD and the redox-active cysteine pair (*12, 13*). The glutamate-histidine dyad juxtaposed to the N-terminal redox active disulfide is conserved throughout the enzyme family that includes TrxR, and indeed, the glutamate variants of TrxR from *Plasmodium falciparum* and human have been shown to have low activity (*2, 5*) The function of this glutamate residue in the catalytic mechanism of TrxR has not been studied in detail despite the previous data showing its involvement in catalysis. Based on the crystal structure of DmTrxR (*14*), the distance between ND1 of His-464' and OE2 of Glu-469' is 2.8Å, as shown in Fig 3.1. In addition, the glutamate and histidine residues are both in a hydrophobic environment. Thus, in analogy to chymotrypsin, it may be possible that a LBHB forms between His-464' and Glu-469' during catalysis, enabling this dyad to facilitate formation of thiolate anion of DmTrxR.

To address the function of the glutamate residue in DmTrxR, we have studied the pH dependence of the steady-state kinetics of two glutamate variants, E469'Q and E469'A DmTrxR, and the effect of pH on the properties of the glutamate variants undergoing the reductive half reaction, including the rates of the three phases and the spectra of the intermediates.

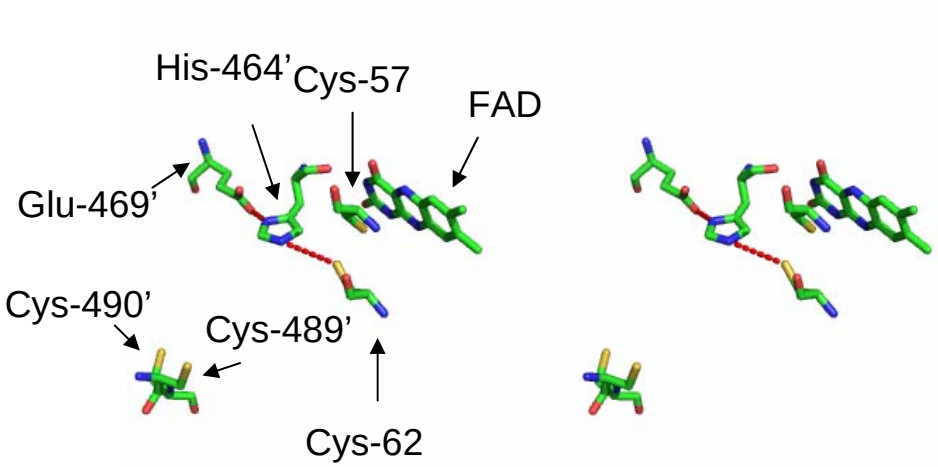

Fig. 3.1 Stereo view showing the relative positions of the amino acid residues in the active site of DmTrxR. The active site contains an FAD, an N-terminal redox-active disulfide (Cys-57 and Cys-62), and a C-terminal terminal redox-active disulfide (Cys-489' and Cys-490'); the Ser-Cys-Cys-Ser motif is at the end of a flexible sequence of amino acid residues that could position Cys-489' or Cys-490' either near the nascent N-terminal dithiol for the interchange reaction, or alternately, near the Trx binding site, as shown here. His-464' is adjacent to the N-terminal redox-active disulfide, and the distance between NE2 of His-464' and the sulfur atom of Cys-57 is 3.69 Å. The distance between ND1 of His-464' and OE2 of Glu-469' is 2.8 Å (*14*). PyMol was applied to generate the image, and the structure used here is based on the structure of rat TrxR (pdb accession code:1H6V) (*15*).

C. Materials and Methods

1. Chemicals

NADPH, lysozyme, FAD, phenylmethylsulfonyl fluoride, leupeptin, pepstatin, tricine, boric acid, citric acid, and GSSG were purchased from Sigma-Aldrich. Nickel-nitrilotriacetic acid agarose for purification of His-tagged proteins was from QIAGEN. Isopropyl-beta-D-thiogalactopyranoside was from Invitrogen. SDS-PAGE gels (4-20%) were purchased from NuSep. All other chemicals and reagents were from Fisher Scientific unless stated.

2. Site-directed mutagenesis

The plasmids of wild-type DmTrxR and DmTrx-2 were kindly provided by S. Gromer, Heidelberg. The cDNA fragments encoding the genes of interest were inserted into the pQE-30 plasmid that allows for expression of N-terminal His-tagged proteins. pQE-30 was obtained from QIAGEN. The sequence of each plasmid was verified by the sequencing core facility at the University of Michigan.

The cloning of the glutamate variants was performed using the QuickChange site-directed mutagenesis kit from Stratagene. The procedure in the manual provided by the manufacturer was followed. A plasmid, pQE-30, having the cDNA fragment of wild-type DmTrxR was used as a template. The sequences of oligonucleotides used in this study are shown in Table A.2.1 (Appendix 2). The sequence of each plasmid was verified by the sequencing core facilitate at the University of Michigan.

3. Preparation of the glutamate variants and DmTrx-2

The preparation methods were similar to those described previously (*16, 17*). Briefly, the bacterial strain, NovaBlue from Novagene, was used for protein expression that was induced by isopropyl-beta-D-thiogalactopyranoside. The harvested cells were suspended in buffer containing 50 mM potassium phosphate, 300 mM NaCl, and 10 mM imidazole. In the preparation of enzymes, 100 μM of FAD was added to the lysate solution to stabilize the enzyme, and the bacteria were treated with lysozyme. The protease inhibitors, phenylmethylsulfonyl fluoride, leupeptin and pepstatin, were added to cell lysates, and the lysates were sonicated. The 6xHis-tagged proteins were isolated from a nickel-nitrilotriacetic acid column by a step-gradient of imidazole. All elution buffers for the preparation of enzymes contained 100 μM FAD. The procedures for isolation of enzymes and substrate were performed in the cold room (4 °C). The purity of each fraction of the glutamate variants and of DmTrx-2 was determined by analysis on 4-20% SDS-PAGE. The imidazole in each fraction was removed by a 10-DG desalting column from Bio-Rad. This procedure, which was quicker than dialysis, avoided the known instability of these proteins during dialysis. The concentrations of the glutamate variants and DmTrx-2 were determined spectrally using values of ε_{462nm} = 11,900 $M^{-1}cm^{-1}$ and ε_{277nm} = 7,320 $M^{-1}cm^{-1}$, respectively (*18, 19*).

4. The determination of activities of the glutamate variant

The activities of the glutamate variants were measured by rates of consumption of NADPH, monitored at 340 nm in the presence of 100 μM NADPH, 50 μM DmTrx-2, and 0.3 mM GSSG in a universal buffer, pH 7.6 (*20*), containing 25 mM borate, 25 mM

monobasic potassium phosphate, 25 mM tricine, and 25 mM citrate (universal buffer). This buffer mixture does not maintain constant ionic strength. Results were corrected for acid-catalyzed hydrolysis of NADPH.

5. Steady-state kinetics of the glutamine variants over a range of pH

The reaction rates of E469'A and E469'Q DmTrxR were determined at various pH values in the universal buffer from the rate of consumption of NADPH using various concentrations of DmTrx-2 and a fixed concentration of NADPH (100 μM) in the presence of GSSG (0.3 mM). Results were corrected for the acid-catalyzed hydrolysis of NADPH. K_m and V_{max} values were derived from a Michaelis-Menten graph of turnover numbers versus concentration of DmTrx-2 fit by the equation for a rectangular hyperbola. The profiles of activity vs. pH were fit to equation 3.1 to obtain the two pK_a values.

$$v = \frac{V_{\max}}{\frac{10^{-pH}}{10^{-pK_a1}} + \frac{10^{-pK_a2}}{10^{-pH}} + 1} \qquad (3.1)$$

6. The kinetics of the reductive half-reactions of the glutamine variants using stopped-flow spectrophotometry

The reductive half-reactions of the glutamate variants were studied by placing NADPH in anaerobic buffer in one syringe, and oxidized enzyme in anaerobic buffer in the other syringe of the Hi-Tech SF-61 DX2 stopped-flow spectrophotometer at 25 °C. Changes in the spectra during the reaction with NADPH were observed using the photodiode array detector, and absorbance changes at single wavelengths were monitored

using the monochromator coupled to a photomultiplier detector. The dead-time of the stopped-flow instrument is 1.5 ms, and the first spectrum was recorded starting 1.5 ms after the stop of flow. The apparent rate constants were derived from single-wavelength data with the KinetAsyst (version 3.16) software from Hi-Tech.

D. Results and discussion

1. The activity of the glutamate variants

The alignment of the protein sequences of TrxRs from different species shows that two adjacent glutamate residues (Glu-469' and Glu-470') are potentially involved in the catalysis of DmTrxR (Fig. A.2.1). Therefore, E469'A and E470'A DmTrxR were cloned and expressed. The activity of E469'A DmTrxR retained 28% of wild-type activity, whereas E470'A DmTrxR retained 70% of wild-type activity (data not shown), indicating that Glu-469' is slightly more important to the catalysis than is Glu-470'. The X-ray structure of DmTrxR, showed that Glu-469' is closer to His-464' in the triad with Cys-57, supporting this conclusion (*14*). Because the proposed role of Glu-469' is to make His-464' a better catalyst, it was of interest to study the effect of pH on the enhancement of His-464' by Glu-469' in DmTrxR, utilizing both polar and apolar replacement residues for Glu-469'. Thus, the effect of pH on the biochemical properties of E469'A and E469'Q DmTrxRs, including steady-state kinetics and the characteristics of the reductive half-reaction, were studied.

In the study of Benen et al., the activities of E455'D and E455'Q lipoamide dehydrogenase from *Azotobacter vinelandii* retained only 1.6% and 1.2% of wild-type activity, respectively, when the NAD^+ analog, 3-acetylpyridine-adenine-dinculedtide, was used as an electron acceptor (lipoamide to NAD^+ direction) (*12*). However, the His variants had even less than one percent of wild-type activity, indicating that Glu was less important than His in the overall catalysis. McMillan et al. showed that E514'A TrxR from *P. falciparum* (PfTrxR) had 7.5 % of the wild-type activity (*2*), again indicating that

Glu was less important than His. E469'A and E469'Q DmTrxR have 28% and 35% of wild-type enzyme activity, respectively, indicating that like other members of the family, this glutamate residue participates, but not critical for the activity of DmTrxR. It is possible that in glutamate variants, the neighboring Glu-470' may provide the function that Glu-469' fulfills in wild type, with only modest alteration of the protein structure. Differences such as that between PfTrxR and DmTrxR might be exploited by medicinal chemists in the design of differential inhibitors that would affect the parasite enzyme to a greater extent than the vector or host enzymes. Thus, similar studies should be extended to the human enzyme.

2. Effect of pH on the steady-state kinetics of the glutamate variants

Because the K_m of NADPH for the wild-type enzyme is less than 2 μM, it is not possible to determine the K_m value of NADPH accurately without resorting to fluorescence techniques. Therefore, in this study, the V_{max} and K_m values for the DmTrx-2 substrate, for E469'A and E469'Q variants at different pH values were determined using a fixed concentration of NADPH (100 μM). As shown in Fig. 3.2, the pH profiles of V_{max} of these two glutamate variants were shifted to more acidic pH values compared to that of the wild-type enzyme. The two pK_a values derived from the pH profiles of V_{max} for E469'A and E469'Q DmTrxRs are identical, pK_a = 6.0 and 8.7. For comparison, the two pK_a values determined for the wild-type enzyme are 6.4 and 9.3. In our previous study, the pK_a of 6.4 in wild-type enzyme in complex with DmTrx-2 was attributed to both Cys-57 and Cys-490' (*1*). This pK_a did not change in H464'Q DmTrxR although the

activity of H464'Q DmTrxR was much less than that of wild-type enzyme, suggesting that the formation of thiolate anion in the variant is feasible but not efficient. In the study presented here, the pK_a of 6.0, contributed by Cys-57 and Cys-490', is quite similar to that of wild-type enzyme, and is consistent with our previous assignment of this macroscopic pK_a value to Cys-57 and Cys490'. The pK_a of 9.3 assigned to His-464' in our previous work, changed to 8.7 in the glutamate variants. This indicates that the basicity of His-464' decreases slightly in the absence of the negatively charged Glu-469'.

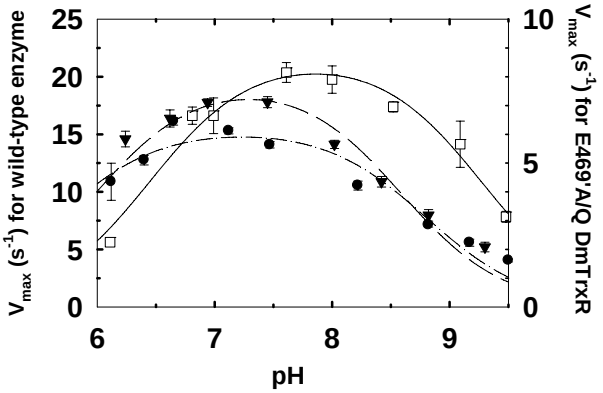

Fig 3.2 The pH profiles of V_{max} for wild-type (□), E469'Q (▼) and E469'A (●) DmTrxR. The turnover numbers were determined from the rate of NADPH consumption with various concentrations of DmTrx2 and a fixed concentration of NADPH (100 μM), in the presence of GSSG (0.3 mM), at different pH values. The K_m and V_{max} values were derived from a graph of turnover number versus concentration of DmTrx-2 fit to an equation for a rectangular hyperbola. The data were fit to Equation 1 to calculate the pK_a values. Note that the y-scales for wild-type and for the E469'A/Q variants are not the same.

The two apparent pK_a values derived from the pH profiles of V_{max}/K_m of the two glutamate variants are 6.8 and 8.9. Both variants have the same apparent pK_a values. The comparison of the values in Fig. 3.3 with those of wild-type enzyme show that they are almost identical (*1*). The pK_a values derived from the pH profile of V_{max}/K_m are the macroscopic pK_a values of free enzyme and substrate. We propose that the pK_a of 6.8 is

contributed by the nascent thiols on Cys-57 and Cys-490'. The pK_a of 8.9 was initially assigned to His-464'. The present work indicates that the assignment should be to the His464'-Glu469' dyad.

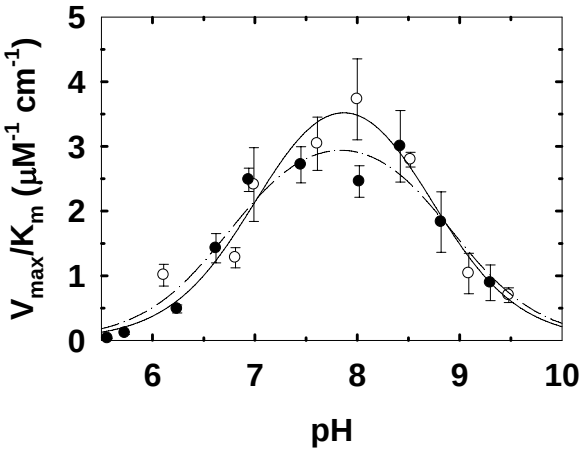

Fig. 3.3 The pH profiles of V_{max}/K_m for wild-type DmTrxR (○) and E469'Q DmTrxR (●). The pH profile of V_{max}/K_m of E469'A DmTrxR is similar to that of E469'Q DmTrxR, but is not shown. The turnover numbers were determined from the rate of NADPH consumption with various concentrations of DmTrx2 and a fixed concentration of NADPH (100 μM) in the presence of GSSG (0.3 mM) at different pH values. The K_m and V_{max} values were derived from a graph of turnover number versus concentration of DmTrx-2 fit to an equation for a rectangular hyperbola. The data in this figure were fit to Equation 1 to calculate the pK_a values.

3. Effect of pH on the reductive half-reaction of E469'Q and E469'A DmTrxR

Our previous results indicated that the rates of flavin reduction and disulfide reduction in the reductive half-reaction of DmTrxR were inhibited profoundly by the mutation of His-464' (reduction and reoxidation of EH_2^A in Scheme 3.1). The reductive half-reactions of E469'Q and E469Q'A DmTrxR were studied here because the proposed function of Glu-469' is to make His-464' a stronger base for its interaction with Cys-57. Figs. 3.4 and 3.5 show spectra observed during the reductive half-reactions of E469'A

and E469'Q DmTrxRs, respectively. Three apparent phases were identified from the kinetic traces shown in the insets. The first phase occurred from the dead time (1.5 ms) to ~10 ms, the second phase from ~10 ms to ~100 ms and the third phase from ~100 ms to ~600 ms. In the first phase, the absorbance at 450 nm decreased and that at 670 nm increased, representing reduction of flavin and the formation of the $FADH^{-}$-$NADP^{+}$ CTC, respectively. These steps are associated with reduction of E_{ox} to EH_2^{A} (Scheme 3.1). In the second phase, the absorbance at 450 nm and 540 nm increased showing partial reoxidation of the flavin and formation of the thiolate-FAD CTC, respectively. Thus, this phase represents the reaction from EH_2^{A} to EH_2^{B} (Scheme 3.1). In the third phase (the slowest one), the absorbance at 450 and 540 nm continued to increase. This phase may not due to a single step, but could reflect the dithiol-disulfide interchange reaction between the N-terminal dithiol and the C-terminal disulfide (EH_2^{B} to EH_2^{D}), and the further reduction of EH_2 with the second molecule of NADPH to EH_4. The data in Figs. 3.4 and 3.5 should be compared with those of the wild-type enzyme in Fig. 2.9.

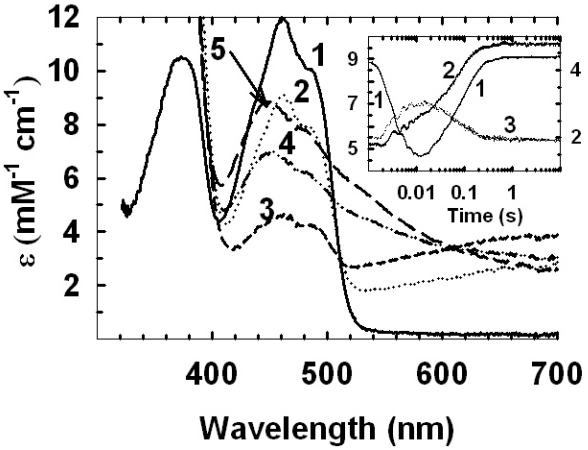

Fig. 3.4 Spectra and kinetics observed in the reductive half-reaction of E469'A DmTrxR. Reduction was carried out at pH 7, 25 °C under anaerobic conditions. Reduction of DmTrxR (10 μM) with 10 equiv of NADPH. Spectrum 1, oxidized enzyme. Spectra 2-5, 3 ms, 10 ms, 100 ms, and 0.6 s after mixing with NADPH. The Inset shows kinetic traces: Curve 1, left y-axis, 450 nm; Curve 2, right y-axis, 540 nm and Curve 3; right y-axis, 670 nm.

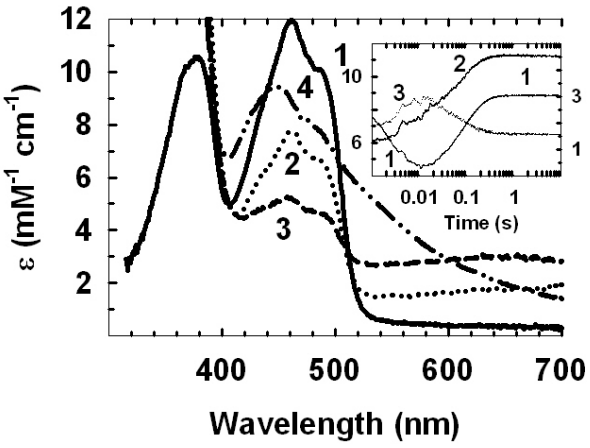

Fig. 3.5 Spectra and kinetics observed in the reductive half-reaction of E469'Q DmTrxR. Reduction was carried out at pH 7, 25 °C under anaerobic conditions. Reduction of DmTrxR (10 μM) with 10 equiv of NADPH. Spectrum 1, oxidized enzyme. Spectra 2-4, 1 ms, 10 ms, and 0.6 s after mixing with NADPH. The Inset shows kinetic traces: Curve 1, left y-axis, 450 nm; Curve 2, right y-axis, 540 nm and Curve 3; right y-axis, 670 nm.

Table 3.1 The apparent rate constants measured during the reductive half reactions of wild-type, E469'Q and E469'A DmTrxR, at different pH values, at 25 °C.

Enzyme[a]	pH	K_d - NADPH (μM)[b]	$k_{1\ app\ max}$ (s^{-1})	$k_{2\ app}$ (s^{-1})	$k_{3\ app}$ (s^{-1})
WT[c]	7	13±4	629±56	237±37	47.4±9.4
WT[c]	8	8±5	562±83	187±12	38±16
WT[c]	9	9±2.8	488±36	170±23	16.4±3.5
E469'A	7	21.5±4.2	432±30	14.2±2.2	8±1.4
E469'A	8	25±3.6	465±25	29±2.0	9.4±3.4
E469'A	9	17±5.5	363±38	69±2.7	26.2±8.2
E469'Q	7	15±2.4	352±17	13.4±1.8	8±1.4
E469'Q	8	20.2±3	370±19	36.6±5.4	10.4±1.4
E469'Q	9	15±6.8	258±7	78.2±6.7	7.1±0.5

[a] The concentration of enzyme was 10 μM.
[b] The $K_{d\ app}$-NADPH values were determined from $k_{1\ app}$ and concentrations of NADPH using an equation for a rectangular hyperbola. The $k_{1\ app}$ reflects the reduction of the flavin.
[c] the data have been shown in Table 2.1.

Compared to those of the wild-type enzyme, the rates of the first phase in the glutamate variants were somewhat smaller (1.2-1.9 fold) (Table 3.1), suggesting that the transfer of hydride ion from NADPH to FAD was only slightly impaired in the glutamate variants. The second phase was much slower than that of the wild-type enzyme at pH 7 (17-18 fold) (Table 3.1), showing that electron transfer from $FADH^-$ to the N-terminal redox-active disulfide was significantly affected by the replacement of Glu-469'. The rate of the second phase of both glutamate variants increased at higher pH values. Because the formation of thiolate anion is favored at higher pH values, the rate of this phase is expected to increase as the pH is increased. As indicated in Table 3.1, the pH effects on the third rate constants for these two glutamate variants are different. The rates observed in the third phase with E469A' DmTrxR were pH dependent (Fig. 3.6), with the rate increasing at higher pH values. As discussed previously, this step is ascribed in part to the dithiol-disulfide interchange reaction between the N-terminal nascent dithiol pair and

the C-terminal redox-active disulfide. Deprotonation of Cys-57, essential for the interchange reaction, will be enhanced at higher pH values.

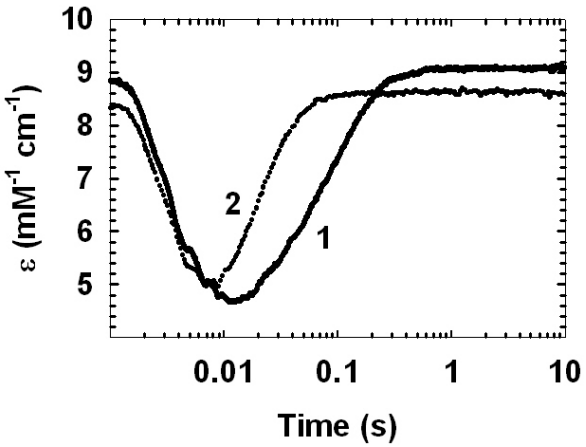

Fig. 3.6 The kinetics at 450 nm in the reductive half-reaction of E469'A DmTrxR at pH 7 (trace 1) and pH 9 (trace 2) cf. wild-type in Fig. 2.9.

In contrast, the rate of the third phase of the reductive half reaction in E469Q' DmTrxR was independent of pH (Fig. 3.7). It is possible that His-464' may still influence the formation of thiolate anion in E469'Q DmTrxR because the active site is more polar ("wild-type"-like) than in E469'A DmTrxR. Our previous study showed that the rate in the third phase with the wild-type enzyme decreased as the pH was increased, as shown in Table 3.1. Although the formation of thiolate anion is favored at high pH, the formation of imidazolium on His-464' is less favorable at higher pH**.** This suggested that the primary function of His-464' is to stabilize the thiolate anion on Cys-57 via ion-pair formation. In E469'Q DmTrxR, a hydrogen bond might form between ND1 of histidine residue and OE1 of glutamine residue. This interaction could facilitate a productive orientation of His-464' toward Cys-57, even if it were not ideal. Thus, the thiolate anion

on Cys-57 would be less stabilized by the imidazolium of His-464'. In addition, deprotonation of Cys-57 in E469'Q DmTrxR is still affected by pH. The interaction of these two linked factors may result in this phase being independent of pH.

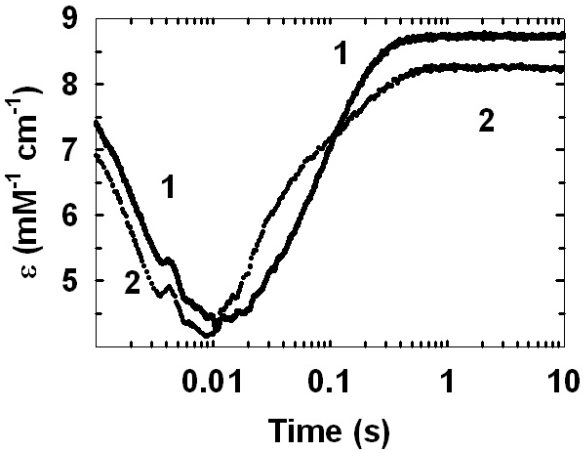

Fig. 3.7 The kinetics at 450 nm in the reductive half-reaction of E469'Q DmTrxR at pH 7 (trace 1) and pH 9 (trace 2) cf. wild-type in Fig. 2.9.

The kinetics of the reductive half reaction of E469'A and E469'Q DmTrxRs at pH 7 are compared with those at pH 9 in Figs. 3.6 and 3.7, respectively. The biphasic nature of the reduction of the N-terminal disulfide by $FADH^-$ was more apparent at pH 9 than at pH 7 with E469'Q DmTrxR. This may reflect two enzyme populations depending on the charge state of His-464'.

Benen et al. showed that the spectra of the reduced glutamate variants of lipoamide dehydrogenase have a high absorbance at 530 nm, contributed by the thiolate-FAD CTC (*13*). In addition, McMillan et al. showed that in E514'A PfTrxR, the thiolate-FAD CTC is enhanced; they proposed that this enhancement might be caused by the hydrophobic side chain of alanine (*2*). Our data shows that the absorbance at 670 nm

contributed by the $FADH^-$-$NADP^+$ CTC was higher in E469'Q and E469'A DmTrxRs than in wild-type enzyme, indicating that the binding of $NADP^+$ to both glutamate variants is tighter (Figs. 3.4 and 3.5, spectrum 3). The thiolate-FAD CTC contributing to absorbance at 540 nm was also enhanced in the glutamate variants (Fig. 3.4, spectra 5 and Fig. 3.5, spectra 4).

The K_d values of NADPH were calculated using plots of the apparent first-order rate constants vs NADPH concentration. As shown in Table 1, the binding of NADPH to the E469'A DmTrxR was slightly less tight than to the wild-type enzyme. Like the wild-type enzyme, the effect of pH on the dissociation constant of NADPH for both glutamate variants was not significant. The second and third rate constants were nearly independent of the concentration of NADPH.

E. Concluding remarks

Malaria is the cause of a serious public health issue globally; 500 million cases are reported and 2.5 million people die of this disease annually (*21*). The malarial parasites of the genus *Plasmodium,* and its vector, *A. gambiae* have extremely high demands for the Trx system because of high rates of production of reactive oxygen species. Structural and mechanistic differences among TrxRs from humans and from *A. gambiae* and *P. falciparum* have been observed. Specifically, in this study, we have discovered that Glu-469' in DmTrxR may be less sensitive to the effects of mutation than is the analogous Glu-514' from the *P. falciparum*. It is hoped that the recognition of these differences may aid in the development of differential inhibitors more specific for TrxR from the parasites.

The thiolate-imidazolium-carboxlate catalytic triad is conserved in the enzymes of the family of pyridine nucleotide-disulfide oxidoreductases, and the glutamate-histidine dyad has been shown to act as an acid-base catalyst (*2-5, 12, 13*). Indeed, the function of the histidine residue in TrxRs has been studied, and this amino acid residue is crucial to catalysis (*1, 2*). However, the role of the glutamate residue in the thioredoxin reductase family had not been fully addressed (*2, 4, 5*). This led us to explore the role of the glutamate residue in the catalysis of DmTrxR.

The examination of sequence alignments shows that TrxRs from dipteran insects have two adjacent glutamate residues (Glu-469' and Glu-470' in DmTrxR), both of which could potentially be involved in the catalysis. Our data showed that Glu-469' is more important than Glu-470' in the catalysis of DmTrxR. It was of interest to study the

biochemical properties of the glutamate variants utilizing both polar and apolar replacement residues for Glu-469'.

The two glutamate variants of Glu-469' lost only ~70 % of their activity, suggesting that this glutamate residue is important but not critical to the catalysis of DmTrxR. The short distance between His-464' and Glu-469' shows that a hydrogen bond exists between these two amino acid residues; formation of a LBHB is possible during the catalysis of DmTrxR if the two residues moved together, as has been observed with the serine proteases. The V_{max} vs pH profile shows that the mutation of Glu-469' causes a slight decrease in the basicity of His-464' in complex of the enzyme with DmTrx-2.

The rates of the three phases of the reductive half-reaction were inhibited in both glutamate variants. The second phase, associated with reduction of the N-terminal disulfide by $FADH^-$, and the third phases, associated in part with dithiol-disulfide interchange, were significantly slower in both glutamate variants. The inhibitory effects due to the mutation of Glu-469' on the second and third phases were less at higher pH values in E469'A DmTrxR, as would be expected because the formation of thiolate anion is favored at higher pH values.

The data from this study, strongly indicate that the function of Glu-469' is to enhance the basicity of His-464', perhaps by facilitating its orientation toward Cys-57.

References

1. Huang, H. H., Arscott, L. D., Ballou, D. P., and Williams, C. H., Jr. Acid-base catalysis in the mechanism of thioredoxin reductase from Drosophila melanogaster (accepted by Biochemistry).
2. McMillan, P. J., Arscott, L. D., Ballou, D. P., Becker, K., Williams, C. H., Jr., and Muller, S. (2006) Identification of acid-base catalytic residues of high-Mr thioredoxin reductase from Plasmodium falciparum, *J Biol Chem 281*, 32967-32977.
3. Pai, E. F., and Schulz, G. E. (1983) The catalytic mechanism of glutathione reductase as derived from x-ray diffraction analyses of reaction intermediates, *J Biol Chem 258*, 1752-1757.
4. Brandt, W., and Wessjohann, L. A. (2005) The functional role of selenocysteine (Sec) in the catalysis mechanism of large thioredoxin reductases: proposition of a swapping catalytic triad including a Sec-His-Glu state, *Chembiochem 6*, 386-394.
5. Gromer, S., Wessjohann, L. A., Eubel, J., and Brandt, W. (2006) Mutational studies confirm the catalytic triad in the human selenoenzyme thioredoxin reductase predicted by molecular modeling, *Chembiochem 7*, 1649-1652.
6. Cleland, W. W., Frey, P. A., and Gerlt, J. A. (1998) The low barrier hydrogen bond in enzymatic catalysis, *J Biol Chem 273*, 25529-25532.
7. Craik, C. S., Roczniak, S., Largman, C., and Rutter, W. J. (1987) The catalytic role of the active site aspartic acid in serine proteases, *Science 237*, 909-913.
8. Ishida, T., and Kato, S. (2004) Role of Asp102 in the catalytic relay system of serine proteases: a theoretical study, *J Am Chem Soc 126*, 7111-7118.
9. Sprang, S., Standing, T., Fletterick, R. J., Stroud, R. M., Finer-Moore, J., Xuong, N. H., Hamlin, R., Rutter, W. J., and Craik, C. S. (1987) The three-dimensional structure of Asn102 mutant of trypsin: role of Asp102 in serine protease catalysis, *Science 237*, 905-909.
10. Frey, P. A., Whitt, S. A., and Tobin, J. B. (1994) A low-barrier hydrogen bond in the catalytic triad of serine proteases, *Science 264*, 1927-1930.
11. Karplus, P. A., and Schulz, G. E. (1987) Refined structure of glutathione reductase at 1.54 A resolution, *J Mol Biol 195*, 701-729.
12. Benen, J., van Berkel, W., Dieteren, N., Arscott, D., Williams, C., Jr., Veeger, C., and de Kok, A. (1992) Lipoamide dehydrogenase from Azotobacter vinelandii: site-directed mutagenesis of the His450-Glu455 diad. Kinetics of wild-type and mutated enzymes, *Eur J Biochem 207*, 487-497.
13. Benen, J., van Berkel, W., Zak, Z., Visser, T., Veeger, C., and de Kok, A. (1991) Lipoamide dehydrogenase from Azotobacter vinelandii: site-directed mutagenesis of the His450-Glu455 diad. Spectral properties of wild type and mutated enzymes, *Eur J Biochem 202*, 863-872.
14. Eckenroth, B. E., Rould, M. A., Hondal, R. J., and Everse, S. J. (2007) Structural and biochemical studies reveal differences in the catalytic mechanisms of mammalian and Drosophila melanogaster thioredoxin reductases, *Biochemistry 46*, 4694-4705.

15. Sandalova, T., Zhong, L., Lindqvist, Y., Holmgren, A., and Schneider, G. (2001) Three-dimensional structure of a mammalian thioredoxin reductase: implications for mechanism and evolution of a selenocysteine-dependent enzyme, *Proc Natl Acad Sci U S A 98*, 9533-9538.
16. Kanzok, S. M., Fechner, A., Bauer, H., Ulschmid, J. K., Muller, H. M., Botella-Munoz, J., Schneuwly, S., Schirmer, R., and Becker, K. (2001) Substitution of the thioredoxin system for glutathione reductase in Drosophila melanogaster, *Science 291*, 643-646.
17. Bauer, H., Kanzok, S. M., and Schirmer, R. H. (2002) Thioredoxin-2 but not thioredoxin-1 is a substrate of thioredoxin peroxidase-1 from Drosophila melanogaster: isolation and characterization of a second thioredoxin in D. Melanogaster and evidence for distinct biological functions of Trx-1 and Trx-2, *J Biol Chem 277*, 17457-17463.
18. Bauer, H., Massey, V., Arscott, L. D., Schirmer, R. H., Ballou, D. P., and Williams, C. H., Jr. (2003) The mechanism of high Mr thioredoxin reductase from Drosophila melanogaster, *J Biol Chem 278*, 33020-33028.
19. Cheng, Z., Arscott, L. D., Ballou, D. P., and Williams, C. H., Jr. (2007) The relationship of the redox potentials of thioredoxin and thioredoxin reductase from Drosophila melanogaster to the enzymatic mechanism: reduced thioredoxin is the reductant of glutathione in Drosophila, *Biochemistry 46*, 7875-7885.
20. Kooter, I. M., Steiner, R. A., Dijkstra, B. W., van Noort, P. I., Egmond, M. R., and Huber, M. (2002) EPR characterization of the mononuclear Cu-containing Aspergillus japonicus quercetin 2,3-dioxygenase reveals dramatic changes upon anaerobic binding of substrates, *Eur J Biochem 269*, 2971-2979.
21. Linares, G. E., and Rodriguez, J. B. (2007) Current status and progresses made in malaria chemotherapy, *Curr Med Chem 14*, 289-314.

Chapter 4: Conclusions and Potential Future Work

Malaria is a serious public health issue in the world; 500 million cases are reported and 2.5 million people, mostly children, die of this disease annually (*1, 2*). Malarial parasites have developed resistance to anti-malarial drugs, which have therefore become less effective for prevention of malaria. Thus, new prophylactics need to be developed to treat this disease. Malarial parasites and their vectors, dipteran insects, require the thioredoxin (Trx) system to provide reducing equivalents for antioxidant activities (*3, 4*). Differences among thioredoxin reductases (TrxRs) from human, *Plasmodium falciparum*, and *Diptera* (e.g., *Drosophila melanogaster* and *Anopheles gambiae*, a vector of malarial parasites) have been identified (*1, 5-10*). Thus, it is hoped that these differences will be useful to medicinal chemists in the development of inhibitors of the host-vector enzyme relative to the enzyme from the parasite. TrxRs from *D. melanogaster* (DmTrxR) and *A. gambiae* are nearly identical, structurally. Therefore, DmTrxR offers a good model to study TrxRs from *Diptera*, as explained earlier is this dissertation.

The catalytic mechanism of DmTrxR has been established, showing that two dithiol-disulfide interchange reactions are essential for catalysis. A dyad of His-464' and Glu-469' has been shown to act as the acid-base catalyst to facilitate the formation of thiolate anion to initiate the interchange reaction. The functions of His-464' and Glu-469' in DmTrxR were investigated in this study. To understand the function of His-464', wild-type and H464'Q DmTrxR were cloned and expressed. The kinetic, spectroscopic, and

catalytic properties of wild-type and H464'Q DmTrxR as function of pH were compared to test how His-464' might function as an acid-base catalyst. The results of steady-state kinetic analysis indicated that two cysteine residues need to be deprotonated, and His-464' must be protonated for maximal activity. Spectroscopic studies showed that H464'Q DmTrxR can be fully reduced to EH_6 in the present of excess NADPH, while wild-type enzyme is only reduced to EH_4, suggesting that the relative redox potentials of the three redox centers are altered in H464'Q DmTrxR. Analysis of rapid kinetic experiments showed that His-464' is involved in both the reductive and oxidative half reactions, which is consistent with His-464' acting as an acid-base catalyst in dithiol-disulfide exchange reactions and stabilizing the thiolate anion on Cys-57 and Cys490' via ion-pair formation.

To address the function of Glu-469', the variants, E469'A and E469'Q DmTrxR, were cloned and expressed. The activity of these two glutamate variants indicated that this glutamate residue is important but not crucial. The rates of the reductive half reactions of the two glutamate variants were slower than those of wild-type enzyme. Based on our observations, Glu-469' facilitates the positioning of His-464' toward the interchange thiol, Cys-57 and also makes His-464' a better base.

When the His-464'-Glu-469' dyad is modified so that it cannot function as an acid-base catalyst, the activity of DmTrxR is observed to decrease, suggesting that the dyad may be a good target for inhibitors of DmTrxR. Certain gold compounds are generally thought to attack thiol groups of cysteine residues of certain enzymes to inhibit their activity. However, it has been shown that a gold compound, $Au(PEt)_3Cl$, is able to interact with a His-133 in the active site of cyclophilins-3 in spite of the presence of 4

solvent-accessible cysteine residues (*11, 12*). Therefore, His-464' could be a target for certain inhibitors of DmTrxR. In addition, in DmTrxR, two glutamate residues (Glu-469' and Glu-470') are potentially able to make His-464' a better catalyst, whereas only one glutamate residue is found in thioredoxin reductase from *P. falciparum* (PfTrxR) (*1*). This difference may help medicinal chemists develop inhibitors affecting PfTrxR to a greater extent than the vector enzyme. Overall, in these studies, the His-464'-Glu-469' dyad has been shown to be very important to the catalysis of DmTrxR and these results may be helpful in the development of inhibitors of host-vector enzyme relative to the enzyme from the parasite.

The results from this study suggest that several further experiments could be done to address the roles of His-464' and Glu-469' in the catalysis of DmTrxR.

Goal 1: Determination of redox potentials of E_{ox}/EH_2 and EH_2/EH_4 of H464'Q DmTrxR

In our study, the redox potentials of three redox centers appeared to be different in H464'Q DmTrxR than in wild-type enzyme. Determination of macroscopic redox potentials of E_{ox}/EH_2 and EH_2/EH_4 of H464'Q DmTrxR would be useful for understanding how DmTrxR functions in cells that do not have His-464' to function as an acid-base catalyst.

Experiment:

Cheng et al. have determined the macroscopic redox potentials of E_{ox}/EH_2 and EH_2/EH_4 of wild-type DmTrxR (*13*). Their methods can be applied to determine the redox potentials of E_{ox}/EH_2 and EH_2/EH_4 of H464'Q DmTrxR. The redox potential of

E_{ox}/EH_2 of H464'Q DmTrxR can be determined by a spectroscopic method. The redox potentials of EH_2/EH_4 can be determined by steady-state kinetics experiments using the Haldane relationship, as was done by Cheng et al.

Anticipated results:

Because H464'Q DmTrxR can be completely reduced by NADPH, the redox potential of and EH_2/EH_4 of H464'Q DmTrxR should be considerably higher than that of wild-type DmTrxR. It has been shown that the macroscopic redox potentials of EH_2/EH_4 of wild-type DmTrxR is more negative than that of DmTrx-2, thereby allowing electron transfer from wild-type DmTrxR to oxidized DmTrx-2 (*13*). In contrast, the redox potential of EH_2/EH_4 of H464'Q DmTrxR should be higher than that of wild-type DmTrxR; therefore, in H464'Q DmTrxR, electron transfer from the histidine variant to oxidized DmTrx-2 should be less favorable.

Goal 2. To determine how electron transfer from the N-terminal redox-active dithiol to the C-terminal redox-active disulfide is affected in H464'Q DmTrxR

The function of His-464' is to facilitate the formation of the thiolate anion on Cys-57; therefore, the rate of transfer of reducing equivalents from the nascent N-terminal dithiol to the C-terminal disulfide should be affected by the mutation of His-464' (k_7 in Scheme 2.1). In our study, the effect of His-464' on this rate was not specifically determined.

Experiment:

The C-terminal dithiol has been shown to be modified by 5,5'-dithiobis-(2-nitrobenzoic acid) (DTNB) when PfTrxR is reduced (*14*). When wild-type and H464'Q

DmTrxR are reduced by dithiothreitol, the C-terminal dithiol of wild-type and H464'Q DmTrxR could be modified by DTNB to form mixed disulfides containing the enzyme thiol and thionitrobenzoate (TNB). As these mixed disulfides are reduced, the release of TNB anion could be detected by an increase in absorbance at 412 nm. Therefore, the rate of release of TNB anion, which can be measured when these enzymes are reduced (e.g., by NADPH), would serve as a monitor of the interchange reaction. The effect of His-464' on this specific step could be determined by this method.

Anticipated results:

The effect of His-464' on the electron transfer from the N-terminal dithiol to the C-terminal disulfide could be determined using this method. Because the function of His-464' is to facilitate the formation of thiolate anion on Cys-57, the rate should decrease in H464'Q DmTrxR compared that of wild-type enzyme.

Goal 3. To investigation whether a lag phase in the oxidative half reactions of wild-type and H464'Q DmTrxR is due to $NADP^+$ dissociation

A lag phase was observed in the oxidative half reaction of wild-type and H464'Q DmTrxR. This phase was also observed in the oxidative half reaction of PfTrxR, and it was postulated that dissociation of $NADP^+$ from the enzyme is the likely cause (*1*).

Experiment:

In order to test this suggestion, alternative reducing agents (e.g., dithionite and NADH) can be applied. Because these reducing agents are not physiological substrates, presumably, their products would not bind tightly and the lag phase would disappear.

Anticipated results:

Because dissociation of $NADP^+$ from enzyme is the likely cause, it is expected that the lag phase in the oxidative half reaction of wild-type and H464'Q DmTrxR would disappear when other non-physiological reducing agents are used.

Goal 4: To investigate whether Glu-470' is an alternate for Glu-469'

DmTrxR has two adjacent glutamate residues (Glu-469' and Glu-470') in the active site. As discussed in Chapter 3, the glutamate variants had ~ 30% of the wild-type activity. We cannot exclude that Glu-470' might fulfill the role of Glu-469'. Therefore, double mutants might help to resolve this speculation.

Experiment:

Site-directed mutagenesis can be applied to create double mutants to test our hypothesis. The activity of the double mutants can be measured to determine whether Glu-470' is an alternate for Glu-469'. In addition, the reductive and oxidative half reactions of the double mutants also can be studied.

Anticipated results:

Assuming Glu-470' is an alternate for Glu-469', the activity of the double mutants should decrease compared to that of the Glu-469' variants. In addition, the apparent rates of the reductive and oxidative half reactions of the double mutants should be much slower than those of the Glu-469' variants.

Goal 5: To determine the effect of Glu-469' on the oxidative half reaction of two glutamate variants

Because the pH effects on the oxidative half reactions of wild-type and H446'Q DmTrxR were not significant, the pH effects on the oxidative half reactions of the

glutamate variants presumably may not be obvious either. However, it will be of interest to study the oxidative half reaction of the glutamate variants to investigate how this glutamate residue affects this half reaction.

Experiment:

The oxidative half reactions of the Glu-469' variants can be studied using double-mixing stopped-flow technique. The Glu-469' variants will be pre-reduced by reducing agents (e.g., NADPH and dithionite) followed by mixing with Trx. The evolving changes in the spectra during the reaction with reducing agents will be observed using the photodiode array detector, and absorbance changes at single wavelengths will be collected using the monochromator and a photomultiplier detector.

Anticipated results:

The oxidative half reactions of E469'A and E469'Q DmTrxR should be slower compared to that of wild-type enzyme because His-464' has been shown to be involved in oxidative half reaction and His-464' does not function well in the Glu-469' variants.

Goal 5: To determine the effect of Glu-469' on the oxidative half reaction of two glutamate variants

Because the pH effects on the oxidative half reactions of wild-type and H464'Q DmTrxR were not significant, the pH effects on the oxidative half reactions of the glutamate variants presumably may not be obvious either. However, it will be of interest to study the oxidative half reaction of the glutamate variants to investigate how this glutamate residue affects this half reaction.

Experiment:

The oxidative half reactions of the Glu-469' variants can be studied using double-mixing stopped-flow technique. The Glu-469' variants will be pre-reduced by reducing agents (e.g., NADPH and dithionite) followed by mixing with Trx. The evolving changes in the spectra during the reaction with reducing agents will be observed using the photodiode array detector, and absorbance changes at single wavelengths will be collected using the monochromator and a photomultiplier detector.

Anticipated results:

The oxidative half reactions of E469'A and E469'Q DmTrxR should be slower compared to that of wild-type enzyme because His-464' has been shown to be involved in oxidative half reaction and His-464' does not function well in the Glu-469' variants.

References

1. McMillan, P. J., Arscott, L. D., Ballou, D. P., Becker, K., Williams, C. H., Jr., and Muller, S. (2006) Identification of acid-base catalytic residues of high-Mr thioredoxin reductase from Plasmodium falciparum, *The Journal of Biologial Chemisrty 281*, 32967-32977.
2. Linares, G. E., and Rodriguez, J. B. (2007) Current status and progresses made in malaria chemotherapy, *Current medicinal chemistry 14*, 289-314.
3. Kanzok, S. M., Schirmer, R. H., Turbachova, I., Iozef, R., and Becker, K. (2000) The thioredoxin system of the malaria parasite Plasmodium falciparum. Glutathione reduction revisited, *The Journal of Biologial Chemisrty 275*, 40180-40186.
4. Kanzok, S. M., Fechner, A., Bauer, H., Ulschmid, J. K., Muller, H. M., Botella-Munoz, J., Schneuwly, S., Schirmer, R., and Becker, K. (2001) Substitution of the thioredoxin system for glutathione reductase in Drosophila melanogaster, *Science (New York, N.Y 291*, 643-646.
5. Arscott, L. D., Gromer, S., Schirmer, R. H., Becker, K., and Williams, C. H., Jr. (1997) The mechanism of thioredoxin reductase from human placenta is similar to the mechanisms of lipoamide dehydrogenase and glutathione reductase and is distinct from the mechanism of thioredoxin reductase from Escherichia coli, *Proceedings of the National Academy of Sciences of the United States of America 94*, 3621-3626.
6. Zhong, L., Arner, E. S., and Holmgren, A. (2000) Structure and mechanism of mammalian thioredoxin reductase: the active site is a redox-active selenolthiol/selenenylsulfide formed from the conserved cysteine-selenocysteine sequence, *Proceedings of the National Academy of Sciences of the United States of America 97*, 5854-5859.
7. Zhong, L., and Holmgren, A. (2000) Essential role of selenium in the catalytic activities of mammalian thioredoxin reductase revealed by characterization of recombinant enzymes with selenocysteine mutations, *The Journal of Biologial Chemisrty 275*, 18121-18128.
8. Bauer, H., Gromer, S., Urbani, A., Schnolzer, M., Schirmer, R. H., and Muller, H. M. (2003) Thioredoxin reductase from the malaria mosquito Anopheles gambiae, *European journal of biochemistry / FEBS 270*, 4272-4281.
9. Bauer, H., Massey, V., Arscott, L. D., Schirmer, R. H., Ballou, D. P., and Williams, C. H., Jr. (2003) The mechanism of high Mr thioredoxin reductase from Drosophila melanogaster, *The Journal of Biologial Chemisrty 278*, 33020-33028.
10. Gromer, S., Johansson, L., Bauer, H., Arscott, L. D., Rauch, S., Ballou, D. P., Williams, C. H., Jr., Schirmer, R. H., and Arner, E. S. (2003) Active sites of thioredoxin reductases: why selenoproteins?, *Proceedings of the National Academy of Sciences of the United States of America 100*, 12618-12623.
11. Zou, J., Taylor, P., Dornan, J., Robinson, S. P., Walkinshaw, M. D., and Sadler, P. J. (2000) First Crystal Structure of a Medicinally Relevant Gold Protein Complex: Unexpected Binding of, *Angew Chem Int Ed Engl 39*, 2931-2934.
12. Urig, S., and Becker, K. (2006) On the potential of thioredoxin reductase inhibitors for cancer therapy, *Seminars in cancer biology 16*, 452-465.

13. Cheng, Z., Arscott, L. D., Ballou, D. P., and Williams, C. H., Jr. (2007) The relationship of the redox potentials of thioredoxin and thioredoxin reductase from Drosophila melanogaster to the enzymatic mechanism: reduced thioredoxin is the reductant of glutathione in Drosophila, *Biochemistry 46*, 7875-7885.
14. Wang, P. F., Arscott, L. D., Gilberger, T. W., Muller, S., and Williams, C. H., Jr. (1999) Thioredoxin reductase from Plasmodium falciparum: evidence for interaction between the C-terminal cysteine residues and the active site disulfide-dithiol, *Biochemistry 38*, 3187-3196.

Appendices

Appendix 1

A. Cellular targets of reactive oxygen species

It is estimated that 1.5×10^5 oxidative events occur in each cell each day and that 1-3% of the reactions in respiration can result in formation of reactive oxygen species (ROS) (*1*). ROS are able to react with macromolecules such as lipids, proteins, and nucleotides, resulting in development of various diseases. Several examples are given in the following sections.

1. Lipid peroxidation

The polyunsaturated fatty acids of phospholipids are vulnerable to ROS. Lipid peroxides are produced from the oxidation of lipids even though there are numerous ROS detoxification systems in cells. The formation of lipid peroxides results in changes in membrane fluidity, dysfunction of the proteins in membranes, and cell death (*2*). Lipid peroxides can undergo lipid peroxidation that is mediated by iron and oxygen to produce reactive aldehydes *in vitro*. Two major products are malondialdehyde (MDA) and 4-hydroxynonenal (HNE) (*2*). MDA is mutagenic in both bacterial and mammalian cells, and exhibits a carcinogenic effect in rats; HNE is a weak mutagen but appears to be a major toxic product of lipid peroxidation (*3, 4*). These two compounds are able to attack DNA and proteins (discussed below). It has been found that oxidation of low density lipoprotein is a cause of atherosclerosis (*5*).

2. DNA adducts

Among ROS, hydroxyl radical and peroxynitrite have redox potentials low enough to form covalent adducts that possibly cause mutagenesis, carcinogenesis, or even cell death (*3*). ROS can attack DNA bases as well as the deoxyribose residue. In addition, the reactive products from lipid peroxidation (e.g., MDA and HNE) are also able to damage DNA (*3*). Due to the limits of detection, certain DNA lesions are not easily detected. A myriad of DNA adducts have been identified, such as 8-oxo-deoxyguanosine (8-oxo-dG), thymine glycol, and 5-hydroxymethyluracil. 8-Oxo-dG may not be the most common form of damaged DNA; however, it has been extensively studied because it is readily detected (*3*). The formation of 8-oxo-dG results in transversion (e.g., G:C to T:A) and this type of change is commonly observed in both oncogenes and tumor suppressor genes (*6*).

3. Protein oxidation

The side chains of amino acid residues, especially cysteine and methionine, can be oxidized by ROS (*4*). Methionine sulfoxide is formed from the oxidation of methionine. The oxidation of cysteine produces sulfenic (–SOH), sulfinic ($–SO_2H$) and sulfonic ($–SO_3H$) acids (*7*). Oxidation of some amino acid residues (e.g. lysine, arginine and proline) will form carbonyl derivatives (*8*) that can also be produced from the oxidation of amino acid residues by the products of lipid peroxidation (*8*). Because carbonyl derivatives are major products in ROS-damaged proteins, they act as the biomarkers of oxidative damage (*1, 8*).

B. Cellular antioxidant systems

To neutralize ROS, several antioxidants constitute an intracellular antioxidant network made up of enzymatic and non-enzymatic components. Superoxide dismutase, catalase, the glutathione (GSH)-glutathione reductase system, and the Trx-TrxR system are examples of enzymatic components and nonenzymatic antioxidants include ascorbate (vitamin C) and vitamin E. The following is a brief review of these components.

1. Superoxide dismutase

Superoxide dismutase (SOD; E.C.1.15.1.1) efficiently catalyzes the dismutation of superoxide anion to form hydrogen peroxide and oxygen (rate constant is equal to 1.6×10^9 M^{-1} s^{-1}; Reaction A.1). If superoxide anions are not scavenged by SOD, superoxide anions will have a chance to interact with hydrogen peroxide to form hydroxyl radicals (Reaction 1.5 in Chapter 1).

Three types of SODs have been identified in eukaryotic cells: cytosolic Cu/Zn SOD (SOD-1), mitochondrial Mn-SOD (SOD-2), and extracellular SOD (SOD-3). Prokaryotic and plant cells possess Fe-SOD (*9*). Cu/Zn SOD is a cytosolic dimeric protein with a M_r of 32,000. Mn-SOD is an 80-kDa tetrameric protein. Extracellular SOD contains Cu and Zn as cofactors and it is tetrameric and glycosylated. Unlike SOD-1, SOD-3 has an affinity to heparin, thereby allowing SOD-3 to bind to endothelial and other cells (*10, 11*). Among these three types of enzymes, Mn-SOD seems very important, because it is associated with apoptosis. Mn-SOD knockout (KO) mice die soon after birth or develop a severe neurodegeneration disorder (*11*). SOD-1 KO mice do

not show any significant anomalies relative to wild-type organisms, but their life spans are decreased (*9*).

Multiple factors, such as copper- and zinc-deficient diets, can contribute to the loss of activity of SOD in the body, because the enzymes require these metal ions as cofactors (*9*). In addition, mutation of SOD-1 is found in some patients with the familiar amyotrophic lateral sclerosis (also called ALS or Lou Gehrig's disease). The evidence indicates that this disease is caused by mutants of SOD-1 that aggregate as plaques from the increased levels of unfolded proteins (*12*).

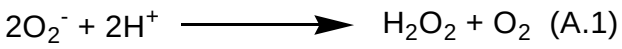

(A.1)

2. Catalase

Catalase (EC 1.11.1.6) catalyzes the conversion of hydrogen peroxide to water and oxygen (Reaction A.2); therefore, it can prevent the formation of hydroxyl radicals via the Fenton reaction. The predominant catalase-containing organelle in mammalian cells is the peroxisome (*11*).

(A.2)

Three subgroups of catalases have been classified. Two of them are heme-containing enzymes: monofunctional heme catalases (typical catalase) and catalase-peroxidase, and the third one is (nonheme) manganese catalase (*13*). A typical catalase is a homotetramer of 50,000-85,000 MW monomers and contains four prosethetic heme groups. It is able to reduce not only hydrogen peroxide but also of short-chain aliphatic

peroxides (*13, 14*). Catalase-peroxidase is only found in fungi in the eukaryotic kingdom. The activity of catalase-peroxidase is 2 to 3 orders of magnitude less than that of a typical catalase and the K_m for hydrogen peroxide for catalase-peroxidase is higher than that of a typical catalase by 1 to 2 orders of magnitude. Three species carrying manganese catalase have been identified; manganese catalase can form an oligomeric structure (*13*).

3. The glutathione-glutathione reductase system and its cellular functions

The glutathione (GSH)-glutathione reductase (GR) system is composed of GSH (tripeptide γ-L-glutamyl-L-cysteinyl-glycine) and GR. The system provides GSH for glutathione peroxidase (GPx), glutaredoxin (Grx), and glutathione-S-transferase (GST) (see below). GSH is the most abundant intracellular thiol antioxidant, being at millimolar concentrations in cells. GSH is highly soluble due to the side chains of the tripeptide. The intracellular redox potentials created by the ratios of GSH/GSSG at very high concentrations are in the range of –260 mV to –150 mV (the more oxidized values are only observed in cells undergoing apoptosis) (*15*). GSH is able to pass reducing equivalents to other enzymes or oxidants by its redox-active sulfhydryl group. The most important function of GSH in cells is to detoxify oxidants. GSH is able to donate reducing equivalents to other detoxification enzymes, such as GPx in order to neutralize peroxides (see discussion below). GSH can interact directly with hydroxyl radical, lipid peroxides, and the tocopherol radical of Vitamin E. GSH also reacts with several electrophiles and xenobiotics via GSH-S-transferase (*16*).

Excess NO will combine with GSH to form the S-nitrosoglutathione adduct (GSNO). GSNO can be reduced by TrxR or by Trx to liberate GSH and NO (Reaction

A.3) (*17*). Thus, this mechanism may prolong the half-life of NO in the body; in addition, GSNO may regulate the activity of the Trx system *in vivo*. Moreover, GSH is involved in several biosynthetic pathways (e.g., formaldehyde dehydrogenase and prostaglandins D_2 and E_2).

$$Trx(SH)_2 + GSNO + O_2 \longrightarrow Trx\text{-}S_2 + GSH + H^+ + {\cdot}NO + {\cdot}O_2^- \quad (A.3)$$

GSH is oxidized to glutathione disulfide (GSSG) after its reaction with oxidants. It is clear that the ratio of GSH to GSSG controls several normal cellular functions. The GSH/GSSG ratio is increased as cells are stimulated by growth factors, while a decrease in the GSH/G ratio by ROS will lead to the expression of multiple genes responsible for antioxidants or apoptotic pathways (*15*). Oxidative stress results in rapid deletion of GSH, which decreases the GSH/GSSG ratio. At least three processes can restore the normal GSH/GSSG ratio. First, the efflux of GSSG from cytosol to an extracellular environment can be mediated by transmembrane transporters. Second, GSSG can be reduced to GSH by GR utilizing NADPH (Reaction A.4). Finally, the depletion of GSH can be restored by *de vovo* synthesis of GSH (*18*).

$$GSSG + NADPH + H^+ \longrightarrow 2GSH + NADP^+ \quad (A.4)$$

As the concentration of intracellular GSSG increases, GSSG can exchange with the sulfhydryl groups of certain proteins to form protein-glutathione mixed disulfides, a process referred to as S-glutathionylation (*19*). S-glutathionylation is recognized as a

regulatory mechanism of protein activity (*20*) because it prevents the sulfhydryl groups of certain cysteine residues from reacting with ROS to form sulfonic acids; a sulfonic acid is resistant to reduction by cellular antioxidants. The mechanism of S-glutathionylation is very complex. The GSH/GSSG ratio modulates S-glutathionylation. As the GSH/GSSG ratio is restored, deglutathionylation by GSH, glutaredoxin, Trx or GST will occur. Some targeted proteins will lose their activities upon S-glutathionylation, but some require S-glutathionylation to achieve complete activation (*21*). Stimulated by ROS, the Ras regulator can be activated by S-glutathionylation, specifically on Cys-118 and will subsequently activate ERK (extracellular signal-regulated kinase) and AKT (acutely transforming retrovirus AKT8 in rodent T cell lymphoma). This regulatory mechanism has recently been reviewed extensively (*21*). S-glutathionylated adducts have been identified in enzymes with critical thiol groups (e.g., carbonic anhydrase III), signal proteins (e.g., MEKK1; MAPK/ERK kinase kinase 1), transcription factors (e.g., NF-κB), heat shock proteins and mitochondrial proteins (e.g., complex I).

GSH is synthesized *de novo* by the action of two ATP-dependent enzymes: glutamate cysteine ligase;GCL (or γ-glutamylcysteine synthetase; γ–GCS), and glutathione synthetase (GS) (Reactions A.5 and A.6) (*19, 22*). GCL catalyzes the formation of the peptide bond between cysteine and the γ-carboxyl group of glutamate; this uncommon peptide bond protects against hydrolysis by peptidases (*22*). The activation of GCL can be stimulated by various factors because the promoter of GCL contains the antioxidant response element as well as an Sp-1 binding site. It is known that the first enzyme is rate-limiting in GSH synthesis (*19*). GSH is able to exhibit non-allosteric negative feedback on GCL, which regulates GSH synthesis, i.e.,

glutathione binds to the glutamate site of GCL rather than to a separate site to inhibit activity of GCL. GCL is a heterodimeric protein that contains a modulatory subunit of 28 kDa, and a catalytic subunit of 73 kDa. The catalytic site and the site for GSH feedback inhibition are located in the heavy subunit, and the regulatory site functions only when these two subunits associate (*19*). GS is a homodimer of 118 kDa. The regulatory mechanism of GS is less well understood (*19*).

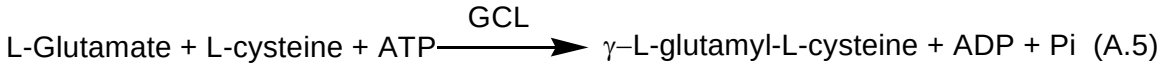

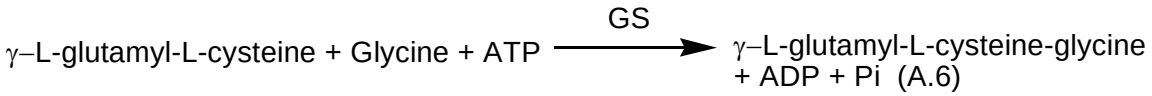

4. Glutathione peroxidase

Mammalian glutathione peroxidases (GPx, EC 1.11.1.9) have been studied extensively (*23*). Mammalian GPx has 6 isoforms: cytosolic Gpx1 (cGPx), gastrointestinal Gpx2 (GIGPx), plasma Gpx3 (pGPx), phospholipid hydroperoxide GPx4 (PHGPx), epididymal GPx5, and olfactory epithelium GPx6 (*24*). The main function of GPx is to catalyze the reduction of hydrogen peroxide and other peroxides (e.g. lipid hydroperoxides and organic hydroperoxides) using GSH as a reducing agent (Reaction A.7). However, pGPx can be regenerated by TrxR/NADPH or TrxR/Trx/NADPH instead of by GSH (*25*). Even though the general reactions catalyzed by GPx are all similar, each isoform of GPx has its own substrate specificity and cellular distribution. cGPx is able to reduce soluble hydroperoxides in lipoproteins to prevent lipid peroxidation (*26*). PHGPx

is a very unique enzyme; unlike other GPxs, PHGPx is able to catalyze the reduction of phospholipid hydroperoxides in lipoproteins to prevent lipid peroxidation. cGPx, GIGPx, pGPx, and PHGPx are selenoenzymes; cGPx, GIGpx, and pGPx are homotetramers, whereas PHGPx is a monomer (*26*). Selenocysteine is replaced by cysteine in GPxs in other organisms such as terrestrial plants, insects, bacteria and humans (*27*). GPxs are able to regulate intracellular hydrogen peroxide; therefore, GPxs are associated with the signaling pathways associated with hydrogen peroxide. Because of its antioxidant activity, cGPx has been shown to inhibit apoptosis in the cells derived from lymphocytes and in HIV-infected cells. Furthermore, PHGPx has been shown to play a role in spermatogenesis and to prevent cardiovascular diseases (*26*).

The general mechanism of GPx has been established: a selenolate anion exists in reduced GPx and this selenolate anion is oxidized to a seleninic acid by peroxides. The first GSH molecule will bind to the seleninic acid of GPx to form a seleneylsulfide adduct (Se-SG). The second GSH molecule will then react to form GSSG and will regenerate an active selenolate anion (*11, 25*).

5. Glutaredoxin

Glutaredoxin (Grx) was discovered in an *E. coli* mutant lacking Trx; Grx is able to donate reducing equivalents to RNR in the mutant (*28*). Grx is widely distributed in organisms ranging from prokaryotes to eukaryotes (*29*). Grx isoforms can be divided into

three subgroups. The first is classic Grx, a small protein (~10 kD_a) characterized by a Trx/Grx fold and a CXXC motif (usually CPYC). The second form is a Grx that is structurally related to glutathione-S-transferase, but retains a redox-active CXXC motif. The third is a Grx with a monothiol (e.g., CGFS) (*29*). Those Grxs having a CXXC motif are able to reduce protein disulfide bonds by a dithiol mechanism, where the solvent-exposed N-terminal cysteine of the redox-active motif forms a thiolate anion to attack a disulfide bond of a protein to form a mixed disulfide between Grx and the target proteins. The C-terminal cysteine residue acts as a so-called resolving cysteine to attack the mixed disulfide forming Grx-S_2 and protein-(SH_2). All three classes of Grxs can carry out deglutathionylation via a monothiol mechanism. The N-terminal cysteine residue of Grx will deprotonate to initiate a nucleophilic attack on a glutathionylated protein, thereby releasing the glutathione from the protein; the resulting Grx-GS mixed disulfide will react with a GSH molecule to produce Grx and GSSG (*29*). Grx appears to be the protein that is mainly responsible for deglutathionylation. Its potency is 50,000 to 100,000 times that of either GSH or dithiothreitol (*30*); the Grx system has a 5000-fold higher catalytic efficiency (k_{cat}/K_m) than the Trx system in the reaction of deglutathionylation (*31*). There are two dithiol Grxs, Grx1 and Grx2, and one monothiol Grx, Grx5, in mammals (*32*). The cytosolic Grx1 is involved in several physiological functions, e.g., regulation of transcription factors, apoptosis, and recycling of dehydroascorbate. The mitochondrial Grx2 catalyzes deglutathionylation very efficiently. Grx2 is the first identified iron-sulfur containing protein in the Grx family. Stimulated by ROS or GSSG, the dimeric Grx2 will monomerize to activate its oxidoreductase activity. Grx2 can also accept electrons from

GSH and the selenoenzyme TrxR (*33*). A monothiol Grx5 has been shown to protect cells against oxidative stress and assembly of iron-sulfur clusters from apoproteins (*33*).

The functions of Trx and Grx partially overlap. For example, either Trx or Grx are able to donate reducing equivalents to activate several targeted enzymes, e.g., RNR for DNA synthesis, PAS reductase, and methionine sulfoxide reductase. However, unlike Trx, Grx can catalyze deglutathionylation efficiently to regulate the activities of several proteins (*29*). Grx is one of the main enzymes that regulate the activities of transcription factors and affect cell differentiation and apoptosis by S-deglutathionylation processes (*30, 31*). In addition to S-deglutathionylation, Grx also has been shown to bind directly to the C-terminal region of ASK-1 to inhibit apoptosis (*30*).

6. Glutathione-S transferase

Glutathione-S-transferases (GST) (E.C. 2.5.1.18) are a group of detoxification enzymes catalyzing the conjugation of GSH to electrophilic atoms of a toxicant to make the compound more soluble for excretion (*34, 35*). In addition, GST exhibits peroxidase, isomerase, and thiol transferase activities. GST is thought of not only as detoxifying but also as being involved in signal transduction and other important physiological functions (*34, 35*). Three major GST groups have been classified: cytosolic GST (cGST), mitochondrial GST, and microsomal GST (*34*). Based on several criteria, including sequence similarities and immuno-reactivity properties, 7 classes of cGSTs in mammalian cells have been identified: alpha, Mu, Pi, Sigma, Theta, Omega, and Zeta, and cGST in nonmammalian cells can be grouped by Beta, Delta, Epsilon, Lambda, Phi, and Tau (*34*). All cGST isoenzymes are found in the cytosol, but the alpha class GST4A-

4 can also be associated with mitochondria (*34*). The structure of the monomer of cGST contains two domains: an N-terminal domain I and a C-terminal domain II. Domain I has a Trx-like fold and domain II has variable numbers (4 to 7) of α-helices (*35*). Each monomer has two binding sites, a GSH binding site (G site) in the N-terminal domain I, and a hydrophobic substrate binding site (H site) formed by the nonpolar side chains of amino acid residues from the C-terminal domain II (*34-36*). Although each monomer has a catalytic site, it should be noted that dimerization is required for full activity (either a homodimer or a heterodimer) (*36*). cGSTs function in many types of antioxidant defense processes. cGSTs can catalyze the conjugation of GSH to exogenous substances including drugs, pesticides, environmental pollutants, and carcinogens. The GSH-conjugates will undergo oxidation to form mercapturic acids for excretion (*34*). cGSTs also display peroxidase activity to neutralize lipid hydroperoxides. In addition to antioxidant activities, cGSTs are able to facilitate a variety of physiological functions. The zeta cGST is able to promote degradation of aromatic amino acids. The alpha cGST is involved in the synthesis of steroid hormones. cGSTs can stimulate the synthesis of prostaglandins (e.g., 15-deoxyl-$\Delta^{12, 14}$-prostaglandin J_2) and regulate the effects of these prostaglandin derivatives on biological functions (*34*). Moreover, cGSTs are able to regulate protein activities by S-glutathionylation: cGSTs catalyze glutathionylation on the sulfenic acid in peroxiredoxin VI to reactivate its antioxidant activity. Furthermore, cGSTs can physically bind to several signaling molecules (e.g., JNK and ASK-1) to regulate their activities (*37*).

The mammalian mitochondrial class Kappa GST is active in a dimeric form; the catalytic properties of this isoenzyme are similar to those of cGSTs: it can catalyze the

conjugation of GSH with some toxic substances (e.g., 1-chloro-2,4-dinitrobenzene) and displays peroxidase activity (*34, 36*).

The microsomal GSTs, also called MAPEG (membrane-associated proteins involved in ecosanoid and glutathione metabolism), can act as detoxification enzymes that catalyze the conjugation of GSH with toxicants. For example, one human isoenzyme, MGST1, can facilitate the conjugation of GSH to several halogenated arenes and the subsequent GSH-dependent reduction of lipid peroxidation (*35*). Some of them (MGST 2 and MGST 3) are found to be involved in the biosynthesis of eicosanoids, leukotrienes and prostaglandins (*35*).

7. Nonenzymatic antioxidants

Nonenzymatic antioxidants are also employed in cells including vitamin C (ascorbic acid) and vitamin E (α-tocopherol).

a. Vitamin C (ascorbate)

Ascorbate can undergo either one or two electron oxidation to form the semidehydroascorbate (SDA) radical or dehydroascorbate (DHA) (*38*). Therefore, ascorbate can act as an intracellular radical scavenger. Ascorbate can provide protection against oxidation of low-density lipoprotein and prolong life spans of patients with nontreatable cancer (*39, 40*). In addition, ascorbate is found to act as a cofactor in several metal-dependent oxygenases (e.g., Cu^{+}-dependent monooxygenase) (*38*).

SDA can be reduced to ascorbate by a variety of enzymes in the cell, e.g., NADH-cytochrome b_5 reductase, Grx, protein disulfide isomerase, GST, 3-α-dehydrogenase, and TrxR. The DHA can be reduced by nonenzymatically by GSH (*38*).

b. Vitamin E

Eight isoforms of vitamin E have been identified: α-, β-, γ-, δ-tocopherol, and α-, β-, γ-, δ-tocotrienols, as shown in Fig A.1 (*41*). The function of vitamin E is to act as a chain-breaking antioxidant in the oxidation of lipids (*39, 40*). In general, tocotrienols are more powerful antioxidants than tocopherols. Among these four isoforms, the α-isoform displays the strongest antioxidant activity (*40*). In the evolution of vitamin E, α-tocopherol has been retained in higher eukaryotes. Vitamin E can be reduced directly by GSH or indirectly via vitamin C (*4*).

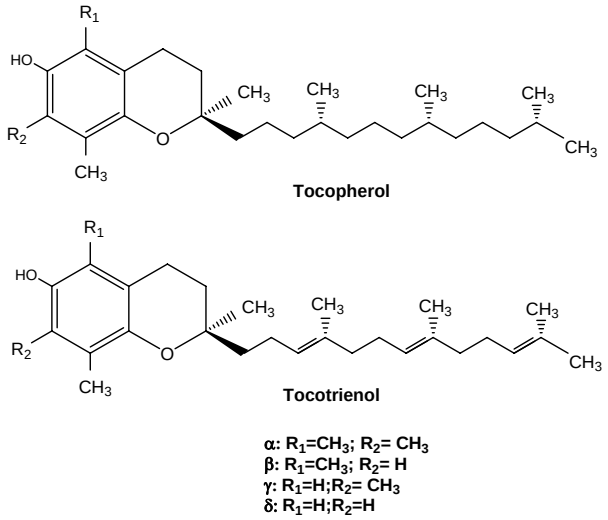

Fig A.1.1 The structures of tocopherol and tocotrienol (*41*)

References

1. Valko, M., Rhodes, C. J., Moncol, J., Izakovic, M., and Mazur, M. (2006) Free radicals, metals and antioxidants in oxidative stress-induced cancer, *Chem Biol Interact 160*, 1-40.
2. Ran, Q., Liang, H., Ikeno, Y., Qi, W., Prolla, T. A., Roberts, L. J., 2nd, Wolf, N., Vanremmen, H., and Richardson, A. (2007) Reduction in glutathione peroxidase 4 increases life span through increased sensitivity to apoptosis, *J Gerontol A Biol Sci Med Sci 62*, 932-942.
3. Marnett, L. J. (2000) Oxyradicals and DNA damage, *Carcinogenesis 21*, 361-370.
4. Valko, M., Leibfritz, D., Moncol, J., Cronin, M. T., Mazur, M., and Telser, J. (2007) Free radicals and antioxidants in normal physiological functions and human disease, *Int J Biochem Cell Biol 39*, 44-84.
5. Yla-Herttuala, S. (1999) Oxidized LDL and atherogenesis, *Ann N Y Acad Sci 874*, 134-137.
6. Seifried, H. E., Anderson, D. E., Fisher, E. I., and Milner, J. A. (2007) A review of the interaction among dietary antioxidants and reactive oxygen species, *J Nutr Biochem 18*, 567-579.
7. Michelet, L., Zaffagnini, M., Massot, V., Keryer, E., Vanacker, H., Miginiac-Maslow, M., Issakidis-Bourguet, E., and Lemaire, S. D. (2006) Thioredoxins, glutaredoxins, and glutathionylation: new crosstalks to explore, *Photosynth Res 89*, 225-245.
8. Stadtman, E. R., and Levine, R. L. (2000) Protein oxidation, *Ann N Y Acad Sci 899*, 191-208.
9. Johnson, F., and Giulivi, C. (2005) Superoxide dismutases and their impact upon human health, *Mol Aspects Med 26*, 340-352.
10. Fridovich, I. (1995) Superoxide radical and superoxide dismutases, *Annu Rev Biochem 64*, 97-112.
11. Nordberg, J., and Arner, E. S. (2001) Reactive oxygen species, antioxidants, and the mammalian thioredoxin system, *Free Radic Biol Med 31*, 1287-1312.
12. Furukawa, Y., and O'Halloran, T. V. (2005) Amyotrophic lateral sclerosis mutations have the greatest destabilizing effect on the apo- and reduced form of SOD1, leading to unfolding and oxidative aggregation, *J Biol Chem 280*, 17266-17274.
13. Zamocky, M., and Koller, F. (1999) Understanding the structure and function of catalases: clues from molecular evolution and in vitro mutagenesis, *Prog Biophys Mol Biol 72*, 19-66.
14. Kirkman, H. N., and Gaetani, G. F. (2007) Mammalian catalase: a venerable enzyme with new mysteries, *Trends Biochem Sci 32*, 44-50.
15. Watson, W. H., Chen, Y., and Jones, D. P. (2003) Redox state of glutathione and thioredoxin in differentiation and apoptosis, *Biofactors 17*, 307-314.
16. Comhair, S. A., and Erzurum, S. C. (2005) The regulation and role of extracellular glutathione peroxidase, *Antioxid Redox Signal 7*, 72-79.

17. Nikitovic, D., and Holmgren, A. (1996) S-nitrosoglutathione is cleaved by the thioredoxin system with liberation of glutathione and redox regulating nitric oxide, *J Biol Chem 271*, 19180-19185.
18. Hill, B. G., and Bhatnagar, A. (2007) Role of glutathiolation in preservation, restoration and regulation of protein function, *IUBMB Life 59*, 21-26.
19. Forman, H. J., and Dickinson, D. A. (2003) Oxidative signaling and glutathione synthesis, *Biofactors 17*, 1-12.
20. Biswas, S., Chida, A. S., and Rahman, I. (2006) Redox modifications of protein-thiols: emerging roles in cell signaling, *Biochem Pharmacol 71*, 551-564.
21. Dalle-Donne, I., Rossi, R., Giustarini, D., Colombo, R., and Milzani, A. (2007) S-glutathionylation in protein redox regulation, *Free Radic Biol Med 43*, 883-898.
22. Njalsson, R., and Norgren, S. (2005) Physiological and pathological aspects of GSH metabolism, *Acta Paediatr 94*, 132-137.
23. Arthur, J. R. (2000) The glutathione peroxidases, *Cell Mol Life Sci 57*, 1825-1835.
24. Herbette, S., Roeckel-Drevet, P., and Drevet, J. R. (2007) Seleno-independent glutathione peroxidases. More than simple antioxidant scavengers, *Febs J 274*, 2163-2180.
25. Epp, O., Ladenstein, R., and Wendel, A. (1983) The refined structure of the selenoenzyme glutathione peroxidase at 0.2-nm resolution, *Eur J Biochem 133*, 51-69.
26. Brigelius-Flohe, R. (1999) Tissue-specific functions of individual glutathione peroxidases, *Free Radic Biol Med 27*, 951-965.
27. Maiorino, M., Ursini, F., Bosello, V., Toppo, S., Tosatto, S. C., Mauri, P., Becker, K., Roveri, A., Bulato, C., Benazzi, L., De Palma, A., and Flohe, L. (2007) The thioredoxin specificity of Drosophila GPx: a paradigm for a peroxiredoxin-like mechanism of many glutathione peroxidases, *J Mol Biol 365*, 1033-1046.
28. Holmgren, A. (1989) Thioredoxin and glutaredoxin systems, *J Biol Chem 264*, 13963-13966.
29. Fernandes, A. P., and Holmgren, A. (2004) Glutaredoxins: glutathione-dependent redox enzymes with functions far beyond a simple thioredoxin backup system, *Antioxid Redox Signal 6*, 63-74.
30. Shelton, M. D., Chock, P. B., and Mieyal, J. J. (2005) Glutaredoxin: role in reversible protein s-glutathionylation and regulation of redox signal transduction and protein translocation, *Antioxid Redox Signal 7*, 348-366.
31. Chrestensen, C. A., Starke, D. W., and Mieyal, J. J. (2000) Acute cadmium exposure inactivates thioltransferase (Glutaredoxin), inhibits intracellular reduction of protein-glutathionyl-mixed disulfides, and initiates apoptosis, *J Biol Chem 275*, 26556-26565.
32. Sagemark, J., Elgan, T. H., Burglin, T. R., Johansson, C., Holmgren, A., and Berndt, K. D. (2007) Redox properties and evolution of human glutaredoxins, *Proteins 68*, 879-892.
33. Lillig, C. H., and Holmgren, A. (2007) Thioredoxin and related molecules--from biology to health and disease, *Antioxid Redox Signal 9*, 25-47.
34. Hayes, J. D., Flanagan, J. U., and Jowsey, I. R. (2005) Glutathione transferases, *Annu Rev Pharmacol Toxicol 45*, 51-88.

35. Frova, C. (2006) Glutathione transferases in the genomics era: new insights and perspectives, *Biomol Eng 23*, 149-169.
36. Torres-Rivera, A., and Landa, A. (2007) Glutathione transferases from parasites: A biochemical view, *Acta Trop*.
37. Tew, K. D. (2007) Redox in redux: Emergent roles for glutathione S-transferase P (GSTP) in regulation of cell signaling and S-glutathionylation, *Biochem Pharmacol 73*, 1257-1269.
38. Linster, C. L., and Van Schaftingen, E. (2007) Vitamin C. Biosynthesis, recycling and degradation in mammals, *Febs J 274*, 1-22.
39. Cameron, E., and Pauling, L. (1976) Supplemental ascorbate in the supportive treatment of cancer: Prolongation of survival times in terminal human cancer, *Proc Natl Acad Sci U S A 73*, 3685-3689.
40. Carr, A. C., McCall, M. R., and Frei, B. (2000) Oxidation of LDL by myeloperoxidase and reactive nitrogen species: reaction pathways and antioxidant protection, *Arterioscler Thromb Vasc Biol 20*, 1716-1723.
41. Zingg, J. M. (2007) Vitamin E: An overview of major research directions, *Mol Aspects Med*.

Appendix 2

Table A.2.1: The primers for site-directed mutagenesis

E469'A	forward	CATCCATCCCACTACCGCCGCGGAATTCACCC
E469'A	reverse	GGGTGAATTCCGCGGCGGTAGTGGGATGGATG
E469'Q	forward	GCATCCATCCCACTACCGCCCAGGAATTCACCC
E469'Q	reverse	GGGTGAATTCCTGGGCGGTAGTGGGATGGATGC
E470'A	forward	CATCCCACTACCGCCGAAGCGTTCACCCGG
E470'A	reverse	CCGGGTGAACGCTTCGGCGGTAGTGGGATG

Fig. A.2.1 Alignment of high M_r TrxRs. The analysis was performed with ClustalW. The sequences of high M_r TrxRs are form NCBI: *Drosophila melanogaster* (Dm; GI:10953879), *Anopheles gambiae* (Ag; GI:20792390), *Plasmodium falciparum* (Pf; GI:886900), *Rattus norvegicus* (Rn; GI:6942216), *Mus musculus* (Ms; GI:110224447) and for *homo sapiens* (Hs; GI:33519430). The highlighted residues correspond to the N-termianl redox-active cysteine pair, the C-terminal redox-active cysteine pair and the dyad of histidine-glutamate.

```
Dm ------------------------------------------------------------
Ag ------------------------------------------------------------
Rn ------------------------------------------------------------
Ms MPVDDCWLYFPASRGRTFVQTVWVAPTCPNCCWFPGFLPPVPRPPHVPRVLLRGPRGAVL 60
Hs ------------------------------------------------------------
Pf ------------------------------------------------------------

Dm ----------------------------------------------------MAPVQG 6
Ag ----------------------------------------------------MAPLNQ 6
Rn ----------------------------------------------------MNDSKD 6
Ms PASRPSKTLPSSSQTPCPTDPCICPPPSTPDSRQEKNTQSELPNKKGQLQKLPTMNGSKD 120
Hs ----------------------------------------------------MNGPED 6
Pf ------------------------MCKDKNEKKNYEHVNANEKNGYLASEKNELTKNKV 35

Dm ---SYDYDLIVIGGGSAGLACAKEAVLNGARVACLDFVKPTPTLGTKWGVGGTCVNVGCI 63
Ag E--NYEYDLVVIGGGSGGLACAKQAVQLGAKVAVLDFVKPSP-RGTKWGLGGTCVNVGCI 63
Rn APKSYDFDLIIIGGGSGGLAAAKEAAKFDKKVMVLDFVTPTP-LGTNGGLGGTCVNVGCI 65
Ms PPGSYDFDLIIIGGGSGGLAAAKEAAKFDKKVLVLDFVTPTP-LGTRWGLGGTCVNVGCI 179
Hs LPKSYDYDLIIIGGGSGGLAAAKEAAQYGKKVMVLDFVTPTP-LGTRWGLGGTCVNVGCI 65
Pf EEHTYDYDYVVIGGGPGGMASAKEAAAHGARVLLFDYVKPSS-QGTKWGIGGTCVNVGCV 94

Dm PKKLMHQASLLGEAVH-EAAAYGWNVDE--KIKPDWHKLVQSVQNHIKSVNWVTRVDLRD 120
Ag PKKLMHQASLLGEAIH-DSQPYGWQLPDPAAIRHDWATLTESVQNHIKSVNWVTRVDLRD 122
Rn PKKLMHQAALLGQALK-DSRNYGWKLED--TVKHDWEKMTESVQNHIGSLNWGYRVALRE 122
Ms PKKLMHQAALLGQALK-DSRNYGWKVED--TVKHDWEKMTESVQSHIGSLNWGYRVALRE 236
Hs PKKLMHQAALLGQALQ-DSRNYGWKVEE--TVKHDWDRMIEAVQNHIGSLNWGYRVALRE 122
Pf PKKLMHYAGHMGSIFKLDSKAYGWKFDN---LKHDWKKLVTTVQSHIRSLNFSYMTGLRS 151

Dm KKVEYINGLGSFVDSHTLLAKLK---SGERTITAQTFVIAVGGRPRYPD-IPGAVEYGIT 176
Ag QKVEYVNGLGYFKDDHTVVAVMKN--QTERELRAKHVVIAVGGRPRYPD-IPGAAEYGIT 179
Rn KKVVYENAYGKFIGPHKIMATNNK--GKEKVYSAERFLIATGERPRYLG-IPGDKEYCIS 179
Ms KKVVYENAYGRFIGPHRIVATNNK--GKEKIYSAERFLIATGERPRYLG-IPGDKEYCIS 293
Hs KKVVYENAYGQFIGPHRIKATNNK--GKEKIYSAERFLIATGERPRYLG-IPGDKEYCIS 179
Pf SKVKYINGLAKLKDKNTVSYYLKGDLSKEETVTGKYILIATGCRPHIPDDVEGAKELSIT 211

Dm SDDLFSLDREPGKTLVVGAGYIGLECAGFLKGLGYEPTVMVRSIVLRGFDQQMAELVAAS 236
Ag SDDIFSLPQAPGRTLLVGAGYIGLECAGFLKGLGYDVSVMVRSILLRGFDQQMATMVGDS 239
Rn SDDLFSLPYCPGKTLVVGASYVALECAGFLAGIGLDVTVMVRSILLRGFDQDMANKIGEH 239
Ms SDDLFSLPYCPGKTLVVGASYVALECAGFLAGIGLDVTVMVRSILLRGFDQDMANKIGEH 353
Hs SDDLFSLPYCPGKTLVVGASYVALECAGFLAGIGLDVTVMVRSILLRGFDQDMANKIGEH 239
Pf SDDIFSLKKDPGKTLVVGASYVALECSGFLNSLGYDVTVAVRSIVLRGFDQQCAVKVKLY 271
```

```
Dm MEERGIPFLRKTVPLSVEKQDDGKLLVKYKNVETG---EEAEDVYDTVLWAIGRKGLVDD 293
Ag MVEKGIRFHHRSRPLAVEKQPDGRLLVRYETVDEAGTATNGEDVFDTVLFAIGRQAETGT 299
Rn MEEHGIKFIRQFVPTKIEQIEAGTPGRLKVTAKSTNSEETIEDEFNTVLLAVGRDSCTRT 299
Ms MEEHGIKFIRQFVPTKIEQIEAGTPGRLRVTAQSTNSEETIEGEFNTVLLAVGRDSCTRT 413
Hs MEEHGIKFIRQFVPIKVEQIEAGTPGRLRVVAQSTNSEEIIEGEYNTVMLAIGRDACTRK 299
Pf MEEQGVMFKNGILPKKLTKMDD-KILVEFS--------DKTSELYDTVLYAIGRKGDIDG 322

Dm LNLPNAGVTVQK----DKIPVDSQE-ATNVANIYAVGDIIYGKPELTPVAVLAGRLLARR 348
Ag LKLANAGVVTAEGGKSDKLEVDETDHRTNVPHIYAVGDVLYRKPELTPVAIHAGRIIARR 359
Rn IGLETVGVKINE--KTGKIPVTDEE-QTNVPYIYAIGDILEGKLELTPVAIQAGRLLAQR 356
Ms IGLETVGVKINE--KTGKIPVTDEE-QTNVPYIYAIGDILEGKLELTPVAIQAGRLLAQR 470
Hs IGLETVGVKINE--KTGKIPVTDEE-QTNVPYIYAIGDILEDKVELTPVAIQAGRLLAQR 356
Pf LNLESLNMNVNK--SNNKIIADHLS-CTNIPSIFAVGDVAENVPELAPVAIKAGEILARR 379


Dm LYGGSTQRMDYKDVATTVFTPLEYACVGLSEEDAVKQFGADEIEVFHGYYKPTEFFIPQK 408
Ag LFGGSEERMDYADVATTVFTPLEYGCVGLSEEAAEAAHGKDGIEVYHAYYKPTEFFVPQR 419
Rn LYGGSTVKCDYDNVPTTVFTPLEYGCCGLSEEKAVEKFGEENIEVYHSFFWPLEWTVPSR 416
Ms LYGGSNVKCDYDNVPTTVFTPLEYGCCGLSEEKAVEKFGEENIEVYHSFFWPLEWTVPSR 530
Hs LYAGSTVKCDYENVPTTVFTPLEYGACGLSEEKAVEKFGEENIEVYHSYFWPLEWTIPSR 416
Pf LFKDSDEIMDYSYIPTSIYTPIEYGACGYSEEKAYELYGKSNVEVFLQEFNNLEISAVHR 439

Dm SVRY--------------CYLKAVAERHGDQRVYGLHYIGPVAGEVIQGFAAALKSGLTI 454
Ag SVRY--------------CYLKAVALREGNQRVLGLHFLGPAAGEVIQGFAAALKCGLTM 465
Rn DNNK--------------CYAKVICNLKDNERVVGFHVLGPNAGEVTQGFAAA-KCGLTK 461
Ms DNNK--------------CYAKIICNLKDDERVVGFHVLGPNAGEVTQGFAAALKCGLTK 576
Hs DNNK--------------CYAKIICNTKDNERVVGFHVLGPNAGEVTQGFAAALKCGLTK 462
Pf QKHIRAQKDEYDLDVSSTCLAKLVCLKNEDNRVIGFHYVGPNAGEVTQGMALALRLKVKK 499

Dm NTLINTVGIHPTTAEEFTRLAITKRSGLDPTPAS-C----CS 491
Ag QVLRNTVGIHPTVAEEFTRLAITKRSGLDPTPAT-C----CS 502
Rn QQLDSTIGIHPVCAEIFTTLSVTKRSGGDILQS-GC----UG 498
Ms QQLDSTIGIHPVCAEIFTTLSVTKRSGGDILQS-GC----UG 613
Hs KQLDSTIGIHPVCAEVFTTLSVTKRSGASILQA-GC----UG 499
Pf KDFDNCIGIHPTDAESFMNLFVTISSGLSYAAKGGCGGGKCG 541
```